

**DEVELOPMENT OF INTERFERENCE MITIGATION SCHEME FOR INBAND
OVERLAY 5G NETWORKS**

BY

AMEH, Ameh Innocent PhD/SEET/2016/924

**DEPARTMENT OF ELECTRICAL AND ELECTRONIC ENGINEERING
FEDERAL UNIVERSITY OF TECHNOLOGY, MINNA.**

JULY 2023

ABSTRACT

The steep growth in mobile data traffic has gained a lot of attention in recent years because the current infrastructure deployments and radio resources, may not be sufficient to service the upcoming demands. Many solutions have been put forward, one of them being Device-to-Device (D2D) communications where users in proximity can transmit directly to one another, bypassing the base station (BS). Fifth generation (5G) networks enable D2D communication between devices in proximity, and this led to the introduction of interference between D2D User Equipment (DUEs) and other D2D Users, known as Co-Tier Interference, as well as interference between D2D users and traditional Cellular User Equipment (CUEs), known as the Cross-Tier Interference. Managing these ensuing interference scenarios is considered one of the most critical issues when D2D is introduced to the cellular network because D2D users share the same licensed spectrum with cellular users. In this research work, two (2) interference mitigation schemes were developed. The Mode Selection and Bandwidth Allocation Scheme (MS-BAS) was developed to mitigate the cross-tier interference in the micro-D2D network. Communication mode is assigned to User Equipment (UEs) based on the separating distance and Signal-to-Interference-Plus-Noise Ratio (SINR) between the transmitting and receiving UEs. 60% and 30% of the spectrum is statically assigned to both the cellular and D2D tiers respectively, while the remainder 10% is dynamically assigned to the communication tier with the higher number of UEs. The second developed scheme is the D2D Power Control Scheme (D2D-PCS) for the mitigation of co-tier interference in the D2D tier of the network, where UEs begin transmission with a set initial transmit power, rather than their maximum transmit power. The UE pathloss is computed and used to compute the D2D SINR. This SINR is compared with both the CUE SINR and a set threshold SINR to determine the interference level. The transmit power is then adjusted based on the interference level. The MS-BAS delivered an average data rate of 43.17 Mbps across the network, indicating a 29.37% improvement when compared with the existing Selective Overlay Mode Operation (SOMO), and an average Signal-to-Interference-Plus-Noise Ratio (SINR) of 2.02 representing a 37.41% improvement. The energy efficient D2D Power Control Scheme (D2D-PCS) for the mitigation of co-tier interference recorded an SINR of 0.39, indicating a 69.57% and 50.00% improvement over the Fixed Power Control (FPC) and Power Control Scheme 1 (PCS1) schemes respectively, an average data rate of 25.48 Mbps, indicating a 47.62% and 32.71% performance improvement over the FPC and PCS1 schemes respectively, and a 17.25 dBm DUE average power utilization against 23.00 dBm and 17.50 dBm for the FPC and PCS1 schemes respectively. The obtained results show the efficacy of the MS-BAS and D2D-PCS in significantly mitigating both cross and co tier interference scenarios respectively in the two-tiered network.

Table of Contents

Content	Page
Cover Page	i
Title Page	ii
DECLARATION	iii
CERTIFICATION	iv
DEDICATION	v
ACKNOWLEDGEMENTS	vi
ABSTRACT	vii
Table of Contents	viii
List of Tables	xi
List of Figures	xii
List of Abbreviations	xiv
CHAPTER ONE	1
1.0 INTRODUCTION	1
1.1 Background to the Study	1
1.2 Statement of the Research Problem	6
1.3 Research Aim and Objectives	7
1.4 Research Motivation	8
1.5 Scope and Limitation of the Study	8
CHAPTER TWO	9
2.0 LITERATURE REVIEW	9
2.1 The Fifth Generation (5G) Networks	9
2.2 5G Use Cases and Applications	11
2.2.1 M2M communication	12
2.2.2 Internet of things (IoT)	13
2.2.2.1 <i>The tactile internet</i>	15
2.2.2.2 <i>Healthcare and wearables</i>	16
2.2.3 Augmented and virtual reality	17
2.2.4 D2D communication	20

2.3	Key Challenges in D2D Communication	23
2.3.1	Peer discovery	24
2.3.2	Security	25
2.3.3	Interference	26
2.3.3.1	<i>Co-tier interference</i>	27
2.3.3.2	<i>Cross-tier interference</i>	28
2.4	Interference Mitigation Techniques	29
2.4.1	Mode selection	29
2.4.2	Resource allocation	30
2.4.3	Power control	32
2.4.4	Bandwidth allocation	32
2.5	Review of Related Works on Interference Mitigation in D2D Networks	33
2.5.1	Summary of review of related works	48
CHAPTER THREE		47
3.0	RESEARCH METHODOLOGY	49
3.1	Research System Model	49
3.2	Mode Selection and Bandwidth Allocation Scheme	50
3.3	Power Control Scheme	58
CHAPTER FOUR		62
4.0	RESULTS AND DISCUSSION	65
4.1	Presentation of Results	65
4.1.1	Results of mode selection and bandwidth allocation scheme	65
4.1.2	Results of power control scheme	78
CHAPTER FIVE		92
5.0	CONCLUSION AND RECOMMENDATIONS	
		92
5.1	Conclusion	92
5.2	Recommendations	93
5.3	Contribution to Knowledge	93
REFERENCES		94
APPENDICES		103

List of Tables

Table	Title	Page
2.1:	Meta analysis Table of related works	43

3.1:	System parameters	50
3.2:	Pseudocode of mode selection and bandwidth allocation scheme	58
3.3:	Pseudocode of power control technique	63
4.1:	A random distribution of UE to DUE and CUE modes	66
4.2:	SINR of MS-BAS with varied DUE distance	67
4.3:	Data rate of MS-BAS with varied DUE distance	68
4.4:	DUE SINR of SOMO & MS-BAS with varied number of D2D pairs	72
4.5:	Data rates of MS-BAS with varied number of D2D pairs	74
4.6:	SINR of D2D-PCS with varied DUE distance	78
4.7:	Data rate of D2D-PCS with varied DUE distance	80
4.8:	SINR of D2D-PCS with varied number of D2D pairs	85
4.9:	Data rates of D2D-PCS with varied number of D2D pairs	87
of Figures		List

Figure	Title	Page
2.1:	A D2D-enabled network scenario	21
2.2:	Categorization of D2D communication	24
2.3:	An interference scenario in a D2D-enabled cellular network	27
2.4:	Interference scenario for different reuse resource	29
2.5:	Bandwidth allocation	33
3.1:	Research network system model	49
3.2:	Block diagram of mode selection and bandwidth allocation	51
3.3:	Flowchart of mode selection and bandwidth allocation scheme	56
3.4:	Block diagram of power control algorithm	59
3.5:	Flowchart of D2D power control scheme	62
4.1:	A random distribution of UE to CUE and DUE modes	66

4.2:	DUE SINR of MS-BAS based on varied DUE distance	68
4.3:	MS-BAS DUE data rate based on varied DUE distance	69
4.4:	MS-BAS CUE data rate based on varied DUE distance	70
4.5:	MSBAS UE data rate based on varied DUE distance	71
4.6:	DUE SINR of MS-BAS based on varied number of D2D pairs	73
4.7:	MS-BAS DUE data rate based on varied D2D pairs	75
4.8:	MS-BAS CUE data rate based on varied D2D pairs	76
4.9:	MS-BAS UE data rate based on varied D2D pairs	77
4.10:	SINR of PCS1 based on varied DUE distance	79
4.11:	D2D-PCS DUE data rate based on varied DUE distance	81
4.12:	D2D-PCS CUE data rate based on varied DUE distance	82
4.13:	D2D-PCS UE data rate based on varied DUE distance	84
4.14:	D2D-PCS Average DUE power against DUE distance	85
4.15:	D2D-PCS DUE SINR on varied D2D Pair	86
4.16:	D2D-PCS DUE data rate based on varied D2D pairs	88
4.17:	D2D-PCS CUE data rate based on varied D2D pairs	89
4.18:	D2D-PCS UE data rate based on varied D2D pairs	90
4.19:	D2D-PCS average power consumption on varied D2D pairs	91

List of Abbreviations

Abbreviation	Meaning
4G	Fourth Generation
5G	Fifth Generation
APC	Active Power Control
BS	Base Station
CID	Cell Identity
CRN	Cognitive Radio Network
CUE	Cellular User Equipment
D2D	Device-to-Device
D2D-PCS	D2D Power Control Scheme
D2DR	Device-to-Device Receiver
D2DT	Device-to-Device Transmitter
DL	Downlink
DoF	Degree of Freedom
DUE	Device-to-Device User Equipment eMBB
	Enhanced Mobile Broad Band FPC
	Fixed Power Control
HetNet	Heterogeneous Network
HSPA	High Speed Packet Access
IA	Interference Alignment
IMEI	International Mobile Equipment Identity
KPI	Key Performance Indicator
LOS	Line of Sight
LTE	Long Term Evolution
Macro - D2D	Macrocell and D2D HetNet
MANETs	Mobile Ad-hoc Networks
MCS	Mode and Coding Scheme
M2M	Machine-to-Machine
MIMO	Multiple Input Multiple Output mMTC
	massive Machine Type Communication

MS	Mode Selection
MS-BAS	Mode Selection-Bandwidth Allocation Scheme
MTC	Machine Type Communication
MUE	Mobile User Equipment
NLOS	Non-Line of Sight
OFDMA	Orthogonal Frequency-Division Multiple Access
PC	Power Control
PCS1	Power Control Scheme 1
PCS2	Power Control Scheme 2
QoS	Quality of Service
RB	Resource Block
SIM	Subscriber Identity Module
SINR	Signal to Interference plus Noise Ratio
SOMO	Selective Overlay Mode Operation
UL	Uplink
URLL	Ultra-Reliable Low Latency
UDN	Ultra-Dense Network
UE	User Equipment
VNI	Visual Network Index
V2V	Vehicle-to-Vehicle

CHAPTER ONE

1.0 INTRODUCTION

1.1 Background to the Study

The world has witnessed four generations of mobile communication, with each new generation emerging roughly ten years after the emergence of the previous generation.

The first generation consisted of the analogue systems introduced in the early 1980s.

They were only supporting voice services and, for the first time, made mobile telephony available to ordinary people (Bhandari *et al.*, 2017).

The second generation (2G), emerging in the early 1990s, took mobile telephony from being used by some people to being available to essentially everyone and everywhere.

Technology-wise, the key feature of 2G was the transition from analogue-to-digital transmission. Although the main service was still voice, the introduction of digital transmission also enabled the first support of mobile data (Bhandari *et al.*, 2017).

The third generation (3G), Wideband Code Division Multiple Access (WCDMA), which later evolved into High-Speed Packet Access (HSPA), was introduced in 2001. 3G lay the foundation for mobile broadband and, especially with HSPA, made true mobile internet access available to ordinary people (Li *et al.*, 2018).

The fourth generation (4G) era of mobile communication with the first Long-Term Evolution (LTE) systems were introduced in 2009. Compared to HSPA, LTE provides even better mobile broadband including higher achievable data rates (up to 1Gbps) and higher efficiency in terms of, for example, spectrum utilization. However, for 5G there's a much wider set of capabilities and requirements (Li *et al.*, 2018).

5G will continue on the path of LTE, enabling higher data rates (more than 1Gbps) and even higher efficiency for mobile broadband. However, the scope of 5G is much wider

than just further enhanced mobile broadband. Rather, 5G is often described as a platform that should enable wireless connectivity for essentially any kind of device or any kind of application that may benefit from being connected, for example the Internet of Things (IoT), Machine to Machine Communication (M2M) or Machine-Type Communication (MTC), the Tactile Internet, etc (Bhandari *et al*, 2017).

The concept of MTC is one part of this extended set of use cases expected in the 5G era. Major steps to further enhance the support for certain types of MTC applications have already been taken as part of the evolution of LTE. More specifically, these steps have focused on massive-MTC applications associated with very low-cost devices with very long battery life but with relatively modest data rate and latency requirements. However, 5G is assumed to enable connectivity for a much wider range of new use cases.

Examples of additional use cases explicitly mentioned in the context of 5G include wireless connectivity for remote control of machinery, wireless connectivity for traffic safety and control, and monitor/control of infrastructure, to just name a few (Bhandari *et al*, 2017). Furthermore, 5G should not only be a platform for providing connectivity for already identified applications and use cases (Jameel *et al.*, 2018). Rather, 5G should be flexible enough to enable connectivity also for future applications and use cases that may not yet even be anticipated.

The very wide range of use cases to be covered by 5G implies that the capabilities of 5G wireless access must extend far beyond that of previous generations. For the first- and second-generation networks, the use case in focus was mobile telephony with the main target to provide good speech quality for as many users as possible. For 3G and 4G, the change of focus toward mobile broadband implied that the quality measure changed from speech quality to achievable end-user data rate. In line with this, the main target for 3G

and 4G has been to enable as high data rates as possible for as many users as possible. However, for 5G there will be a much wider set of capabilities and requirements, some of which may even be partly contradicting each other (Jameel *et al.*, 2018).

The evolution of the cellular network generations is primarily influenced by a continuous growth in wireless user devices, data usage, and the need for a better quality of experience (QoE). It was projected that more than 50 billion connected devices will utilize the cellular network services by the end of the year 2020 (Ericsson, 2011), and that would result in a tremendous increase in data traffic, as compared to the year 2014 (Ericsson, 2015). However, state-of-the-art solutions are not sufficient for the challenges mentioned above. Specifically, the fifth generation (5G) of the cellular networks will highlight and address three broad views:

- i. user-centric (by providing 24×7 device connectivity, uninterrupted communication services, and a smooth consumer experience),
- ii. service-provider-centric (by providing a connected intelligent transportation system, road-side service units, sensors, and mission critical monitoring/tracking services),
- and iii. network-operator-centric (by providing an energy-efficient, scalable, low-cost, uniformly monitored, programmable, and secure communication infrastructure).

Therefore, 5G networks are perceived to actualize the three views above through these features:

- i. **Ubiquitous Connectivity:** In the future, many types of devices will connect ubiquitously and provide an uninterrupted user experience. In fact, the usercentric view will be realized by ubiquitous connectivity.
- ii. **Zero Latency:** 5G networks will support life-critical systems and real-time applications and services with zero delay tolerance. Hence, it is envisioned that 5G networks will realize zero latency, i.e., very low latency of the order of 1

millisecond (Nokia Networks, 2016; Wubben *et al.*, 2014). In fact, the serviceprovider-centric view will be realized by the zero latency.

- iii. High-Speed Gigabit Connection: The zero-latency property could be achieved using a high-speed connection for fast data transmission and reception, which will be of the order of Gigabits per second to users and machines (Nokia Networks, 2016).

A few more key features of 5G networks are enlisted and compared to the fourth generation (4G) of the cellular networks, as below (5GPPP 2015, GSMA intelligence 2014, METIS 2015):

- i. 10-100 times the number of connected devices,
- ii. 1000 times higher mobile data volume per area,
- iii. 10-100 times higher data rate, iv. 1 millisecond latency,
- v. 99.99% availability, vi. 100% coverage, vii. 10 times less of the energy consumption as compared to the year 2010, viii. real-time information processing and transmission, ix. 5 times less of the network management operation expenses, and
- x. seamless integration of the current wireless technologies.

Therefore, the revolutionary scope and the consequent advantages of the envisioned 5G networks demand new architectures, methodologies, and technologies, e.g., energyefficient heterogeneous frameworks, cloud-based communication (Software-Defined Networks (SDN) and Network Function Virtualization (NFV)), full duplex radio, SelfInterference Cancellation (SIC), Device-to-Device (D2D) communications, machine-to-machine (M2M) communications, access protocols, cheap devices, cognitive networks (for accessing licensed, unlicensed, and shared frequency bands), dense-deployment, security-privacy protocols for communication and data transfer, backhaul

connections, massive multiple-input and multiple-output (mMIMO), multi-Radio Access Technology (RAT) architectures, and technologies for working on millimeter wave (mmWave) 30– 300 GHz. Interestingly, 5G networks will not be a mere enhancement of 4G networks in terms of additional capacity, they will encompass a system architecture visualization, conceptualization, and redesigning at every communication layer (Ge *et al.*, 2014).

Device to device (D2D) wireless communication network is one of the enabling technologies in wireless communication where user devices connect with themselves directly and exchange information without routing such information through a base station (Li *et al.*, 2018). The sole aim of D2D communication is to depopulate the macrocell network, reduce latency in communication, increase network coverage and capacity (Ravindra and Siddesh, 2019). D2D technology was first introduced in fourth generation (4G) network and is one of the enabling technologies of fifth generation (5G) network, which aims at achieving 5G application of an enhanced mobile broadband (eMBB).

5G has basically two limited resources, which are spectrum and power to be maximized. These two main network resources are often traded off to mitigate interference in the network. 5G being an ultra-dense network (UDN) with millions of connections makes interference mitigation to be consequential (Jameel *et al.*, 2018).

Network capacity, coverage and throughput are related directly to the user traffic density on the network. As the number of users in a network increases, the interference increases, and the cell capacity and coverage decrease. To reduce interference and increase capacity, coverage and throughput of cellular communication, technologies such as

antenna sectorization, use of small cells and D2D technology were introduced (Jameel *et al.*, 2018).

The integration of D2D network in already existing macrocell network to form a heterogeneous network (HetNet) introduces a new D2D network layer (tier) to macrocell (large) network layer, which gives rise to a two-tier (Macro - D2D) network. This enabling technology in 5G moves some of the macrocell user equipment to D2D communication layer (tier) to decongest the macrocell network, increase macrocell network coverage, capacity, and throughput. There are problems however, in Macro - D2D HetNets, which includes handover, neighbour discovery, interference, security, communication mode selection, and mobility management. Addressing interference problem is consequential in 5G Macro - D2D to adequately harness and preserve the potentials therein (Jameel *et al.*, 2018).

1.2 Statement of the Research Problem

With an ever-growing number of connected devices using the cellular network (Safaei *et al.*, 2017), service providers are faced with the challenge of improving spectrum reuse, throughput, energy efficiency, coverage, and reduction of end-to-end latency. Network performance would be driven up if closely located user pairs are allowed direct communication with each other, rather than through the traditional Up-link and Downlink communication channels of the Base Stations (BS). Additionally, the creation of new peer-to-peer services and location-based applications would all be driven by an efficient Device-to-Device (D2D) communication system, which incidentally, is one of the identified enabling technologies for the 5th generation cellular network, 5G. This integration of D2D comes with such challenges as neighbour discovery, selection of communication mode (D2D or cellular), security of the transmitted information, security of the UEs, denial of service (DoS), and interference (Asadi *et al.*, 2014). With enabled

D2D communication between devices in proximity, there would be an introduction of interference between D2D User Equipment (DUEs) and other D2D Users, known as CoTier Interference, as well as interference between D2D users and traditional Cellular User Equipment (CUEs), the Cross-Tier Interference.

The interference problems are what this research seeks to mitigate by developing a Mode Selection and Bandwidth Allocation Scheme (MS-BAS) to mitigate the cross-tier interference, and a D2D Power Control Scheme (D2D-PCS) to mitigate the co-tier interference.

1.3 Research Aim and Objectives

The research aims at developing an interference mitigation scheme for an inband overlay 5G network. The objectives are, to:

- i. develop a Macro-D2D network system model.
- ii. develop a mode selection and bandwidth allocation scheme for the mitigation of cross-tier interference in the Macro-D2D network.
- iii. develop a Power Control Scheme to mitigate co-tier interference in the D2D tier of the network.
- iv. evaluate the performance of the schemes developed in (ii) and (iii) by comparison with related works for Signal to Interference plus Noise Ratio (SINR), Data Rates, and Power utilization.

1.4 Research Motivation

A quick look into recent wireless network statistics reveal that global mobile traffic grew 63% in 2016 and almost half a billion (429 million) mobile devices and connections were added in 2016 (Cisco, 2017). Globally, smart devices represented 46% of the total mobile devices and connections in 2016; they accounted for 89% of the mobile data traffic.

Another interesting finding is that smartphones represented only 45% of total mobile devices and connections in 2016 but represented 81% of total mobile traffic. Cisco's Visual Networking Index (VNI) forecasted that by 2021, nearly three-quarters of all devices connected to the mobile network will be "smart" (Cisco, 2017). Inspired by the above, this research focuses on one of the key elements identified as a 5G technology enabler, D2D Communication.

Since it is already clear that not all these challenges can be accommodated even by the current wireless network, the next-generation (5G) networks should take this role and act as an enabler for upcoming communication use-cases.

1.5 Scope and Limitation of the Study

This work focused on the development of two schemes to mitigate co-tier and cross-tier interference in Macro-D2D communication HetNet. The schemes were simulated in MATLAB based on the research parameters and system model. The performance of the schemes in terms of power utilization, SINR, and user equipment data rates were benchmarked with that of related schemes.

CHAPTER TWO

2.0 LITERATURE REVIEW

2.1 The Fifth Generation (5G) Networks

Over the last few years, it was not clear what 5G really stands for, and what kind of technologies, communication protocols and applications will be the biggest drivers of this new cellular infrastructure. As the technology pillars in the architecture of future 5G mobile networks were identified, a diversity of wireless technologies will collaborate to support the 5G communication networks with their demanding applications and services. Despite decisive progress in many enabling solutions, next-generation cellular

deployments may still suffer from a lack of bandwidth due to inefficient utilization of radio spectrum, which calls for expedited action (Masek, 2017).

As a technical envelope of 5G vision, there are several broadly discussed performance criteria which are expected to be delivered by the fifth generation (5G) systems. In this research, the most important of them are (Kujur and Shukla, 2018):

- i. Virtually unlimited capacity and ubiquitous coverage introducing the “anytime and anywhere” connectivity.
- ii. Tremendous increase of network throughput (1 – 10 Gbps). High degree of flexibility and network intelligence of all involved technology components to deliver most of the services on-demand with respect to meeting agreed Quality of Service (QoS) and Quality of Experience (QoE).
- iii. Significantly lower end-to-end latency (below 1 ms) to enable new application scenarios e.g., Tactile Internet (TI).
- iv. Unrestricted mobility to enable the mobile broadband even for very fast-moving objects (up to 500 km/h) e.g., Controlled Dynamic Spectrum Sharing at the airport.
- v. Energy efficient communication to reduce power consumption at the side of end users and telecommunication operators.

Despite very active research during the last couple of years resulting in a variety of promising solutions created across academia and industry, the true 5G landscape is still not there yet. However, the main essentials are already known - all technical and user requirements can be barely fulfilled by a single Radio Access Technology (RAT).

Therefore, as fundamentally different from previous generations of cellular systems, the 5G networks will not be just an incremental advancement of 4G, but rather constructed as a set of directly bounded communication technologies and protocols (Andrews *et al.*,

2014). While in recent cellular systems, the selected wireless technologies have been developing and operating individually, the 5G needs significant increase in network capacity and throughput. Therefore, it requires a tighter interconnection and cooperation between different types of RATs. As a result, it becomes unavoidable to aggregate different radio technologies as part of a common converged radio network – to be transparent to the end-users and develop techniques that can efficiently utilize the radio resources available across different spectral bands (Shuminoski and Janevski, 2013). Following this vision, the Heterogeneous Networks (HetNets) represent a key building block of next generation 5G systems, where different RATs operating in licensed, e.g., Long Term Evolution (LTE) as well as unlicensed spectrum (for example, WiFi) are collectively providing the multiplied performance (Talwar *et al.*, 2013; Andreev *et al.*, 2016).

With respect to the convergence of various RATs, the telecommunication operators increase the density of their mobile networks by deploying new cells with different coverage – to boost the overall network capacity (Hwang *et al.*, 2013) – since the multiRAT concept together with continuing network densification are still not providing satisfactory outputs (from 5G perspective), especially due to limited space and narrow frequency bandwidth of all legacy wireless technologies. Therefore, the heterogeneous deployments (infrastructures) must be provided by novel wireless communication technologies – utilizing extremely high frequency millimeterWave (mmWave) band ranging from 3 to 300 GHz (Khan *et al.*, 2012). Of course, the mentioned mmWave communications are naturally not suitable for long-range use-cases since the wavelength cannot infiltrate from dense materials efficiently. Therefore, it can be easily dispersed by rain drops, gases, and flora. Nevertheless, mmWave and Visible Light Communication (VLC) technologies can improve the transmission data rates for indoor setups, because

they have come up with large bandwidth. This, in fact, particularly supports one of the key ideas of designing the 5G cellular architecture – the outdoor and indoor scenarios should be physically separated, so that penetration loss through building walls can be limited or even fully avoided (Wang and Fapojuwo, 2017).

2.2 5G Use Cases and Applications

A wide variety of emerging 5G applications put pressure on the commercial roll out of 5G wireless systems. 5G network architecture is expected to provide network solutions for a wide range of public and private sectors, that is, energy, agriculture, city management, healthcare, manufacturing, and transport, with significantly improved user experience (5GPPP, 2015). Aside from the enormous number of connections, 5G networks also must support diverse nature of devices and their associated service requirements (Agyapong *et al.*, 2014).

Although research and development in some of these applications are already underway in 4G wireless, original 4G LTE standards, 3GPP LTE Release 8 (3GPP Release 8.0, 2014) did not include support to any of these applications. Rather, these applications were spawned later, and started explosive increase in wireless data usage, thereby imposing additional utilization of resource constrained 4G wireless networks. Naturally, later releases of 4G LTE networks, often named as LTE Advanced, gradually started to include these applications. On the other hand, it is expected that massive bandwidth of 5G mmWave communications will provide a native support for these emerging applications. In this section, some of the demanding applications i.e., D2D communications, M2M communications, IoV, IoT and healthcare are discussed.

2.2.1 M2M communication

Comparable to D2D communications, M2M communications are also expected to play crucial roles with their native support in 5G wireless systems. Based on the information given in Asadi *et al.*, (2014), and Wang and Fapojuwo, (2017) M2M communication can be described as Data communication among machines or devices that does not require human mediation nor impose specific restrictions on communication ranges. The communication between machines is routed through the core networks via base stations and remote servers, even if source and destination are proximate to one another. In comparison, D2D communication presumes a distance limit between devices and relies only on local device capabilities without centralized infrastructure support. Moreover, M2M is application-oriented and technology-independent approach, whereas D2D is technology-dependent and focuses on proximity services, which assumes opportunistic connectivity (Asadi *et al.*, 2014, Wang and Fapojuwo, 2017).

The main application of M2M is to automatically collect and deliver measurement information. D2D communication, as a new communication pattern, can be used for M2M communication to improve network performance and reduce transmission delay (Wang and Fapojuwo, 2017). Major features of M2M communications comprise automated data generation, processing, transfer, and data exchange between smart devices (machines), and infrequent data transmission, with minimum human interaction.

M2M communication envisions:

- i. considerable number of devices with small amount of data, ii. sporadic transmissions, iii. high reliability, iv. low latency, and
- v. real-time operation.

Major reviews of published M2M research works contain various commercial, hardware and proof-of-concept frameworks as well as major architectural improvements, network functionalities and research challenges (Ghavimi and Chen, 2015). Latest advances and development directions in architecture, communication protocols, standards and security for M2M evolution from 4G to 5G are outlined in (Ratasuk *et al.*, 2015). Network unpredictability and mobility often lead to complex interference within M2M devices, as well as between M2M networks and cellular networks (Jo *et al.*, 2014). Therefore, it is expected that Cognitive Radio (CR) or other approach e.g., Licensed Shared Access (LSA) will emerge and assist in developing novel cognitive M2M architecture for sensing and using the available frequency bands (Zhang *et al.*, 2012).

2.2.2 Internet of things (IoT)

Looking back, first patterns of IoT connectivity can be dated back to the 1980s, with the legacy Radio Frequency Identification (RFID) technologies, and back to the 1990s, with the Wireless Sensor Networks (WSN). Due to their promising application scenarios, they gained a lot of attention both in business and consumer markets. Therefore, going further, for the first decade of the 21st century, industrial alliances invested a lot of effort in developing standardized low power IoT solutions (Masek *et al.*, 2016).

The first solutions available on the market were proprietary-based, such as WirelessHART and Z-Wave. Those solutions have delayed the initial take-off of the IoT, due to interoperability issues, among different vendors. Based on this experience, more generic communication technologies have been developed by industrial alliances and working groups i.e., Institute of Electrical and Electronics Engineers (IEEE), European Telecommunications Standards Institute (ETSI), 3rd Generation Partnership Project (3GPP), and Internet Engineering Task Force (IETF), providing the interconnection and Internet-connection of constrained devices – Bluetooth, and the IEEE 802.15.4 standard

have played an important role in the IoT evolution since they were on the market right on time. Recently, the IEEE 802.15.4 Physical (PHY) and Medium Access Control (MAC) layer have been complemented by an IP-enabled IETF protocol stack. The IETF 6LoWPAN (Kushalnagar *et al.*, 2007) and IETF ROLL working groups have played a key role in facilitating the integration of low-power wireless networks into the Internet, by proposing mainly distributed solutions for address assignment and routing. At the same time, the 3GPP has been working towards supporting M2M applications on 4G broadband mobile networks, such as Universal Mobile Telecommunication System (UMTS) and LTE, with the final aim of embedding M2M communications within the 5G systems (Andreev *et al.*, 2016).

None of these technologies have emerged as a market leader, mainly because of technology shortcoming and business model uncertainties. Now, the IoT connectivity field is at a turning point with many promising radio technologies emerging as true M2M connectivity contenders:

- i. Low-Power Wi-Fi,
- ii. Low-Power Wide Area Networks (LPWAN),
- iii. Narrow-Band NB-IoT,
- and, iv. LTE-M (LTE-MTC) (Andreev *et al.*, 2016).

These solutions are therefore attractive for IoT deployments, being able to fulfill availability and reliability requirements. A few application use cases of the IoT are as briefly discussed in the following sub-sections.

2.2.2.1 The tactile internet

After creating the mobile Internet, connecting billions of smart devices (smart phones and laptops), the focus of mobile communications is moving towards providing

ubiquitous connectivity for machines and devices, thereby creating the Internet of Things paradigm (Atzori *et al.*, 2010). With the present technological advancements, the communication stage is ready for the emergence of the Tactile Internet (TI) in which the ultra-reliable and ultra-responsive network connectivity will enable to deliver requested real-time control and physical tactile experiences remotely.

The Tactile Internet will, therefore, provide a true communication paradigm shift from content-delivery to skill-set delivery networks, and thereby reform every segment of the society. Following the information given by International Telecommunication Union (ITU), the Tactile Internet will add a new dimension of human-to-machine interaction by delivering low latency (communication delay) to setup real-time interactive communication systems. Further, the TI has been described as a communication infrastructure linking the following together:

- i. lower latency (<1 ms),
- ii. short transition time,
- iii. high service availability, and
- iv. heightened security (Wubben *et al.*, 2014).

Associated with cloud computing proximity through e.g., mobile edge-clouds and combined with the virtual or augmented reality for sensors and haptic controls, the Tactile Internet addresses areas with reaction times in order of a millisecond e.g., realtime gaming, transportation systems, health, and education.

Because the Tactile Internet will be servicing the mission-critical use-cases of society (e.g., automation in industry, autonomous driving, robotics, healthcare, virtual and augmented reality), it will need to be ultra-reliable, with a maximum outage of a second per year (Simsek *et al.*, 2016), support very low latencies, and serve sufficient capacity to communicate with each other simultaneously and autonomously. Following the

mentioned facts, the proposed architecture will be able to interconnect TI with traditional representatives like wired Internet, the mobile Internet, and the IoT – forming an Internet of new dimensions and capabilities.

Since the state-of-the-art fourth generation (4G) mobile systems do not fulfill the given technical requirements for the TI, the fifth generation (5G) mobile communications systems are expected to underpin the TI at the wireless edge.

2.2.2.2 *Health care and wearables*

Advancements in sensing and communication technology have opened up new possibilities for health monitoring. Wearable technologies promise to provide health care solutions to growing world strained by the aging population. Devices with capabilities of measuring multiple signals in ambulance are being developed. The record of multiple physiological signals over a long period helps in understanding the disease pathophysiology (Binkley, 2003). Improved addressing, extended security services and higher bandwidth enables new possibilities of healthcare (Oleshchuk and Fensli, 2011). Emerging 5G wireless and Body Area Network (BAN) are facilitating a paradigm shift in real-time remote patients' health monitoring.

The major constraint in real-time data collection and monitoring is bandwidth limitation. Higher bandwidth and data rates of 5G wireless are expected to resolve these bandwidth constraints. An IoT based system, using big data and cloud computing concepts, for emergency medical services is presented in Dunne *et al.*, (2014). In view of these, 5G wireless architecture is expected to resolve big data challenges of real-time health care applications bringing huge benefits to humanity (Xu *et al.*, 2014).

2.2.3 Augmented and virtual reality

Leveraging recent advances in storage / memory, communication / connectivity, computing, big data, artificial intelligence (AI), machine vision, and other areas, will enable the implementation of immersive communication technologies as augmented reality and virtual reality (AR, VR). These technologies will enable the transmission of ultra-high-resolution video and sound in real time through the relay of its various sights, sounds, and emotions. The use of VR will go beyond early adopters such as gaming to enhancing cyber-physical and social experiences such as conversing with family and acquaintances, business meetings, and disabled persons. Adding this to the growing number of drones, robots, and other self-driving vehicles taking cameras to places humans could never imagine reaching, a rapid increase of new content from fascinating points of view around the world shall be seen. Ultimately, VR will provide the most personal experience with the closest screen, providing the most connected, most immersive experience (Bastug *et al.*, 2017).

AR and VR represent two ends of the communication spectrum. On the one hand, AR is based on reality as the focus, and the virtual information is presented over the reality. On the other hand, VR is based on virtual data as the focus, immersing the user into the middle of the simulated reality virtual environment. One can also imagine a mixed reality where AR works together with the VR, by merging the physical and virtual information seamlessly (Shafi *et al.*, 2017). Current online social networking sites i.e., Facebook, Twitter are just precursors of what will come when social networking encompasses immersive VR technology. At its foundation, social VR allows two geographically separated people to communicate as if they were face to face. They can make eye contact and can manipulate virtual objects that they both can see. Current VR technology is in its inception since headsets are not yet able to track exactly, where eyes are pointed, by instead looking at the person to whom one is talking.

Moreover, current state-of-the-art VR technology is unable to read detailed facial expressions and senses (Masek, 2017).

Finally, and perhaps most importantly, most powerful VR prototypes are wired with cables because the amount of transmitted high-resolution video at high frame rates simply cannot be done using today's wireless technology (4G / LTE), let alone the fact that a perfect user interface is still in progress. These shortcomings have started efforts to make social VR happen soon (Shafi *et al.*, 2017).

Being connected has become a defining feature of the modern economy and a significant trend of the 21st century. Cisco forecasts that by 2023, nearly two-thirds of the global population will have Internet access, and the number of devices connected to networks will be more than three times the global population (Cisco, 2020). However, current internet speeds cannot take us that far, and would severely restrict economic development. To unlock a digital data-driven economy, the UK Government has set an ambitious agenda for building world-digital infrastructure (UK Government, 2017). The fifth-generation technology standard for wireless cellular networks, or 5G for short, is the next generation of wireless cellular network or mobile network, which is capable of ultra-fast data speeds, and low latency, and has been began deployment worldwide in 2019 (DCMS, 2017). Communication networks are generally composed of three key parts, core network, bearer network, and radio access network. Compared with early communication networks, 5G networks will require more antennas, greater bandwidth and higher base station density (Alsharif and Nordin, 2017).

According to Metcalfe's law, the value of a network is equal to the square of the number of nodes in the network, and the value of the network is proportional to the square of the number of connected users (Cheng *et al.*, 2022). Therefore, with respect to social impacts,

5G is not simply 4G plus 1G, but will be more revolutionary and of higher value. It will not only provide infrastructure support for the deep integration of cross-domain, all-round, and multi-level industries, but also fully release the magnification, superposition, and multiplication effects of digital applications on economic and social development. However, the total power consumption of a single 5G base station is about four times that of a single 4G base station and considering the high density the overall power consumption of 5G networks may be 12 times that of 4G networks (Chih-Lin *et al.*, 2020). Such energy consumption cannot be tolerated because it will cause corresponding environmental and economic problems. The construction of a new generation of wireless cellular networks is also costly, that often exceed billions of pounds. The technical complexity of 5G makes its implementation cost even higher. This also implies that upgrading the existing network to 5G will not be a one-off action, but a step-by-step evolutionary process, from a socio-technical perspective. The transition from 4G to 5G is not only a technological change, but also a competition for deployment and operations management. Countries who fail to adapt will likely lose first-mover advantage, while Mobile Network Operators (MNOs) who fail to adapt will likely lose market share.

2.2.4 D2D communication

D2D communication is one of the enabling technologies in 5G networks; it is a communication network in which User Equipment (UEs) in proximity communicate with each other without going through the base station (Alquhali *et al.*, 2020, Ansari *et al.*, 2018 and Melki, 2017). One of the main benefits of D2D communication is the short signal traversal path which results in an ultra-low latency in communication (Kar and Sanyal, 2017). It allows local data services (information sharing, data and computation offloading), coverage extension, and IoT. D2D helps greatly in fulfilling the requirement of 5G technology. It is expected to give a significant improvement in the utilization of

communication resources, energy productivity and in general, throughput, which are all significant interests of 5G networks (Alquhali *et al.*, 2020). The device-centric nature of the emerging 5G applications is expected to enable the smart device in proximity to transmit data directly without the need to communicate with the Base Station (BS) for sharing the relevant content.

Today, the number of hand-held devices is drastically increasing, with a rising demand for higher data rate applications. In order to meet the needs of the next generation applications, the present data rates need a refinement. The fifth generation (5G) networks are expected and will have to fulfill these rising demands. A competent technology of the next generation networks (NGNs) is Device-to-Device (D2D) Communication, which is expected to play an indispensable role in the approaching era of wireless communication. The use of D2D communication did not gain much importance in the previous generations of wireless communication, but in 5G networks, it is expected to be a vital part. With the introduction of device-to-device (D2D) communication, direct transmission between devices is possible. This is expected to improve the reliability of the link between the devices, enhance spectral efficiency and system capacity (Chai *et al.*, 2013), with reduced latency within the networks. Such a technique is essential for fulfilling the main goals of the mobile network operators (MNOs).

D2D communication allows communication between two devices, without the participation of the Base Station (BS), or the evolved NodeB (eNB). Proximate devices can directly communicate with each other by establishing direct links. Due to the small distance between the D2D users, it supports power saving within the network, which is not possible in case of conventional cellular communication. It promises improvement in energy efficiency, throughput and delay. It has the potential to effectively offload

traffic from the network core. Hence, it is a very flexible technique of communication, within the cellular networks.

A network scenario, supporting D2D communication along with some general use cases is depicted in Figure 2.1.

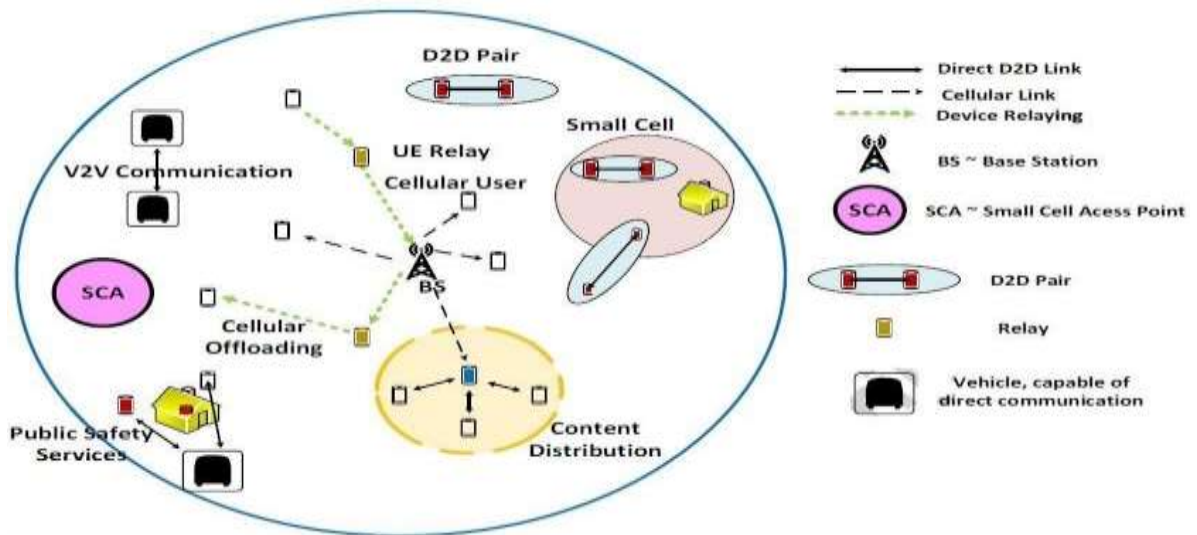


Figure 2.1: A D2D enabled network scenario (Gandotra and Jha, 2016)

Despite the numerous benefits offered by device-to-device (D2D) communication, several concerns are involved with its implementation. When sharing the same resources, interference between the cellular users and D2D users need to be controlled. For this, numerous interference management algorithms have been proposed in literature. Other concerns include peer discovery and mode selection, power control for the devices, radio resource allocation and security of the communication.

The two-tier cellular network architecture is advantageous over the conventional cellular architecture. The benefits offered are as follows:

- i. **One hop communication:** The devices can communicate with each other through a single hop. Lesser resources are, therefore, required for the communication, resulting in an efficient utilization of the spectrum. Since proximity users directly communicate with each other in D2D communication, latency is greatly reduced. These

are desirable aspects in a cellular network. The mobile network operators are also benefitted by these aspects of D2D communication.

ii. Spectrum Reusability: With D2D communication in cellular networks, same spectrum is shared by the D2D users as well as the cellular users. This supports spectrum reusability, thereby improving the spectrum reuse ratio.

iii. Optimization of Power Levels: Since D2D links exist between proximate devices, over a small distance, transmission power is less. This enhances the battery life of the devices. As a result, higher energy efficiency can be achieved with D2D communication in cellular networks.

iv. Improved Coverage Area: D2D communication is possible with relays. This supports communication over greater ranges, thus increasing the overall coverage area.

Despite the number of advantages that are offered by D2D communication over the conventional cellular communication, some limitations exist, like the possibility of use of D2D communication within the cellular systems. Feasibility of D2D communication is determined by the distance restriction. Another concern is the interference, which may be between the users of the same tier or different tiers. In cases of base-station assisted D2D communication, the BS acts as a central controlling entity and can overcome interference problem to some extent. The base station (BS) manages spectrum allocation and aids in avoiding interference among the devices.

2.3 Key Challenges in D2D Communication

Device to device (D2D) communication may use the licensed spectrum (inband) or the unlicensed spectrum (outband) for direct link formation. Inband D2D communication is categorized as underlay and overlay. Underlay D2D communication allows set up of direct links and cellular links in the cellular spectrum. In overlay D2D, on the other hand,

a dedicated portion of the available spectrum is used for Device-to-Device (D2D) communication, with rest of the spectrum used for cellular communication. As out band D2D communication exploits the unlicensed spectrum for the formation of direct links, it is categorized as autonomous and controlled (Asadi *et al.*, 2014). When controlled, the radio interfaces in D2D are managed by the eNB, while in autonomous, these are coordinated by the user equipment (UEs) themselves. The categorization of D2D communication has been depicted in Figure 2.2.

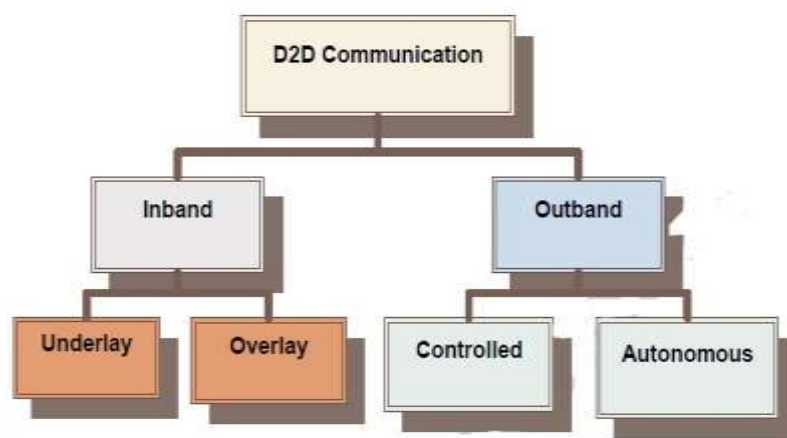


Figure 2.2: Categorization of D2D communication (Gandotra and Jha, 2016)

To utilize the limited available spectrum in the most efficient manner, one must know where to use which category of D2D communication. For implementing D2D communication in cellular networks, a number of key issues need to be efficiently addressed to obtain complete advantage of Device to Device (D2D) communication.

Some of these are discussed in the following sub-sections.

2.3.1 Peer discovery

Since D2D communication is gaining popularity, identifying efficient means of discovering proximate users has become necessary. The process of peer discovery should be efficient, so that D2D links are discovered and established quickly. It is also important for ensuring optimum throughput, efficiency and resource allocation within the system.

Setting up of direct links requires devices to discover each other first. Once discovered, direct links are set up, and then occurs transmission over those links. Researchers are working on different approaches for device discovery. In Lee *et al.*, (2016), spatial correlation of wireless channels is considered for low power peer discovery. The simulation results show that peers can be discovered with very low power consumption. It provides a very accurate method of peer discovery. Peer discovery techniques can be either restricted discovery or open discovery. In case of restricted discovery, the UEs cannot be detected without their prior explicit permission, thus maintains user privacy. In the case of open discovery, UEs can be detected during the duration for which they lie in proximity of other UEs. From the perspective of the network, device discovery can be controlled by the base-station either tightly or lightly (Fodor *et al.*, 2011).

2.3.2 Security

Providing efficient security is a major issue in D2D communication. The D2D communication network is prone to many security risks because of the routing of user data through other users' devices. This data can be hacked, which would breach privacy and confidentiality. Since D2D communication could be vulnerable to malicious attacks (for example, masquerading, eavesdropping, man-in-the-middle attack etc.), enhanced authentication and key agreement mechanisms are required to secure D2D communication in cellular networks. The security of devices can be ensured if closed access is applied to devices. In closed access, a device has a list of certain reliable devices, like the users in the close vicinity or office, with whom one is familiar, otherwise the users that have been legitimated through a reliable party like an association, can unswervingly communicate with each other, sustaining a level of discretion, whereas the devices not on this list need to use the macro cell level to communicate with it. Instead of this, in open access, each device can turn in to relay for other devices deprived of any

limits. Meanwhile, in such an instance security is an open research problem. Interference exploitation can be used as an aid to provide secret communication in D2D communication (Ma *et al.*, 2015).

Prior to the acceptance and implementation of the D2D technique in cellular networks, security needs to be well addressed. The channels are vulnerable to several security attacks like eavesdropping, message modification, and node impersonation. To prevent these, cryptographic solutions can be used to encrypt the information before transmission. The security schemes provided by the cellular operators can be used by the D2D users if they are under their coverage, but users outside the coverage of the operators can't be secured. In this case, security signals may be passed on through relays, but relays are highly susceptible to malicious attacks, like eavesdropping attack, free riding attack, denial of service attack (Osanaiye *et al.*, 2016). Thus, designing security schemes for D2D communication is an important challenge to be addressed.

2.3.3 Interference

Interference is an undesired signal picked up by neighbouring receivers which have a mathematical relationship with signal-to-interference-plus-noise ratio (SINR), throughput, and transmit power, as expressed below:

$$Interference \propto transmit\ Power \tag{2.1}$$

$$Interference \propto \frac{1}{throughput} \tag{2.2}$$

$$Interference \propto \frac{1}{SINR} \tag{2.3}$$

Therefore;

$$Interference \propto \frac{transmit\ power}{SINR * throughput} \tag{2.4}$$

Due to the introduction of D2D communication to the cellular network, the cellular architecture changes and now includes two tiers (Tehrani *et al.*, 2014). The first tier is the conventional macrocell layer, which involves the communication between eNB and device. The new tier, called the device tier involves D2D communication. Thus, such system is called two-tier architecture. The device tier is an unplanned and random distribution of D2D user equipment (DUE). The new architecture has significant improvement in terms of throughput, coverage, and end to end latency if designed carefully (Tehrani *et al.*, 2014). However, it introduces several technical challenges and issues for both DUE and cellular user equipment (CUE). Among these challenges, interference management between CUE and DUEs becomes one of the most critical issues for D2D communication in sharing mode; where the same radio resources are used for both cellular and D2D communication (Noura and Nordin 2016).

Enabling D2D links within a cellular network poses a big threat of interference to the cellular links in the network. D2D links can cause interference between cellular users and D2D users, resulting in cross-tier and co-tier interference as discussed in the following sections.

A general scenario of interference in a D2D-enabled cellular network is depicted in Figure 2.3:

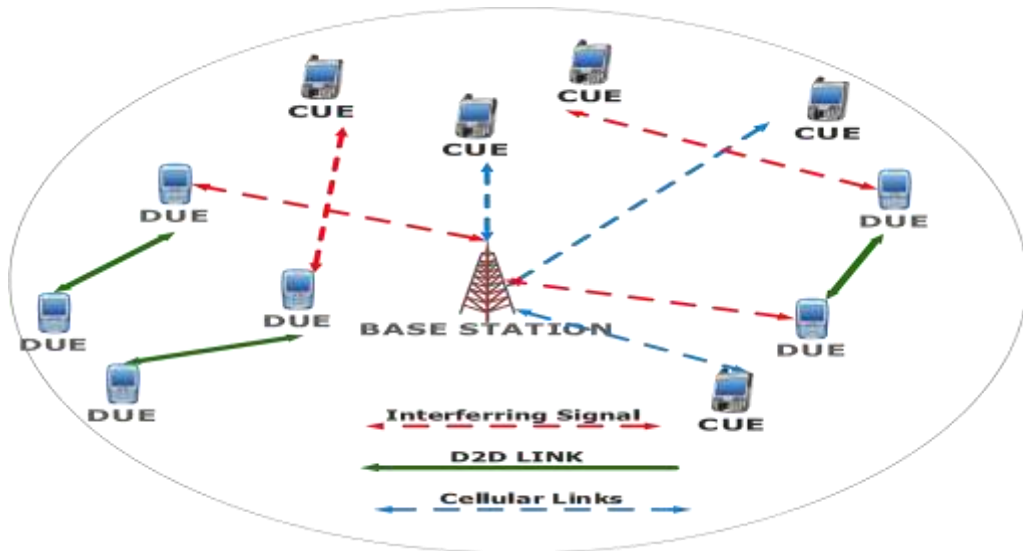


Figure 2.3: An interference scenario in a D2D-enabled cellular network.

2.3.3.1 Co-tier interference

This type of interference is produced between network elements which belong to the same tier in the network. In the case of D2D enabled cellular network, co-tier interference occurs between a D2D user and another D2D user in the same tier. The D2D users causing interference to each other are immediate neighbouring D2D users, since they are located near each other. To set up a direct link between D2D users, the signal to interference plus noise ratio (SINR) value must be higher than a predefined threshold parameter. Otherwise, if the DUE SINR falls below the defined threshold parameter due to co-tier interference, a communication link cannot be established (Noura and Nordin, 2016).

In OFDMA systems, the co-tier interference is caused when the same set of resource blocks are allocated to multiple DUEs. In this case the interference is always generated from the D2D transmitter to D2D receiver in a D2D pairs which are assigned the same cellular resources regardless of the resource reuse direction (UL/DL). Furthermore, the co-tier interference incurred at a D2D receiver from neighbouring D2D transmitter can

be mitigated through proper user pairing and frequency assignment techniques (Noura and Nordin 2016).

2.3.3.2 *Cross-tier interference*

This type of interference is produced between network elements which belong to different tiers, i.e., interference between DUE and CUE. The cross-tier interference could be between (i) a CUE and a DUE, and between (ii) a CUE and multiple DUEs. This interference scenario occurs when the resource blocks allocated to a cellular user are reused by one (or more) D2D users. In this type of interference, the aggressor (or the source of interference) and the victim of interference are different depending on the resource reuse direction (UL/DL) (Noura and Nordin 2016).

Case 1: Interference from D2D to cellular network: When D2D links use the same frequency resources as CUEs in the uplink direction, D2D transmitter is the aggressor interfering with eNB and also the cellular uplink user is the aggressor interfering with D2D receiver, as seen in Figure 2.4 (a).

Case 2: Interference from cellular network to D2D user: On the other hand, when downlink resources of licensed band are reused in D2D links, eNB is the aggressor interfering with D2D receivers and D2D transmitter is the aggressor interfering with cellular downlink user (Noura and Nordin 2016), as seen in Figure 2.4 (b).

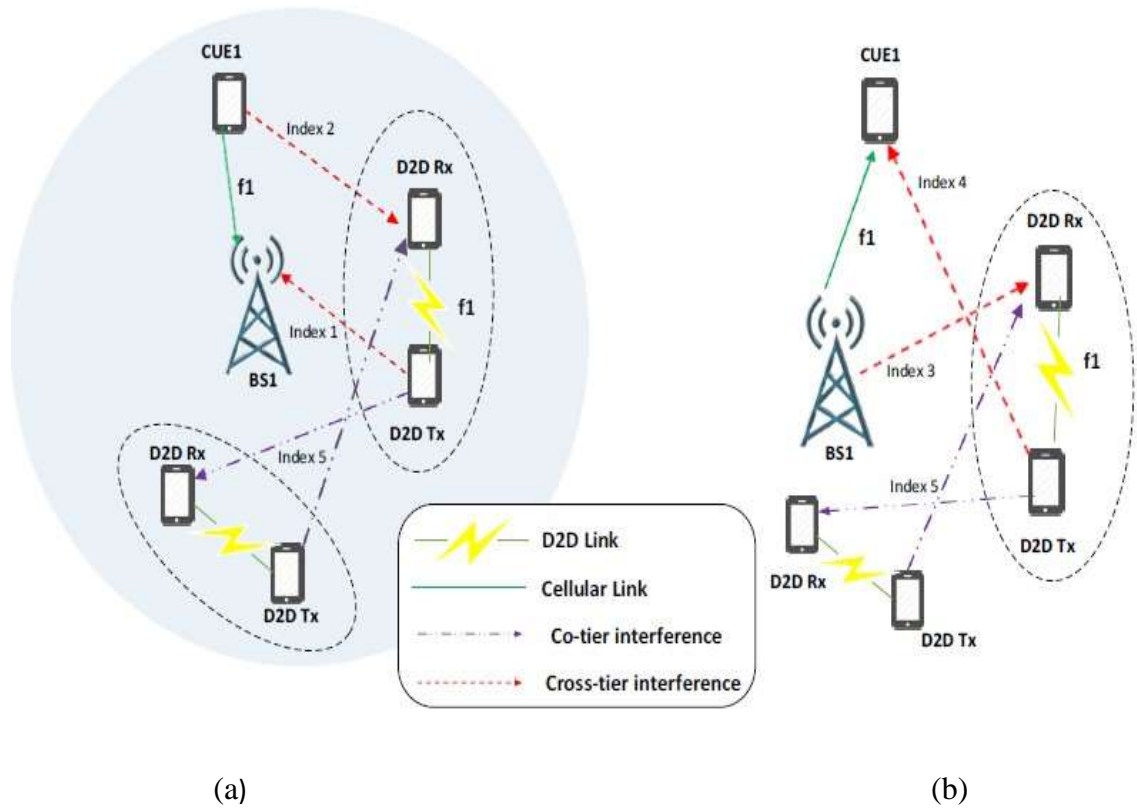


Figure 2.4: Interference scenarios for different reuse resources (Noura and Nordin, 2016)

2.4 Interference Mitigation Techniques

Interference can be mitigated through one or a combination of several techniques. These include, mode selection, optimum resource allocation, power control, and bandwidth allocation (Kamruzzaman *et al.*, 2019). These techniques are briefly discussed below.

2.4.1 Mode selection

Selecting transmission mode (Cellular or D2D mode) is one of the difficult tasks in communication for potential D2D users after discovery. Although they may be in proximity to each other, it might not be optimal for them to operate efficiently and effectively (Alquhali *et al.*, 2020 and Ansari *et al.*, 2018). Therefore, mode selection enables the BS and the D2D users to decide which communication mode to operate in, based on some distinguishing criteria like interference among D2D pairs, distance between D2D pairs, and Cellular users. The quality of the channel condition and

Signal-to-interference plus noise ratio (SINR) is one of the most common selection metrics. Predefined SINR threshold is often considered as the mode selection criteria for D2D communication. Therefore, proper mode selection determines the performance of D2D communication (Librino and Quer, 2018).

It is possible to avoid the effect of cross-tier interference between the cellular and D2D user or co-tier interference among DUE with a proper mode selection (MS) algorithm. Although D2D candidates may be in range for direct communication with each other, it may not be optimal for them to work in D2D mode because of the interference imposed on DUE or CUE. In this sense, D2D MS algorithm decides on the optimal communication mode so that the overall network throughput is maximized and the QoS requirements of the communication links are satisfied. Each of the communication modes affects the amount of interference between cellular users and D2D users or between multiple DUEs (Chen *et al.*, 2018).

2.4.2 Resource allocation

After device discovery, availability of resources is important for enabling communication over the direct links. Radio resource allocation is thus important for enhancing the spectral efficiency of D2D communication. Resource allocation is a crucial part in D2D communication as licensed spectrum blocks are needed to be allocated for D2D transmissions efficiently. However, in such types of communications, sharing of resource blocks with the cellular users generates substantial cross-tier interferences. Investigation shows that the existing interference mitigation techniques are broadly categorized as centralized, distributed and semi-distributed (Barik *et al.*, 2020).

In the centralized method, the interference between D2D and cellular users is completely managed by the eNB. This central entity combines information about each user in the

network, such as the quality of the channel, Channel State Information (CSI), and interference level. Additionally, it selects the channels that must be allocated to each user in the network with the appropriate format and power level. The central entity assigns the resources to each CUE or DUE depending on the collected information. The major issue of centralized methods is the massive amount of signalling necessary to exchange CSI and feedback. Furthermore, because the process is conducted by a single entity, which must handle massive amounts of data, the complexity of interference management increases significantly with the users' number in the network. Therefore, centralized methods are appropriate only for limited scale D2D networks (Alzubaidi *et al.*, 2022).

In the distributed method, the interference management process does not need a central entity and is conducted independently by DUEs. Due to finite CSI and feedback, the distributed method minimizes control and computational cost. Thus, due to the difficulty of interference coordination, this method is better suited for large-scale D2D networks (Alzubaidi *et al.*, 2022).

Although both centralized and distributed methods have benefits and drawbacks, tradeoffs can be made between them. Interference management strategies of this type are referred to as semi-distributed or hybrid. Various levels of participation can be established in the strategies of semi-distributed interference management. Such strategies can be appropriate for relatively massive networks (Alzubaidi *et al.*, 2022).

2.4.3 Power control

Power Control is the most popular interference avoidance technique. Adjusting the transmit power of the D2D transmitter while maintaining the minimum SINR requirement of the cellular communication, interference can be avoided or reduced. This

constraint can be set up by the eNB. However, this simple power control scheme may lead to under-utilization of D2D communications. The positioning of the D2D pairs, CUEs, and eNBs plays a vital role in the power control technique. If the D2D pairs are in proximity but they are far away from the eNB or cellular user equipment (CUE), D2D communication performance will not be affected much by reducing the power, but if the reverse is the case, reducing the power may completely stop the D2D communication to take place. So, it is certain that the conventional power control technique itself may not contribute highly to interference management (Koushik and Shahedur, 2021).

Setting the optimum transmission power for reusing the frequency is an area of interest for research. It is particularly important in case of uplink transmissions because of the near-far effect and co-channel interference. Once a maximum power level is allocated to the D2D users, then the Quality of Service (QoS) of the cellular users is maintained in the network. Controlling power effectively mitigates interference in cellular networks. A limit is set upon the power level of the D2D transmitter and the CUE counterparts, in order to maximize the overall system throughput (Nasser *et al.*, 2019).

2.4.4 Bandwidth allocation

The easiest way to coordinate the cross-tier interference between the cellular and device tier is to use bandwidth allocation, otherwise known as spectrum splitting, which will simplify the interference between DUEs and CUEs (Cross-tier interference). Cho *et al.* (2013) used spectrum splitting, where it is suggested to divide the spectrum band into two parts, as shown in Figure 2.5. One part would be dedicated to CUEs and the other part would be assigned to DUEs. This would only leave the co-tier interference unsolved. However, dedicated channels for D2D communication will lead to inefficient use of the available

channels depending on the number of D2D terminals and the proportion of available spectrum for them.

Effective resource allocation in heterogeneous networks is required to balance the amount of bandwidth assigned to DUEs and the amount of bandwidth to be allocated to CUEs. A large amount of bandwidth given to CUEs will enhance the throughput CUEs; nevertheless, this improvement is achieved at the expense of DUEs. Similarly, allocating a large amount bandwidth to DUEs increases the throughput of DUEs but the throughput of CUEs will decrease (Shami *et al.* 2019).

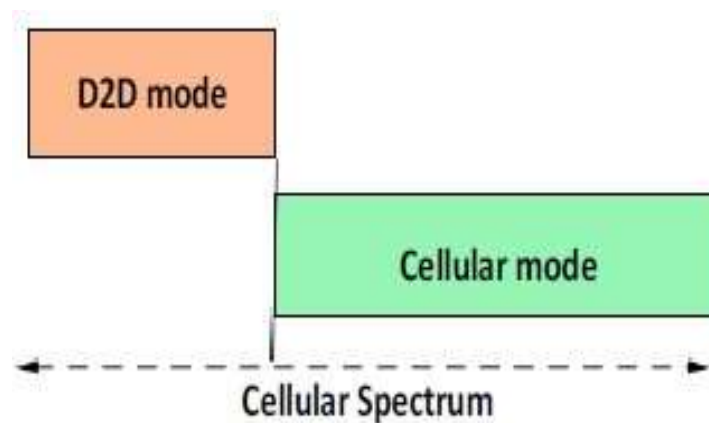


Figure 2.5: Bandwidth allocation (Noura and Nordin, 2016)

2.5 Review of Related Works on Interference Mitigation in D2D Networks

The introduction of enhanced technologies introduced by 3GPP standardization made interference research area to become significant in wireless network deployment, especially in Long Term Evolution-Advanced (LTE-A) systems (Salihu *et al.* 2014).

Therefore, as demand for higher data rate and QoS continue to increase, which brought about the release of 5G, interference between UEs would also continue to rise.

The most common and major impairment of D2D communication network is the interference caused by the DUEs to the CUEs, and vice-versa (Ansari *et al.*, 2018).

Interference mitigation remains a major challenge in the implementation of multiple access technologies to realize 5G mobile networks (Hassan *et al.* 2018). DUEs will suffer from either intracellular or intercellular interference depending on the network operational mode (uplink or downlink) from which the D2D is operating (Adnan and Zuriati, 2020). Therefore, many researchers have identified this issue and proposed different solutions to tackle it.

Jänis *et al.* (2009) introduced Multiple-input and Multiple-output (MIMO) transmission schemes for interference avoidance, resulting in a great enhancement of D2D SINR. Due to interfering signals, the received signal contains three components - Desired signal, Outside interference signal, and D2D interference signal. Interference at the receiver must be minimized so that a higher value of SINR is achieved. This can be achieved by Modulation and Coding Scheme (MCS), which supports error-free reception of information. The D2D interference signals can be mitigated, but interference from outside sources is hard to avoid.

Simple mode selection (MS) can be performed based on the path loss, received signal strength over the D2D link or the distance between the terminals. However, these schemes do not reflect exact channel quality or interference issues. MS has been performed based on the channel quality, Jänis *et al.* (2009) considers sum rate of the connection between D2D pair and of the cellular connection between BS and CUE as the MS criterion. Four communication modes are defined as: (i) Downlink resource sharing, (ii) Uplink resource sharing, (iii) separate resource sharing and (iv) cellular mode sharing. The mode with the maximum sum rate is selected.

A more sophisticated MS strategy is proposed by Doppler *et al.* (2010), which takes the link quality of both D2D and cellular users, the interference situation (cross-tier

interference from DUE to cellular network) for each possible mode and the load situation of the cell into account for a multi-cell scenario. The MS strategy proposed in this work is as follows. Initially, the D2D terminals send probing signals to each other and estimate the received signal powers. Then, the D2D terminal estimate interference plus noise power in both uplink and downlink. Next, the obtained information is sent to the eNB, when it can decide about the amount of resources it would allocate to the DUE in UL/DL based on cellular load as well as the maximum transmit power of DUE for the different direct modes. Then, eNB estimates the expected SINR for each communication mode and the expected throughput based on SINR and available amount of resources for each communication mode. Finally, the communication mode with the highest throughput is selected. The result of this study provides an improvement of 50% in sum-rate with limited interference to the cellular network. However, Power Control (PC) was not considered in this scheme and it was assumed that the BS has all the Channel State Information (CSI) available to choose the best resource sharing mode.

Xing and Hakola (2010) used the joint consideration of mode selection, resource scheduling, link adaption, and power control to tackle co-channel interference. Although the work provided a detailed description of system parameters and simulation results, there were too many techniques and parameters involved in the scheme.

Wang *et al.* (2012) proposed a novel interference coordination scheme for improving system throughput and efficient resource utilization in a multicast D2D network. The work, however, was inconclusive on the attainment of spectral efficiency in the system following the application of the scheme.

In a similar work, Zhou *et al.* (2015) takes into consideration a D2D underlaying communication network for interference cancellation, along with the transmission

powers for maximizing the utility of the network. Although significant gains were enjoyed by the users in terms of spectral efficiency, the problem of cross-tier interference inherent with underlying communication was, however, not addressed.

Also, Guo, *et al.* (2015) concentrated on managing interference between D2D users and cellular users by discussing the range of an Interference Suppression Area (ISA) which classifies the strength of the interference between the cellular and D2D users and influences the system performance. Adequate adjustment of the range of ISA can help achieve optimal system performance but adopted methodology and mathematical models were cumbersome and difficult to comprehend.

In a different approach, Mumtaz *et al.* (2014) proposed a novel Resource Allocation scheme which mitigates the interference between D2D and CUEs. The RA schemes increased the throughput and reduced the overall energy cost of the system. Simulation results also show that the proposed schemes obtained higher throughput and saved significant amount of energy when compared with other works. The method, however, did not consider the signalling overhead of the D2D system, and it was driven by a cumbersome set of mathematical equations and model.

In their own approach, Lei *et al.* (2014) considered a dynamic MS procedure to limit the cross-tier interference between cellular and D2D users. They proposed three routing modes - D2D, cellular and hybrid, for D2D communications underlying cellular networks. Although with a well-structured and detailed methodology, their scheme led to the emergence of too many communication modes (seven), leading to ambiguous results.

Hao *et al.* (2015) proposed a D2D pair forming and game theory to reduce interference and enhance the overall system capacity. Lindner *et al.* (2019) proposed a novel joint radio resource scheduling and allocation for D2D communication that utilizes two strategies from field of game hypothesis to mitigate interference. Simulation results were simple and clearly presented, but the scheme considers instantaneous channel conditions, and their algorithm failed to differentiate between CUEs and DUEs at some points during the simulations.

In Li *et al.* (2016), a non-uniform user model that depends on the distance to the serving base station was considered. The users in the macro and small cells may have different density distribution models. The work focused more on user density distribution rather than Quality of Service (QoS) and system performance indicators.

Soft frequency reuse (SFR) has been identified as an effective frequency planning scheme that has been greatly employed to help reduce interference in cellular network (Li *et al.*, 2016, Adejo *et al.*, 2017a and Li, 2019). SFR also improve spectral efficiency (Iskandar and Nuraini 2016, and Adejo, *et al.*, 2017b), it increases system capacity (Qian *et al.*, 2012) and it improves system throughput and fairness performance (Attia *et al.*, 2017).

Gupta *et al.* (2016) proposed a resource allocation for D2D link in Fractional Frequency Reuse (FFR) and Soft Frequency Reuse (SFR) network. The authors proposed three frequency allocation schemes namely: Fractional Frequency Allocation (FFA) when macro base station uses FFR and Soft Frequency Allocation (SFA) when macro base station uses SFR to reduce interference of the D2D link at same time ensure that the quality of service of the cellular network is highly secured. Although results were clear,

the high number of schemes led to too many equations and ambiguous mathematical models.

Similarly, Ningombam *et al.* (2017) proposed a distance-based throughput enhancement strategies for D2D communication in a sectorized multicellular framework using FFR technique in order to improve system performance by mitigating interference. Results showed improved spectral efficiency and throughput but assumed that each section of the cell consists of at least one D2D pair which has the ability to reuse channel resource of cellular link, and this is not always the case.

In a related work, Ningombam and Shin (2019) proposed a resource sharing optimization where a multicast D2D shares resources with cellular network in a non-orthogonal manner in order to mitigate interference. Although simulation results were clearly presented, the methodologies employed were too complex, and the Metaheuristic-tabu Search Algorithm is based on unrealistic assumptions.

Hassan *et al.* (2017) tackled interference by using two-phase resource allocation algorithms (Fair and restricted); in the fair the DUEs have the flexibility to share the base station resources of one of the cellular networks. In the restricted, D2D are blocked from sharing any cellular resources in order to reduce interference in the system. The methodology is however, inimical to the proliferation of the desired D2D links for the accommodation of the growing UEs.

From the reviewed works, it is, however, clear that resource management plays an important role in minimizing interference and when resources are properly allocated in the system, interference is reduced. More so, the spatial distribution of users in the network is also critical in the mitigation of interference in the system.

Zhai *et al.* (2017) proposed a unified resource management scheme to minimize the total transmit power of all UEs by jointly optimizing mode selection, resource allocation, and power control, to tackle the incidence of interference and power consumption by UEs arising from complicated spectrum sharing pattern. The work achieved an enhancement of energy efficiency and network capacity, although it was not validated through comparison with other schemes.

Yang *et al.* (2017) considered the effects of both the interference caused by the generic D2D transmitter to others, and the interference caused by all others to the generic D2D receiver. The work achieves higher energy efficiency compared with the blind power control scheme, although increasing the energy means increasing the interference and hence decreasing the spectrum efficiency.

Swetha and Murthy (2017) proposed the resource management scheme in overlay D2D network where bandwidth is allocated to D2D overlay devices by the base station, based on the bandwidth resource blocks earmarked for D2D mode. The challenge is the maximization of the reserved bandwidth if not optimally utilized. When the resource block assigned for D2D mode is exhausted the base station assigns subsequent UE to CUE mode. Both line of sight (LOS) and non-line of sight (NLOS) transmission pathlosses were computed using equations (2.5) and (2.6) respectively (Swetha and Murthy, 2017).

$$P_{LOS} = 65 + 21\log_{10}(d) \quad (2.5)$$

$$P_{NLOS} = 71.1 + 34\log_{10}(d) \quad (2.6)$$

The static allocation of bandwidth to communication tiers without recourse to the number of UEs per tier was a limitation of this work. This lead to wastage of scarce spectral resources, leading to degraded data rates.

Li *et al.* (2018) considered a relay mode for D2D UEs. Additionally, they proposed an evolutionary game-based approach for D2D mode selection in order to address a potentially large population of DUEs. The evolutionary game was formulated with a utility function that takes into account both the achievable throughput of DUEs and the radio resource consumption. The work yielded a higher number of D2D connections than the baseline schemes, but it did not consider other D2D communication modes (direct reuse and relay) in its performance evaluation, only DUEs in cellular mode scenarios were evaluated.

Li (2019) proposed SFR for both the licensed and unlicensed band. Using unlicensed band that considers resource allocation based on SFR gives a good design, but portends a severe security risk for the UEs, especially when operating in the unlicensed band.

Song *et al.* (2019) adopted an interference limited area control method; this constraint is used to reduce interference between D2D communication and cellular network. The authors proposed an improved Hungarian algorithm to allocate channels to the joint uplink and downlink channels. Explicit simulation results were obtained, but a major flaw of the scheme was the unrealistic assumption that each channel (either uplink or downlink) could be reused by at most one D2D and each D2D link is allowed to reuse not more than one channel.

Hassan and Gao (2019) proposed an Active Power Control (APC) technique, which not only reduces cross-tier interference in a Macro User Equipment (MUE), generated from the downlink transmission power of an inadequately deployed femtocell, but also reduces unnecessary power consumption to achieve a green femtocell network. The work, however assumed all UEs were static throughout their simulation. This is very unrealistic in a mobile communication network.

Gao *et al.* (2019) proposed an energy-efficient resource block (RB) assignment and power control strategy for underlay device-to-device (D2D) communication in multi-cell networks, where more than one D2D pair is allowed to share the same RBs with cellular user equipments (CUEs). Although there was significant reduction in energy loss, there was inconsistency in network energy efficiency, as it first increases and then decreases when the transmit power increases.

Adejo *et al.* (2020) employed SFR to adequately model an interference frame considering the overlapping bandwidth allocation. This requires a BS to be tuned repeatedly to achieve the desired network performance, thus leading to the disadvantage of a high signalling overhead.

Authors in Rana *et al.* (2021) proposed two D2D interference mitigation scheme referred to as power control scheme 1 (PCS1) and power control scheme 2 (PCS2) which both centred on the difference between computed SINR and target SINR to basically mitigate interference caused by number of D2D pairs in a D2D cellular communication network. The difference between the two Power Control Schemes is in the scaling factors used. In PCS1 a scaling factor of 2 dBm was used and that of PCS2 used power scaling factor of 3 dBm. Equation (2.7) was used in computing the path loss between different communication paths; from D2D Transmitter (D2DT) and macro base station during uplink transmission or from macro base station to D2D Receiver (D2DR) during downlink transmission (Rana *et al.*, 2021).

$$PL_{diff\text{layer}}(dB) = 128.1 + 37.6 * \log d(km) \quad (2.7)$$

where $PL_{diff\text{layer}}(dB)$ is path loss either base station to D2DR or from D2DT to CUE, d is the distance between transmitter and receiver in kilometres (km). Equation 2.8 was used to measure the path loss between D2D communication path.

$$PL \text{ (dB)} = 148 + 40 * \log d(km) \quad (2.8)$$

SINR was computed using (2.9) and compared with the target SINR value

$$\gamma_B = \frac{P_x G_x}{\sum_{y \neq x} P_y G_y + N_o} \quad (2.9)$$

where γ_B is receiver's SINR, P_x is desired transmit power of D2DT, G_x is channel gain when considering the desired transmitter and receiver. P_y is the transmit power of aggressor, G_y is the channel gain of aggressor, N_o is noise and w is an SINR factor that is either 0 when D2D and CUE do not use the same resources otherwise it is 1.

When γ_B is greater than target SINR, the next transmit power will be less than the present power by power scaling power within the range of accepted minimum and maximum transmit power. When γ_B is less than the target SINR, the next transmit power will be greater than the present power by same power scaling factor. And when γ_B is equal to the target SINR, the next transmit power will be the same with the present transmit power.

Although the power control schemes were consistent in their output, they, however, utilized very high power for their operation. This lead to increased noise and interference. Energy consumption by the UEs was also high, and the pathloss model used also lead to high losses when compared with other works. Table 2.1 is a Meta Analysis table of reviewed related works.

Table 2.1 Meta Analysis Table of Related Works

Title/Author/Year	Methodology	Strengths	Weaknesses
Mode selection for device-to-device communication underlying an LTE-advanced network, Doppler <i>et al.</i> (2010)	This work considered the link quality of both D2D and cellular users, the Interference situation (cross-tier interference from DUE to cellular network) for each possible mode and the load situation of the cell into account for a multi-cell scenario.	The result of this study provides an improvement of 50% in sumrate with limited interference to the cellular network.	Power control was not considered in this scheme. It was assumed that the BS has all the CSI available to choose the best resource sharing mode.
The Investigation of Power Control Schemes for a Device-to-Device Communication integrated into OFDMA Cellular System, Xing and Hakola (2010).	The authors used the joint consideration of mode selection, resource scheduling, link adaptation and power control to tackle co channel interference	Presentation of detailed description of system parameters. Availability of detailed simulation results.	Too many techniques involved. Too many parameters to handle. Did not provide any solution for cross-tier interference
Resource sharing optimization for device-to-device communication underlying cellular networks, Yu <i>et al.</i> , (2011).	The system aims to optimize the throughput over the shared resources while fulfilling prioritized cellular service constraints, like interference.	The obtained numerical results show substantial gain from D2D communication handling local traffic.	Authors made too many assumptions, There was no consideration for Overlaying networks.

Title/Author/Year	Methodology	Strengths	Weaknesses
Dynamic Power Control Mechanism for Interference Coordination of Device-to-Device Communication in Cellular Networks, Gu <i>et al.</i> 2011.	Authors proposed a dynamic power control mechanism to reduce interference and improve performance of cellular systems.	Simulations results show that the proposed dynamic power control mechanism could improve performance of the entire communication systems.	The proposed mechanism excludes cellular communication UE with same resource, base station, and areas of adjacent cells from the coverage area of D2D communication UE. Proposed mechanism appeared too complex, with too many parameters.
Energy Efficient Interference-Aware Resource Allocation in LTE-D2D Communication, Mumtaz <i>et al.</i> 2014.	Authors proposed a novel Resource Allocation scheme, which mitigates the interference between D2D and CUEs.	The RA schemes increased the throughput and reduced the overall energy cost per bit of the system. when compared with the conventional methods, the simulation results show that the proposed schemes obtained higher throughput and saved significant amount of energy per bit.	The method did not take into account the signaling overhead of D2D system. Too many parameters to deal with. Method was mathematically cumbersome.
Queuing Models With Applications to Mode Selection in Device-to-Device Communications Underlying Cellular Networks, Lei <i>et al.</i> 2014.	Authors considered a dynamic MS procedure to limit the cross-tier interference between cellular and D2D users. They proposed three routing modes - D2D, cellular and hybrid, for D2D communications underlying cellular networks.		Too many communication modes resulted (seven) Overlaying scenarios were not considered. Method did not address co-tier interference challenges. There were many parameteres to handle. Cumbersome mathematical equations and models.

Title/Author/Year	Methodology	Strengths	Weaknesses
Interference Canceling Power Optimization for Device to Device Communication Zhou <i>et al.</i> 2015.	Authors considered D2D communication underlying cellular uplink communication when single stage interference cancellation receivers are available to improve local service. The interference cancelation configurations and transmission powers are jointly optimized in the network to maximize a network utility.	From simulation results, where sum rate or proportionally fair network utility was maximized, significant gains in the spectral efficiency enjoyed by users was observed.	There was no consideration for overlaying networks.
Distributed interference and energy-aware power control for ultra-dense D2D networks: A mean field game, Yang <i>et al.</i> , (2017).	The authors considered the effects of both the interference caused by the generic D2D transmitter to others, and the interference caused by all others to the generic D2D receiver.	Achieves higher energy efficiency compared with the blind power control scheme.	Increasing the energy means increasing the interference and decreases the spectrum efficiency

<p>Energy-saving resource management for D2D and cellular coexisting networks enhanced by hybrid multiple access technologies, Zhai <i>et al.</i> (2017).</p>	<p>The authors proposed a unified resource management scheme to minimize the total transmit power of all UEs by jointly optimizing mode selection, resource allocation, and power control, to tackle the incidence of interference and power consumption by UEs arising from complicated spectrum sharing pattern.</p>	<p>Enhancement of energy efficiency and network capacity.</p>	<p>Enhancement was not validated through comparison with other schemes</p>
---------------------------------------------------------------------------------------------------------------------------------------------------------------	------------------------------------------------------------------------------------------------------------------------------------------------------------------------------------------------------------------------------------------------------------------------------------------------------------------------	---------------------------------------------------------------	----------------------------------------------------------------------------

Title/Author/Year	Methodology	Strengths	Weaknesses
<p>Joint mode selection and interference management in Device-to-Device communications underlaid MIMO cellular networks, Chou <i>et al.</i> (2017).</p>	<p>The authors adopted the degrees-of-freedom (DoF) as the mode-selection criterion and exploited the linear interference alignment (IA) technique to tackle the effect of D2D mode selection on the network interference profile.</p>	<p>Better performance than in high SNR regime, low interference environment, large MIMO systems, and small-cell networks</p>	<p>No accomodation for large cell networks.</p>
<p>Selective Overlay Mode Operation for D2D communication in dense 5G cellular networks, Swetha and Murthy (2017)</p>	<p>The authors proposed a resource management scheme in overlay D2D network where bandwidth is statically allocated to D2D overlaying devices by the base station, based on the bandwidth resource blocks earmarked for D2D mode.</p>	<p>CUEs report higher data rates due to biased bandwidth allocation to the CUE tier.</p>	<p>The maximization of the allocated bandwidth is not optimal, leading to possible spectrum wastage. When the resource block assigned for D2D mode is exhausted, the base station assigns subsequent UE to CUE mode, even if they would communicate better in D2D mode.</p>

<p>A distributed mode selection approach based on evolutionary game for Device-to-Device communications, Li <i>et al.</i> (2018).</p>	<p>The authors considered a relay mode for D2D UEs. Additionally, they proposed an evolutionary game-based approach for D2D mode selection in order to address a potentially large population of D2D UEs. The evolutionary game was formulated with a utility function that takes into account both the achievable throughput of D2D UEs and the radio resource consumption.</p>	<p>Achieves higher number of D2D connections than the baseline schemes. Did not consider other D2D communication modes.</p>
---------------------------------------------------------------------------------------------------------------------------------------	----------------------------------------------------------------------------------------------------------------------------------------------------------------------------------------------------------------------------------------------------------------------------------------------------------------------------------------------------------------------------------	-----------------------------------------------------------------------------------------------------------------------------

Title/Author/Year	Methodology	Strengths	Weaknesses
Energy-efficient resource block assignment and power control for underlay Device-to-Device multicell networks, Gao <i>et al.</i> (2019).	This work proposed an energyefficient resource block (RB) assignment and power control strategy for underlay device-to-device (D2D) communication in multi-cell networks, where more than one D2D pair is allowed to share the same RBs with cellular user equipments (CUEs).	Reduction in energy loss.	Inconsistent network energy efficiency as it first increases and then decreases when the transmit power increases.

An Active Power Control Technique for Downlink Interference Management in a Two-Tier Macro-Femto Network. Hassan and Gao (2019)

The authors proposed an Active Power Control (APC) technique, which not only reduces cross-tier interference in a Macro User Equipment, generated from the downlink transmission power of an inadequately deployed femtocell, but also reduces unnecessary power consumption to achieve a green femtocell network.

Energy efficient approach.

and green

Unrealistic assumption that all UEs were static throughout their simulation, in a mobile communication network.

Interference Mitigation in D2D Communication Underlying Cellular Networks. Rana *et al.* (2021)

The authors proposed two D2D interference mitigation schemes referred to as power control scheme 1 (PCS1) and power control scheme 2 (PCS2) which both centred on the difference between computed SINR and target SINR to basically mitigate interference caused by number of D2D pairs in a D2D cellular communication network.

Algorithm yielded consistent outputs for both schemes.

Schemes were not energy efficient as they utilized very high power for their operation, leading to increased noise and interference. Energy consumption by the UEs was also high, and the pathloss model used also lead to high losses when compared with other works.

2.5.1 Summary of review of related works

From the review of related works, it is evident that a lot of work has been done towards the mitigation of interference in D2D enabled networks, using a wide variety of schemes ranging from mode selection, resource block assignment, soft frequency reuse, to power control, link adaptation, as well as a combination of two or more of the schemes. Some of the works yielded good results, but with complex or cumbersome methodologies as outlined in Table 2.1. Energy inefficiency, as well as ease of system manipulation (simplicity of system parameters) were partly or wholly lacking in various schemes. Being the primary users of the network, the cellular tier of the Macro-D2D network tended to receive greater priority in bandwidth allocation schemes, which was simply borne out of the assumption that more users would be operating in cellular mode, unfortunately this is not always the case. This assumption led to spectrum wastage, as well as the partial loss or complete non-realization of such benefits of D2D communication as coverage expansion (more connections within the network), energy conservation (especially from less pressure on the base station), reduced latency (improved response time), improved data rates (due to spectral efficiency), improved signal quality (due to higher SINR), as well as reduced interference within the network.

The development of the Mode Selection and Bandwidth Allocation Schemes (MS-BAS) in this work, would tackle the incidence of spectrum redundancy and wastage arising from the assumption that the primary users (CUEs) would always outnumber the secondary users (DUEs). This would consequently drive up SINR and throughput, thereby reducing interference according to equations (2.2) and (2.3). Additionally, the D2D Power Control Scheme (D2D-PCS) would ensure that minimal transmit power is used for each transmission, thereby mitigating interference according to equation (2.1).

CHAPTER THREE

3.0

RESEARCH METHODOLOGY

This chapter contains the methodologies employed towards the attainment of the objectives of the research, which includes details of the system model, system parameters, algorithms of the Cross-tier and Co-tier interference mitigation schemes, and their block diagrams, equations, flowcharts, and pseudocodes.

3.1 Research System Model

The research system model as shown in Figure 3.1 captures transmission in cellular and D2D communications. It gives an illustration of D2D communication between a D2D user equipment (DUE) and communication between a cellular user equipment (CUE) and its serving base station.

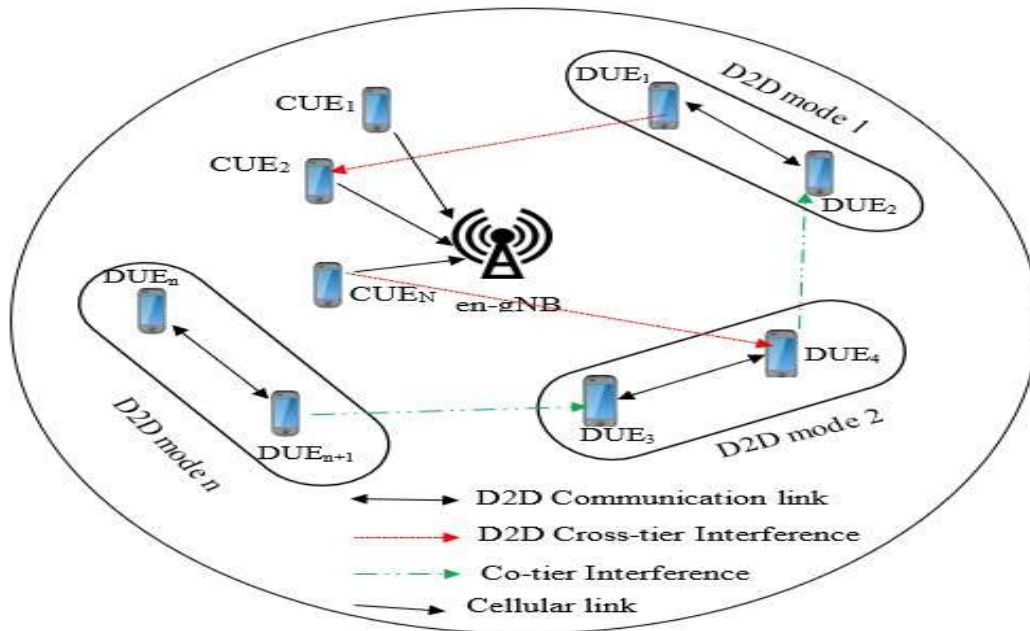


Figure 3.1: Research Network System Model

The simulation of the D2D communication schemes on MATLAB (see codes in Appendix B) was guided by the research system parameters in Table 3.1, where cellular user equipment were represented as $CUE_1, CUE_2 \dots CUE_N$; macrocell base station as $en - gNB$; and D2D

user equipment as $DUE_1, DUE_2, DUE_3, DUE_4 \dots DUE_n$. The system co-tier interference scenario where signal from neighbouring D2D pair is received as interference by nearby D2D pair and cross tier interference as a result of common bandwidth shared among macro-tier and D2D-tier network. Table 3.1 presents the system parameters sourced from referenced literatures (Swetha and Murthy, 2017), and (Rana *et al.*, 2021).

Table 3.1: System parameters

S/No.	Parameter	Value
1.	Minimum transmit power of UE (DUE and CUE)	0 dBm
2.	Maximum transmit power of UE (DUE and CUE)	23 dBm
3.	System bandwidth	60 MHz
4.	Carrier frequency	2.6 GHz
5.	Thermal noise density	-174 dBm/Hz
6.	Number of macrocells	1
7.	Number of D2D pairs	1 – 10
8.	Initial transmit power of CUE and DUE	20 dBm
9.	Target D2D distance	10m
10.	Target SINR for DUEs	0 db

3.2 Mode Selection and Bandwidth Allocation Scheme

The mode selection and bandwidth allocation schemes begin with the communication mode selection, which is determined based on received SINR and distance between transmitting UE and receiving UE, while the bandwidth allocation phase of the scheme is centred on the mode of UE communication, and the number of UEs in that mode. Being the primary users of the network, a greater priority is given to CUEs during bandwidth allocation; they receive a higher reserve of the bandwidth at 60%, while 30% is reserved for D2D communication. The number of UEs in D2D mode determines the allocation of the remainder 10% bandwidth. The block diagram of the mode selection and bandwidth allocation scheme is

presented in Figure 3.2, which shows the various components of the scheme and their relationship.

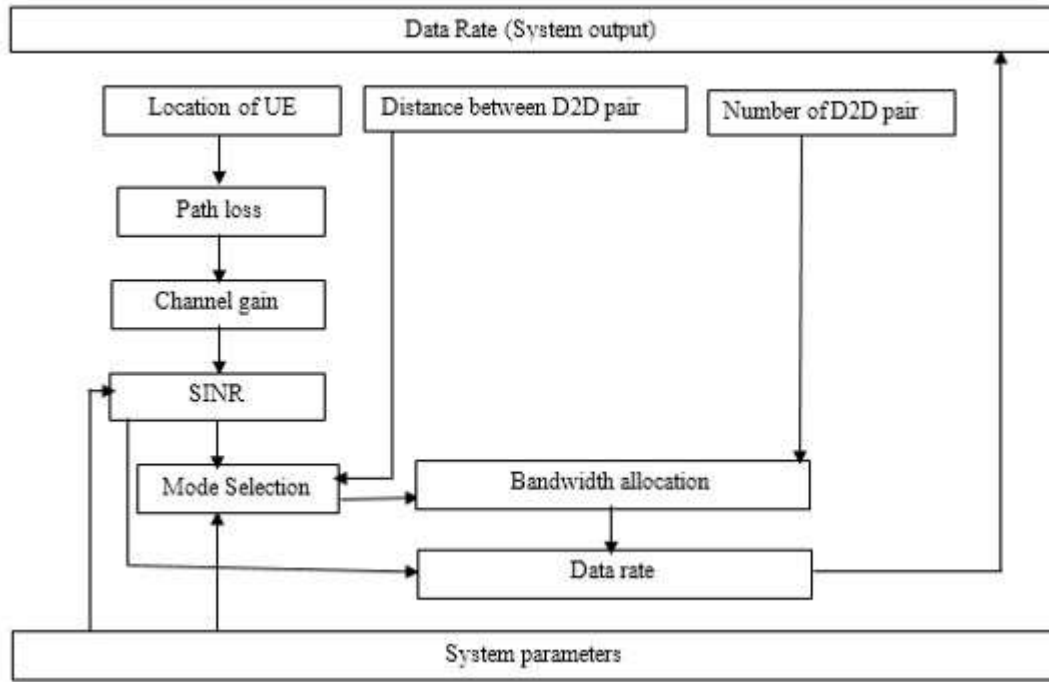


Figure 3.2: Block Diagram of Mode Selection and Bandwidth Allocation

From Figure 3.2, the path loss block works with inputs from location of UE and specified path loss model to compute the propagation path loss between a transmitter and receiver. The path loss model for D2D communication is presented in equation (3.1) adopted from Swetha and Murthy (2017); and that of cellular communication is captured in equation (3.2), (Zhao *et al.*, 2018, Hassan *et al.*, 2018).

$$L_{D2D} = 65 + 21 \log_{10}(d(m)) \quad (3.1)$$

$$L_{cell} = 15.3 + 3.7 \log_{10}(d(km)) \quad (3.2) \text{ where } d \text{ is the distance between the}$$

transmitter and the receiver. The channel gain block computes the propagation channel gain (G) based on computed propagation path loss between a transmitter and a receiver, using equation (3.3) (Onu *et al.*, 2018, Zhao *et al.*, 2018, Swetha and Murthy, 2017).

$$G = 10^{(-Path\ loss)/10} \quad (3.3)$$

The SINR block computes the receiver's SINR using specified thermal noise value from system parameters block, channel gain and SINR mathematical model in equation 3.4 (Junjie *et al.*, 2021, Zhao *et al.*, 2018, Xiaoqin and Yang, 2018).

$$SINR_{rx} = \frac{P_{tx} G_p}{P'_{tr} G'_p + \sum_{co=1}^{n-1} P'_{tr} G'_p + \sum_{cx=1}^{n-1} P'_{tr} G'_p + N_o}$$

(3.4) where;

$SINR_{rx}$ = receiver's SINR,

P_{tx} = desired transmit power,

G_p = channel gain between transmitter and its receiver,

P'_{tr} = interfering signal transmit power,

G'_p = propagation channel gain of the aggressor and its victim,

N_o = thermal noise,

$\sum_{co=1}^{n-1} P'_{tr} G'_p$ = summation of all co-tier interfering signals in the network, and

$\sum_{cx=1}^{n-1} P'_{tr} G'_p$ = summation of all cross-tier interfering signals in the network.

The number of D2D pairs determines the D2D co-tier interfering signals in the network. For n^{th} D2D pairs, there would be $(n - 1)$ D2D interfering signals. Likewise, the number of CUEs in the network determines the CUE co-tier interference.

The mode selection algorithm determines the mode of communication of all UEs in the network. The criteria for mode selection are based on the distance between D2D pairs, and computed D2D SINR. When the distance between the D2D pair is less than or equal to a target distance of 10 m (Swetha and Murthy, 2017), the UE is assigned to D2D mode subject to reference computed SINR, otherwise it is assigned to cellular mode. When the reference

SINR of UE is greater than the set target SINR of 0 (Swetha and Murthy, 2017), the UE is assigned D2D mode, otherwise, it is assigned cellular mode.

Equation (3.5) explains the mode selection mathematically.

$$\begin{aligned} &\{ \text{if } d_{D2D} \leq d_{\text{threshold}} \text{ and } SINR_{\text{computed}} \geq SINR_{\text{threshold}} \text{ assign UE to D2D Mode} \\ &\text{otherwise} \qquad \qquad \qquad \qquad \qquad \qquad \qquad \qquad \qquad \text{assign UE to CUE mode} \end{aligned} \quad (3.5)$$

The bandwidth allocation block assigns bandwidth to both cellular and D2D communication modes. The allocation of bandwidth is centrally done by the base station based on the number of UE in cellular and D2D modes at a particular time. 60% of the network bandwidth is reserved for CUE mode, 30% of network bandwidth is reserved for D2D mode and the remaining 10% is allocated dynamically to either D2D or cellular mode based on the user traffic. When the number of DUEs is greater than or equal to the number of CUEs, the 10% dynamic network bandwidth is allocated to D2D mode; otherwise, it is allocated to cellular mode. The piecewise function for bandwidth allocation by nodes to either D2D or cellular mode, within a macrocell is presented in equations (3.6) and (3.7).

$$\text{if } N_{DUE} \geq N_{CUE} = \{ BW_{CUE \text{ mode}} = 60\% \text{ of network bandwidth} \quad (3.6)$$

$$\begin{aligned} \text{if } N_{DUE} < N_{CUE} = \{ & \text{D2D mode} = 30\% \text{ of network bandwidth } BW \\ & \text{BW} \qquad \qquad \qquad = 40\% \text{ of network bandwidth} \end{aligned} \quad (3.7)$$

$$BW_{CUE \text{ mode}} = 70\% \text{ of network bandwidth}$$

where N_{DUE} is the number of of DUE, N_{CUE} is the number of CUE, $BW_{D2D \text{ mode}}$ is the bandwidth allocated to D2D mode, and $BW_{CUE \text{ mode}}$ is the bandwidth allocated to cellular mode.

The mode selection and bandwidth allocation scheme allocate spectrum to UEs based on the number of UEs per communication tier of the network. The DUEs operate in a different spectrum from that of the CUEs to avoid cross-tier interference.

The mode selection by UEs is divided into two stages: the idle and the active stages of mode selection. The idle stage of the mode selection involves neighbour discovery, and populating neighbourhood database. When a UE is powered on, it discovers its neighbours by broadcasting a Hello packet periodically. The Hello packet contains such information as Cell Identity (CID) of UE, Subscriber Identity Module (SIM) and International Mobile Equipment Identity (IMEI). Each UEs on receiving the hello packet will document the information contained in the hello packet in their neighbourhood database and reply to the UE that sends the hello packet directly with a hello reply packet. The hello reply packet contains same information as that of hello packet which is used by the receiving UE to also update its neighbourhood database.

The active stage of mode selection involves exchanging packets between UEs in order to effectively communicate in D2D mode. When a UE has information for another UE, it first checks its neighbour table to get relevant information about the intending receiver. If the information about the receiver is not in its D2D neighbour database, it will communicate to the receiver in cellular mode. But when the receiver is found on its D2D neighbour database, it would first send to the receiver a wake-up packet. The receiver on receiving the wake-up packet will switch from idle stage to active stage and reply with a wake-up acknowledgement packet.

The intending D2D transmitter will send a D2D initiation Packet directly to its receiver, following which the receiver would use the Initiation Packet to determine the distance between the DUEs, and then use the initial transmit power of the transmitting UE to compute

received signal to interference plus noise (SINR) ratio. The received SINR is compared with the target SINR, and their distance apart compared with the target distance value and send either D2D Initiate connect packet or D2D Initiate disconnect packet. When the computed SINR is greater than the target SINR, and their distance apart is not greater than the target distance, the receiving UE will send a D2D Initiate connect packet and the two UEs will proceed into D2D mode of communication and exchange information. Otherwise, the receiving UE will send a D2D Initiate disconnect packet and the two UEs will communicate in cellular mode. Figure 3.3 is the flowchart of the integrated mode selection and bandwidth allocation scheme (MS-BAS).

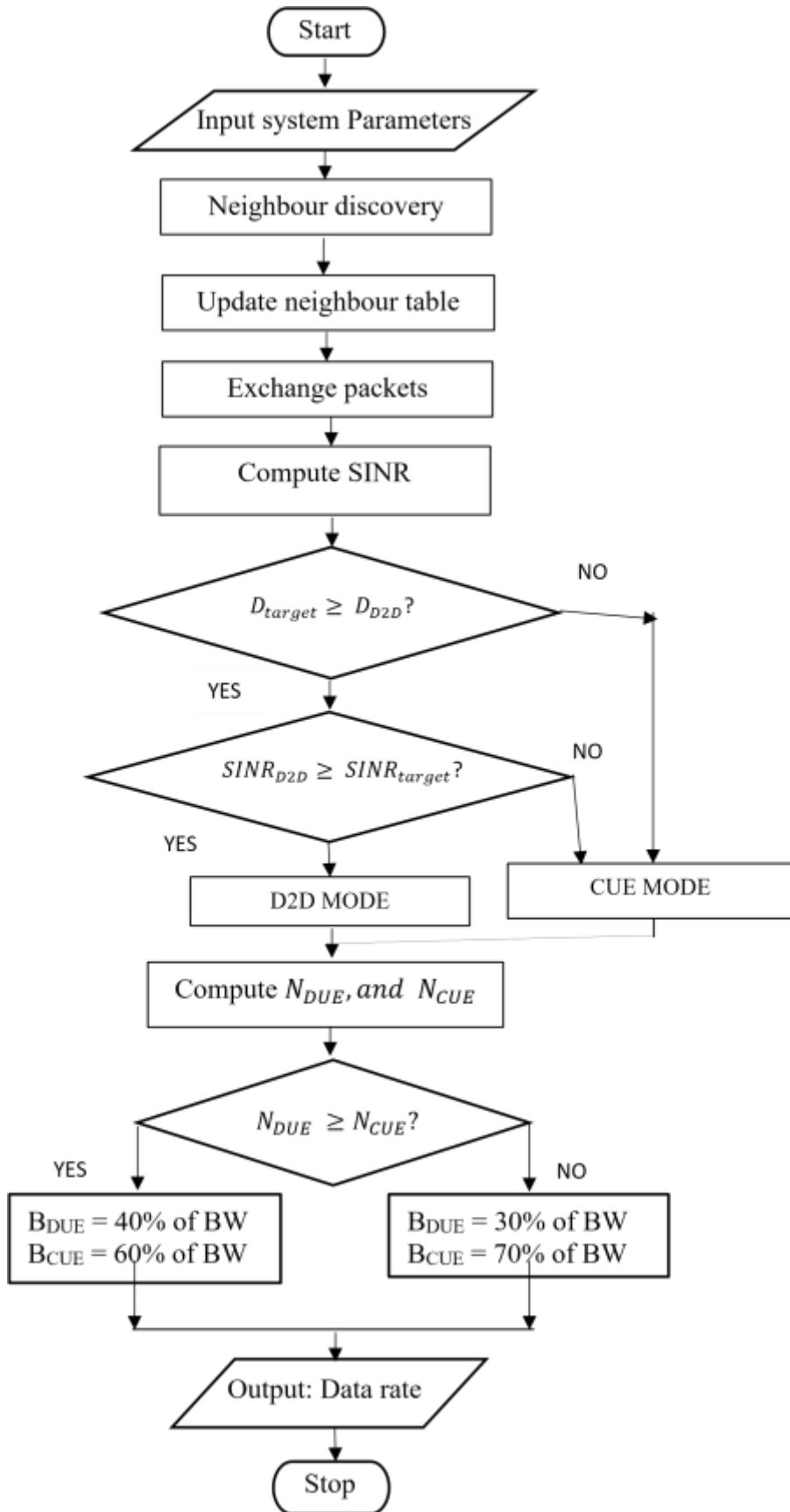


Figure 3.3: Flowchart of Mode Selection and Bandwidth Allocation Scheme

After mode selection, spectrum is centrally allocated by the base station, based on the distributed traffic density of UEs on the network. UEs periodically update the base station with their current operating mode, so that it maintains an updated number of UEs in a particular mode (D2D or cellular) per time. The base station assigns 60% of the spectrum to CUEs, and 30% to D2D. The remaining 10% is dynamically allocated based on the conditions in equations (3.6) and (3.7) to minimize spectrum redundancy in the network. The number of DUE is limited by distance of D2D devices, which often accommodate less UE compared to CUE mode.

The system output of mode selection and bandwidth allocation scheme displays the data rate of DUE, CUE, both CUE and DUE, and average data rate of both DUE and CUE all computed at data rate block using equations (3.8) – (3.11).

$$D_{D2D} = BW_{D2D\ mode} \log_2(1 + SINR_{D2D}) \quad (3.8)$$

$$D_{CUE} = BW_{CUE\ mode} \log_2(1 + SINR_{CUE}) \quad (3.9)$$

$$D_{UE} = BW_{D2D\ mode} \log_2(1 + SINR_{D2D}) + BW_{CUE\ mode} \log_2(1 + SINR_{CUE}) \quad (3.10)$$

$$D_{UES\ Average} = \sum_{i=1}^p \frac{D_{D2D}^i + \sum_{n=1}^n D_{CUE}^n}{p + n} \quad (3.11)$$

where:

D_{D2D} = data rate of D2D

D_{CUE} = data rate of CUE

$D_{UES\ Average}$ = average data rate when considering both D2D and CUE

$SINR_{D2D}$ = signal-to-interference-plus-noise ratio of D2D

$SINR_{CUE}$ = signal-to-interference-plus-noise ratio of CUE

$\sum_{i=1}^p (D_{D2D}^1 + D_{D2D}^2 + \dots + D_{D2D}^p)$ = sum of D2D data rate considering p

number of iterations

$\sum_{i=1}^n (D_{CUE^1} + D_{CUE^2} + \dots + D_{CUE^n})$ = sum of CUE data rate considering n number of iterations.

Where p and n are maximum number of iterations for D2D and CUE respectively.

Table 3.2 is the pseudocode for the mode selection and bandwidth allocation scheme.

Table 3.2: Pseudocode of mode selection and bandwidth allocation scheme

PSEUDOCODE FOR MODE SELECTION AND BANDWIDTH ALLOCATION	
1.	Initialization: Booting of UEs and base station
2.	Load input parameters into the memory of UEs and base station
3.	Idle State of UEs: <ul style="list-style-type: none"> - Neighbour discovery using broadcast packet - Update neighbour Table 4. Active state of UEs: - Exchange packets with discovered neighbours - Compute: <ul style="list-style-type: none"> • Path loss using (3.1) and (3.2) • SINR using (3.4) • Channel gain using (3.3) - Decision: <p style="text-align: center;"><i>if $D_{D2D} \leq D_{target}$ {YesNo:: tthhenen assign $SINR_{D2D} \geq t_{CUE SINR mode target}$</i></p> <p style="text-align: center;"><i>Yes: then assign UE to D2D</i></p> <p style="text-align: center;"><i>if $SINR_{D2D} \leq SINR_{target}$ {No: then assign UE to CUE mode</i></p>
5.	Base station updates Active UE Mode Table Periodically (180 seconds)
6.	Base station Computes Number of Active DUE and D2D 7. Bandwidth Request by UEs 8. Decision: <p style="text-align: center;"><i>$N_{DUE} < N_{CUE}$ {YesYes::tthhenen $BB_{DUECUE} == 7030\%$ of of BandwidtBandwidththh</i></p> <p style="text-align: center;"><i>$N_{DUE} \geq N_{CUE}$ {YesYes::tthhenen $BB_{DUECUE} == 6040\%$ of of BandwidtBandwidththh</i></p>
9.	Compute data rate using equations (3.8) – (3.11)
10.	Output computed data rate
11.	End

3.3 Power Control Scheme

The D2D power control scheme (D2D-PCS) was implemented by UEs in D2D communication mode regulating the use of scarce power resources for an optimal interference mitigation. In D2D-PCS, the UE does not start transmitting with their maximum transmit power, rather it starts with a set initial transmit power. The UEs in D2D communication computes CUE and DUE path loss using equations (3.1) and (3.2) respectively. Channel gain, SINR, average DUE transmit power, data rate and average data rate is computed using equations (3.3), (3.4), (3.15), (3.16) and (3.17) respectively.

Figure 3.4 is the block diagram of the power control scheme for mitigating co-tier interference in the D2D tier of the communication network.

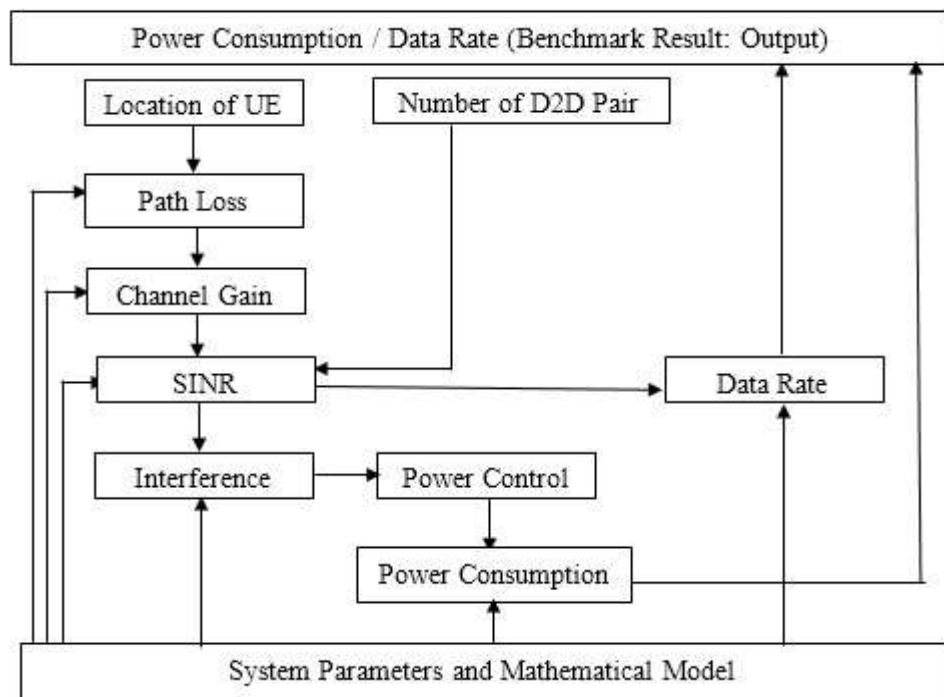


Figure 3.4: Block Diagram of Power Control Algorithm

The block diagram in Figure 3.4 shows the various blocks of the power control scheme. The pathloss block, channel gain and SINR blocks are similar to that of Figure 3.2. The Interference block determines interference in the network based on the quality of signal received. The target SINR, is compared with the computed SINR to determine the level

of interference and denoted as λ . When λ is less than the target (0), interference is high and a positive step power factor Δ of 0.5 is applied. When λ is more than 0, interference is low and a negative step power factor of -0.5 is applied. At the threshold interference where λ is 0, no step power factor is applied to the transmit power. Equations (3.12) and (3.13) mathematically expresses the decision-making process of interference block (Dawar *et al.*, 2021; Rana *et al.*, 2021).

$$\lambda = SINR_{computed} - SINR_{target} \quad (3.12)$$

$$if \lambda = \begin{cases} < 0, \Delta = + 0.5 \\ > 0, \Delta = - 0.5 \\ = 0, \Delta = 0 \end{cases} \quad (3.13)$$

where λ is the difference between computed and target SINR, and Δ is a step power factor.

Based on the outcome of the interference block, the power control block adjusts the transmit power of UE using power step value, and power control model in equation (3.14) (Dawar *et al.*, 2021, Rana *et al.*, 2021, Hassan and Gao 2019).

$$P_{tx} = \max (P_{min}, \min ((P_{tx} + \Delta), P_{max})) \quad (3.14) \text{ where;}$$

P_{tx} = transmit power of UEs

P_{min} = minimum transmit power

P_{max} = maximum transmit power of UEs

The power consumption block computes the average power consumption of each DUE in the network using equation 3.15. An array of transmit power used by transmitting UEs at different positions and instances was used to get the average transmit power.

$$P_{DUEsAverage} = \frac{\sum_{i=1}^{i=L} (\sum_{NDUE=n}^{NDUE} (P^1 + P^2 + \dots + P^n))}{L \times n} \quad (3.15)$$

Where;

$P_{DUEs}^{Average}$ = average power consumed by DUE

P_{tx}^n = transmit power of n^{th} DUE

n = last number of DUE

L = last number of iterations

$\sum_{NDUE=1}^{NDUE=n} (P_{tx}^1 + P_{tx}^2 + \dots + P_{tx}^n)$ = Summation of all DUEs transmit

power The data rate block, when considering the power control scheme compute data rate and average data rate using mathematical model captured in equations (3.16) and (3.17) respectively (Sihan *et al.*, 2019; Budhiraja *et al.*, 2018; Adejo *et al.*, 2017b).

$$D_{DPS2D} = BW \log_2(1 + SINR_{rx}) \quad (3.16)$$

$$D_{AveragePS_D2D} = \sum_{i=1}^L (\sum_{NDUE=1}^{NDUE=n} (D_{DPS2D1} + D_{DPS2D2} + \dots + D_{DPS2Dn})) \quad (3.17)$$

where;

$D_{AveragePS_D2D}$ = average DUE data rate

BW = system bandwidth

$$\sum_{i=1}^L (\sum_{NDUE=1}^{NDUE=n} (D_{DPS2D1} + D_{DPS2D2} + \dots + D_{DPS2Dn})) =$$

Summation of DUE data rate

The system output block displays the computed DUE SINR, average DUE data rate and DUE average transmit power.

Figure 3.5 is the flowchart of the power control scheme for co-tier interference mitigation in Macro-D2D HetNet. Where one was assigned to i , which stands for the initial number of iteration and L stands for the maximum number of iterations. The iteration controls

the number of D2D pair distance and number of D2D pair that would be used in the simulation of the scheme.

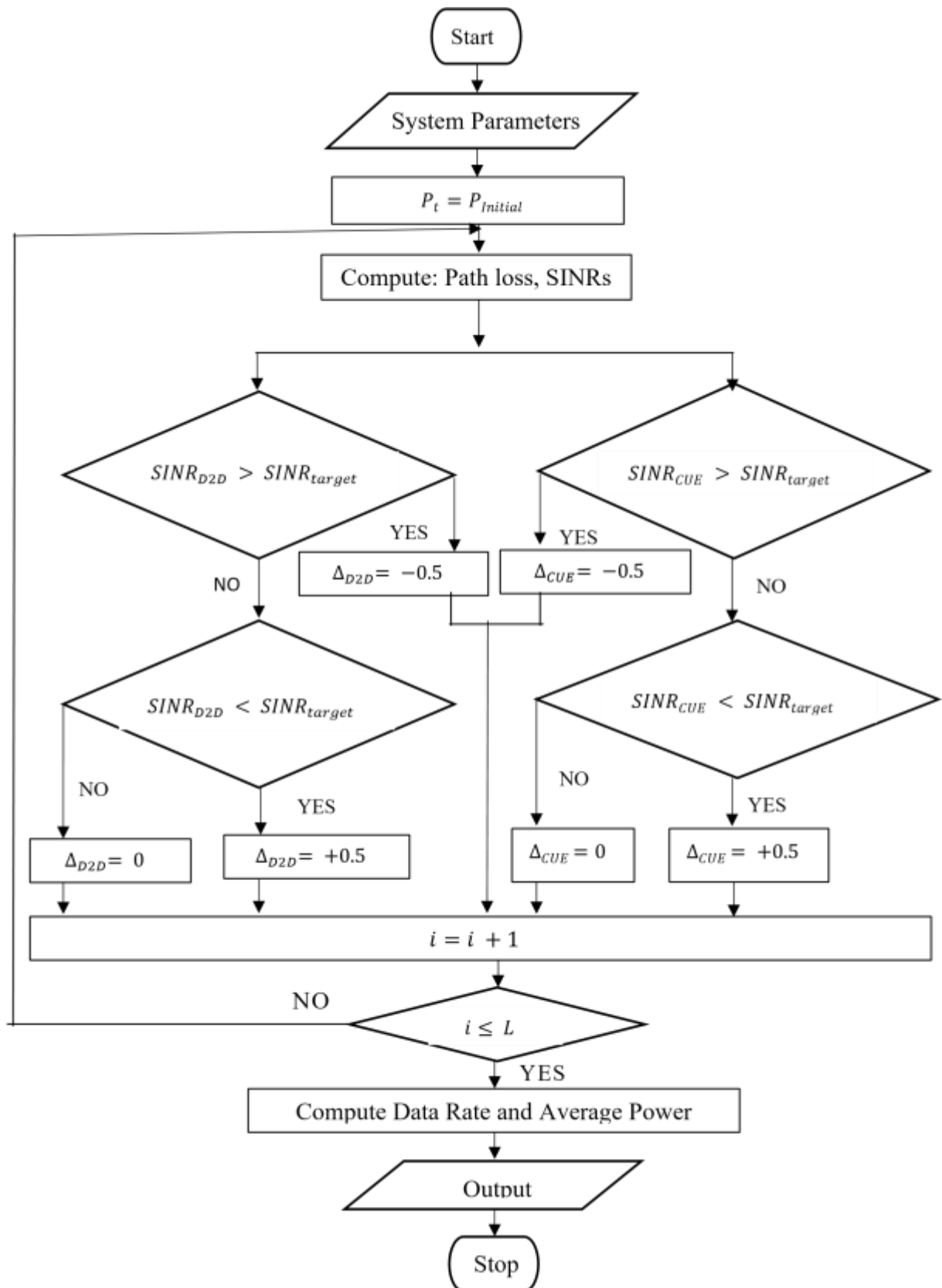


Figure 3.5: Flowchart of D2D Power Control Scheme

The program executes at different D2D pair distance and number of D2D pair until the number of iterations exceed the value of L then the iteration stops. The program computes the average power utilization, and average data rate considering DUE transmit power, and data rate during each iteration.

Table 3.3 presents the pseudocode for the D2D Power Control Scheme.

Table 3.3: Pseudocode of power control technique

PSEUDOCODE OF POWER CONTROL SCHEME FOR D2D COMMUNICATION

1. Booting of UEs
2. Load input variables
3. Set initial transmission power.
 - $P_t = P_{initial}$
4. Compute:
 - UE path loss using (3.1) and (3.2)
 - D2D SINR using (3.4)
5. First decision:
 - Yes: then $SINR_{D2D} > SINR_{target}$*
 - $SINR_{D2D} \geq SINR_{CUE}$ {No: then $SINR_{CUE} > SINR_{target}$*
6. Second decision:
 - Yes: then $\Delta = -0.5$*
 - $SINR_{D2D} > SINR_{target}$ {No: then $SINR_{D2D} < SINR_{target}$*
7. Third decision:
 - Yes: then $\Delta = 0.5$*
 - $SINR_{D2D} < SINR_{target}$ {*
 - No: then $\Delta = 0$*
8. Control iteration:
 - Increase counter:
 - $i = i + 1$
 - Check for limit:
 - $i \leq L$
9. Compute:
 - Average transmit power of DUE using (3.15)
 - DUE data rate using (3.16) - Average data rate using (3.17)
10. Output:
 - Average transmit power of DUE.
 - DUE SINR
 - DUE data rate
 - DUE average data rate

The Percentage Improvement (P_{MSBAS}) of DUE, CUE, and UE SINR and Data rate values for MS-BAS over the SOMO scheme was computed with equation (3.18):

$$P_{MSBAS} = \left(\frac{MSBAS-SOMO}{SOMO} \right) 100\% \quad (3.18)$$

Similarly, the Percentage Improvement (P_{D2DPCS}) of DUE, CUE, and UE Power efficiency for D2D-PCS over the FPC and PCS1 schemes was computed with equations (3.19) and (3.20) respectively:

$$P_{D2DPCS} = \left(\frac{D2DPCS-FPC}{(FPC)} \right) 100\% \quad (3.19)$$

$$P_{D2DPCS} = \left(\frac{D2DPCS-PCS1}{(PCS1)} \right) 100\% \quad (3.20)$$

CHAPTER FOUR

4.0 RESULTS AND DISCUSSION

The chapter presents and discusses the results obtained from the simulation of the research Macro - D2D communication HetNet. The results are in sections based on the set objectives of the study. The power utilization, SINR and data rates were used as key performance indicators (KPIs) to determine the performance of the schemes in mitigating interference, in accordance with equations (2.5) - (2.9).

4.1 Presentation of Results

The simulation results are categorized into two (2) sections based on the developed schemes:

- i. Performance of the Mode Selection and Bandwidth Allocation Scheme (MS-BAS), and, ii. Performance of the D2D Power Control Scheme (D2D-PCS).

The performance of the mode selection and bandwidth allocation scheme (MS-BAS) was compared with that of Selective Overlay Mode Operation (SOMO) for D2D communication, as presented in Swetha and Murthy (2017), while the performance of the D2D Power Control Scheme (D2D-PCS) was compared with that of the Power Control Scheme 1 (PCS1) presented in Rana *et al.* (2021), as well as an arbitrary Fixed Power Control Scheme (FPC), where a fixed transmit power was set throughout the communication.

4.1.1 Results of mode selection and bandwidth allocation scheme

The performance of the mode selection and bandwidth allocation scheme (MS-BAS) was analysed based on varying distance between device-to-device user equipment (DUEs), and the number of D2D pairs. Considering 20 UEs, the distribution of UE based on mode selection, when simulated gave the number of UE, DUE and CUE in each iteration as presented in Table 4.1.

Table 4.1: A random distribution of UE to DUE and CUE modes

S/N	Number of DUE	Number of CUE	Number of UE
1.	14	6	20
2.	10	10	20
3.	8	12	20
4.	10	10	20
5.	4	16	20
6.	6	14	20
7.	12	8	20
8.	8	12	20
9.	10	10	20
10.	6	14	20

The values in Table 4.1 were plotted and presented in Figure 4.1. Table 4.1 and Figure 4.1 indicates that the integration of D2D communication depopulates the macrocell network, by moving some UEs that would normally have all communicated in CUE mode to DUE mode.

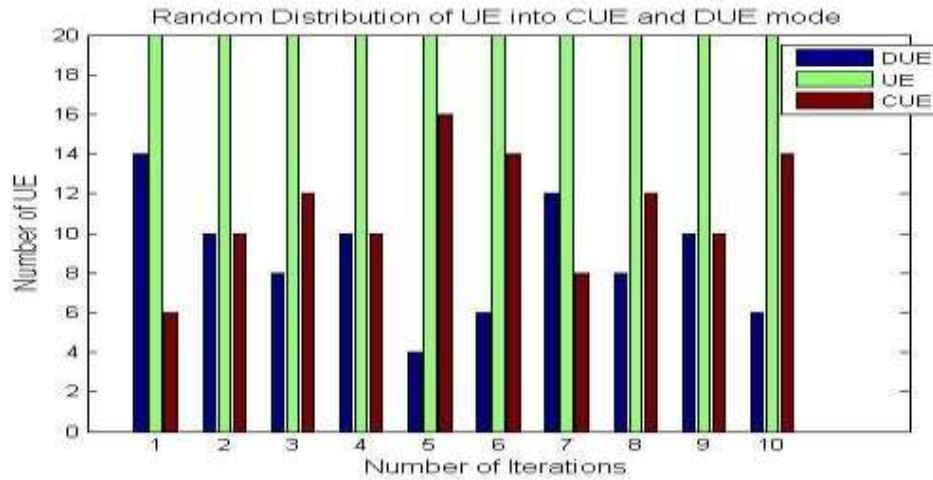


Figure 4.1: A random distribution of UE to CUE and DUE modes.

As captured in Figure 4.1 the distribution of 20 UE to DUE and CUE mode was centred on randomly generated distance between pair of UE. When the distance between the UE pairs is less than or equal to target D2D distance; the UE would be allocated to DUE mode, otherwise it would be allocated to CUE mode. The number of DUEs and CUEs will keep on changing for different iterations.

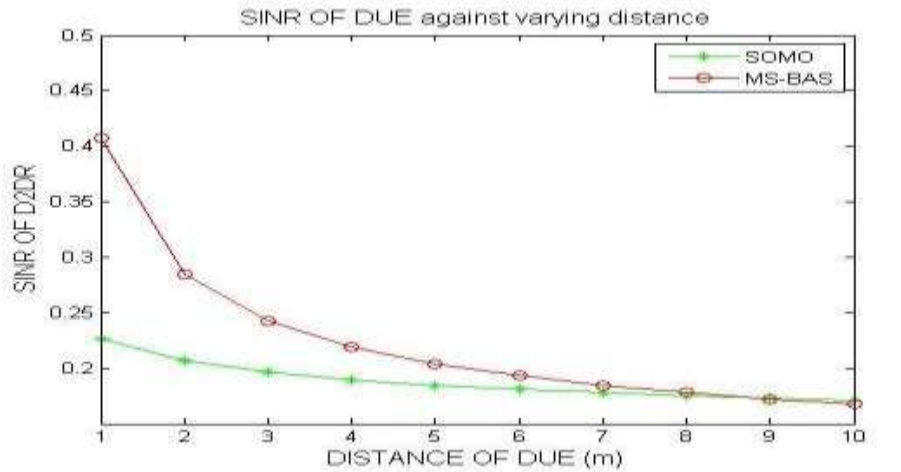
At constant number of D2D pair, the distance between DUE was varied from 0 – 10 m. The range of distance used was in accordance with the adopted D2D target distance of 10m (Swetha and Murthy, 2017). Table 4.2 presents the values of MS-BAS and SOMO SINR when DUE distance was varied.

Table 4.2: SINR of MS-BAS with varied DUE distance

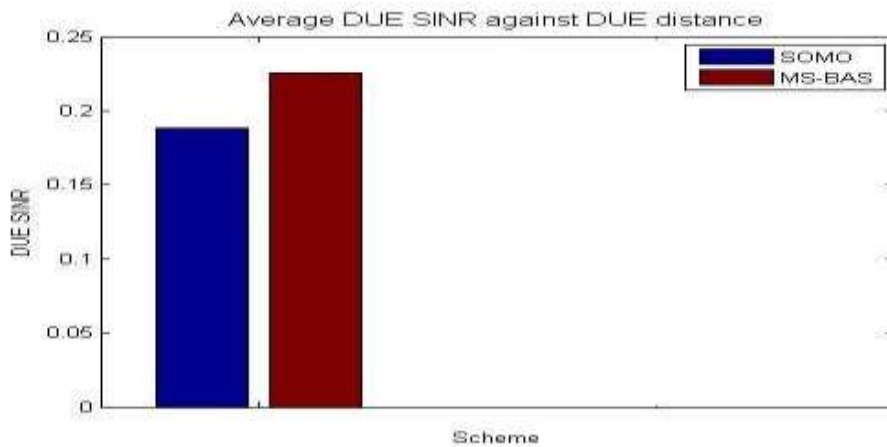
Distance of DUE (m)	DUE SINR	
	SOMO	MS-BAS
1	0.23	0.41
2	0.21	0.29
3	0.20	0.25
4	0.19	0.22
5	0.18	0.21
6	0.18	0.20
7	0.18	0.19
8	0.18	0.18
9	0.17	0.18

10	0.17	0.17
Average	0.19	0.23

The values in Table 4.2 show SOMO and MS-BAS DUE SINR at varying DUE distance, and the average DUE SNR were plotted; and the results presented in Figure 4.2.



(a)



(b)

Figure 4.2: DUE SINR of MS-BAS based on varied DUE distance.

(a) Benchmarked MS-BAS SINR of DUE at varying DUE distance

(b) Average MS-BAS SINR of DUE at varying DUE distance

As presented in Figure 4.2, and from equation (3.18), the performance of MS-BAS in terms of DUE SINR when distance of DUE was varied, outperformed that of SOMO by

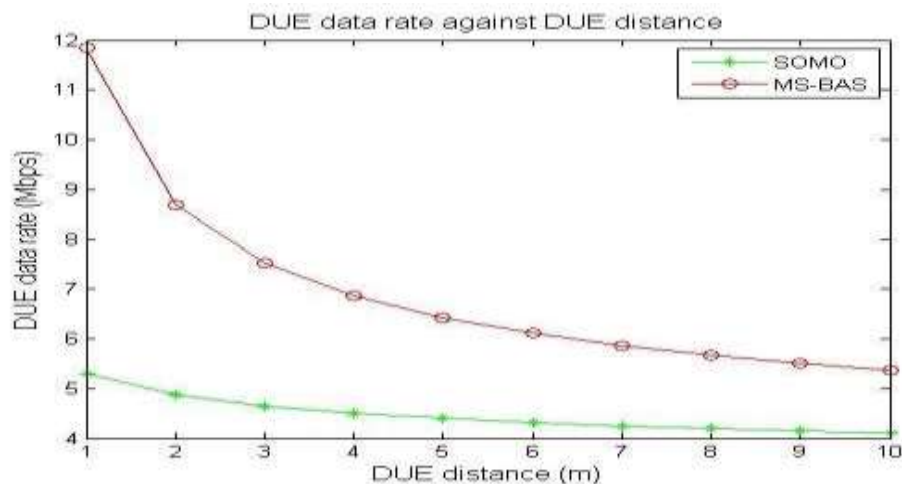
78.26%, 38.10%, 25.00%, 15.79%, 16.67%, 11.11%, 5.56%, 0.00%, 5.88%, and 0.00%, respectively, while the average MS-BAS DUE SINR outperformed that of SOMO by 21.05%.

Table 4.3 gives the data rate performance of MS-BAS at varying DUE distance.

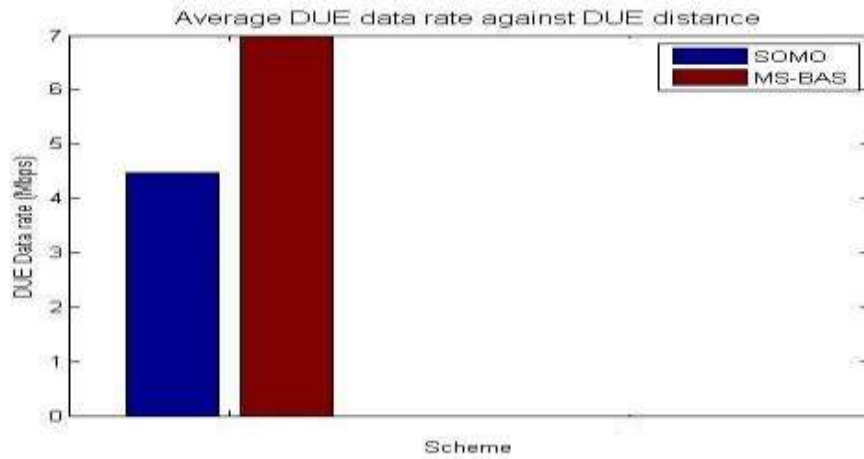
Table 4.3: Data rate of MS-BAS with varied DUE distance

Distance DUE (m)	of DUE data rate		CUE data rate (Mbps)		UE data rate (Mbps)	
	SOMO	MS-BAS	SOMO	MS-BAS	SOMO	MS-BAS
1	5.30	11.98	8.01	6.87	13.31	18.85
2	4.87	8.80	8.01	6.87	12.88	15.66
3	4.65	7.61	8.01	6.87	12.66	14.48
4	4.51	6.95	8.01	6.87	12.52	13.82
5	4.40	6.51	8.01	6.87	12.41	13.38
6	4.32	6.19	8.01	6.87	12.33	13.06
7	4.25	5.95	8.01	6.87	12.26	12.81
8	4.20	5.75	8.01	6.87	12.21	12.62
9	4.15	5.58	8.01	6.87	12.16	12.45
10	4.10	5.44	8.01	6.87	12.12	12.31
Average	4.48	7.08	8.01	6.87	12.49	13.94

The DUE data rate when DUE distance was varied as captured in Table 4.3 were plotted and results presented in Figure 4.3, where Figure 4.3a presents the DUE data rate at each DUE distance and Figure 4.3b gave the average DUE data rate.



(a)



(b)

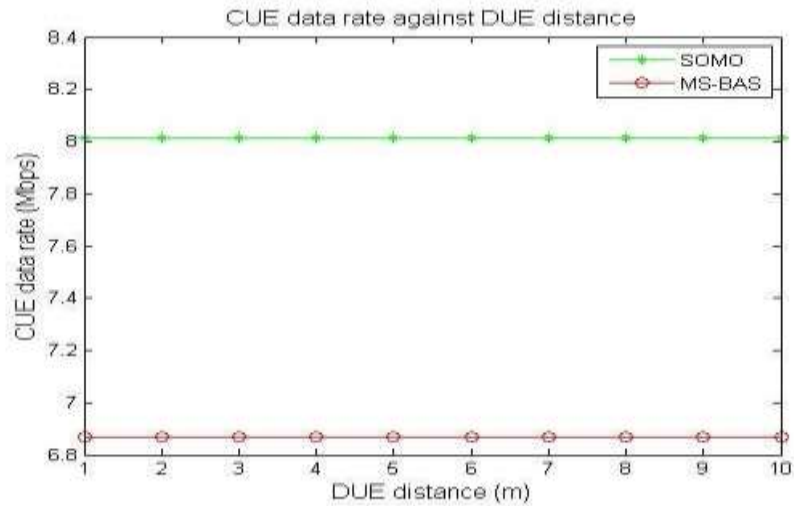
Figure 4.3: MS-BAS DUE data rate based on varied DUE distance.

(a) Benchmarked MS-BAS DUE data rate against DUE distance

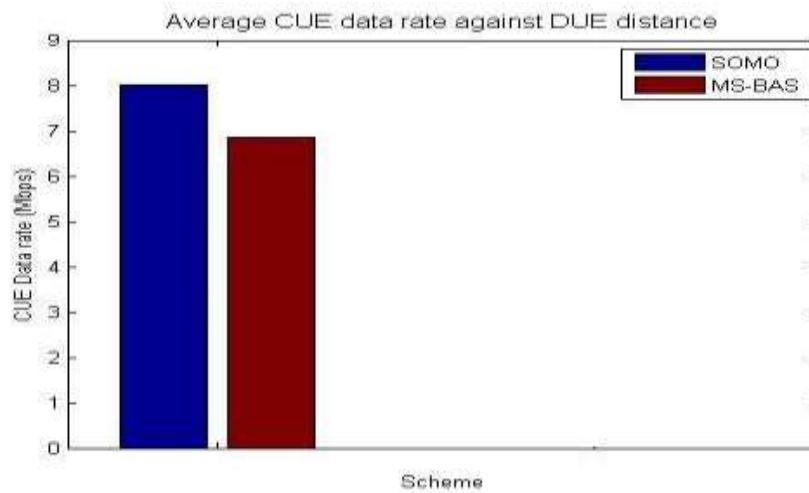
(b) Average MS-BAS DUE data rate performance when DUE was varied.

According to Figure 4.3 and Table 4.3, the performance of MS-BAS in terms of DUE data rate outperformed that of SOMO at DUE distance of 1 – 10 m. At 1 -10 m the MSBAS DUE data rate was better than that of SOMO by 126.42%, 80.88%, 63.12%, 54.43%, 48.86%, 43.75%, 40.59%, 37.50%, 34.14%, and 32.68%, respectively, as computed from equation (3.18). The MS-BAS average DUE data rate performance when DUE distance was varied, performed better than SOMO by 58.93% as shown in Figure 4.3b.

The performance of MS-BAS scheme in terms of CUE data rate at varying DUE distance was plotted and the result presented in Figure 4.4.



(a)



(b)

Figure 4.4: MS-BAS CUE data rate based on varied DUE distance.

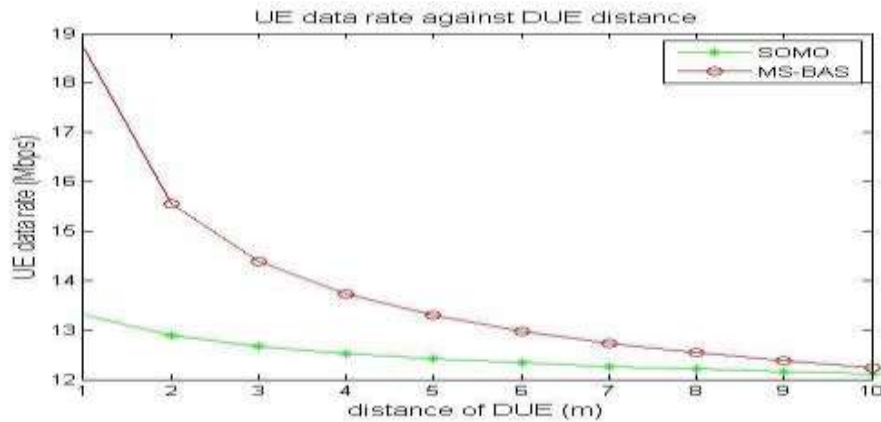
(a) Benchmarked MS-BAS CUE data rate against DUE distance

(b) Average MS-BAS CUE data rate performance when DUE was varied.

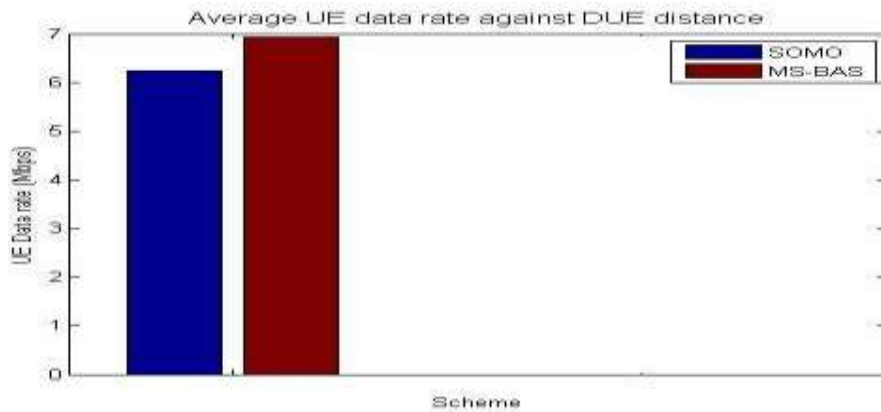
From Figure 4.4a, both MS-BAS and SOMO had a constant data rate when DUE distance was varied. The SOMO scheme had CUE data rate which outperformed that of MS-BAS by 16.59%, at each DUE distance, and its average CUE data rate (Figure 4.4b) was better than that of MS-BAS by 16.59%.

The result of MS-BAS scheme UE data rate performance when DUE distance was varied was captured in Figure 4.5. Where Figure 4.5a captured UE data rate at varying DUE

distance and Figure 4.5b presented average MS-BAS UE data rate performance at varying DUE distance against that of SOMO.



(a)



(b)

Figure 4.5: MSBAS UE data rate based on varied DUE distance.

(a) Benchmarked MS-BAS UE data rate against DUE distance

(b) Average MS-BAS UE data rate performance when DUE was varied.

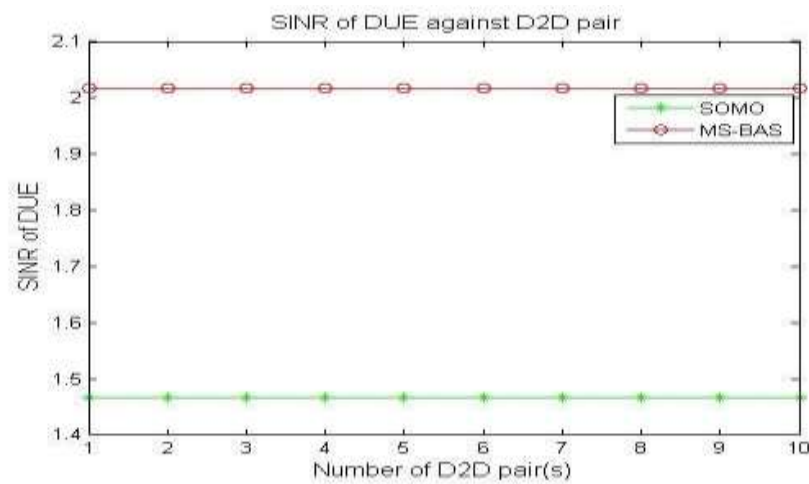
The data rate of all UE in the Macro - D2D network while varying DUE distance was computed and the results presented in Table 4.3. Figure 4.5 indicates that MS-BAS had better overall UE data rate when compared to that of SOMO. At DUE distance ranging from 1 – 10 m, MS-BAS outperformed SOMO UE data rate by 41.34%, 21.50%, 14.38%, 10.27%, 8.00%, 6.03%, 4.69%, 3.46%, 2.63%, and 1.98% respectively in accordance with equation (3.18). MS-BAS average UE data rate when DUE distance was varied, as captured in Figure 4.5b outperformed that of SOMO by 11.35%.

Table 4.4 gives the DUE SINR value of SOMO and MS-BAS schemes while varying the number of D2D pairs.

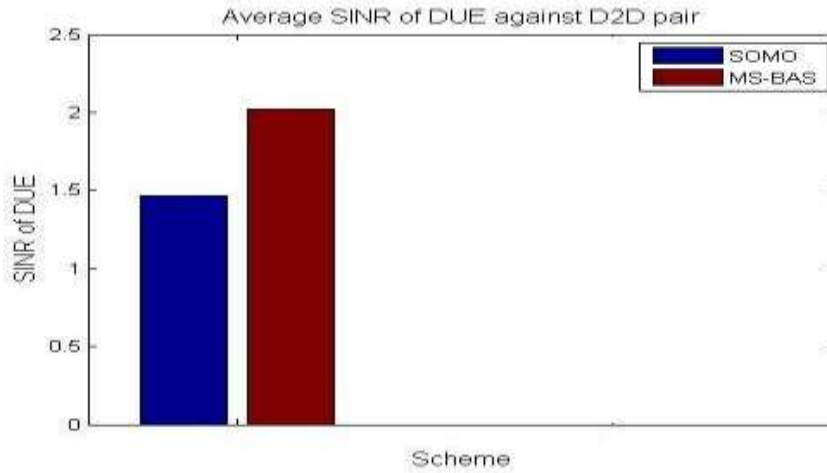
Table 4.4: DUE SINR of SOMO and MS-BAS with varied number of D2D pairs

Number of D2D Pairs	DUE SINR	
	SOMO	MS-BAS
1	1.47	2.02
2	1.47	2.02
3	1.47	2.02
4	1.47	2.02
5	1.47	2.02
6	1.47	2.02
7	1.47	2.02
8	1.47	2.02
9	1.47	2.02
10	1.47	2.02
Average	1.47	2.02

The plot of DUE SINR at varying number of D2D pairs, which shows the performance of MS-BAS scheme, is presented in Figure 4.6.



(a)



(b)

Figure 4.6: DUE SINR of MS-BAS based on varied number of D2D pairs.

(a) Benchmarked performance of MS-BAS SINR of DUE when D2D pair was varied

(b) Average performance of MS-BAS SINR of DUE when D2D pair was varied

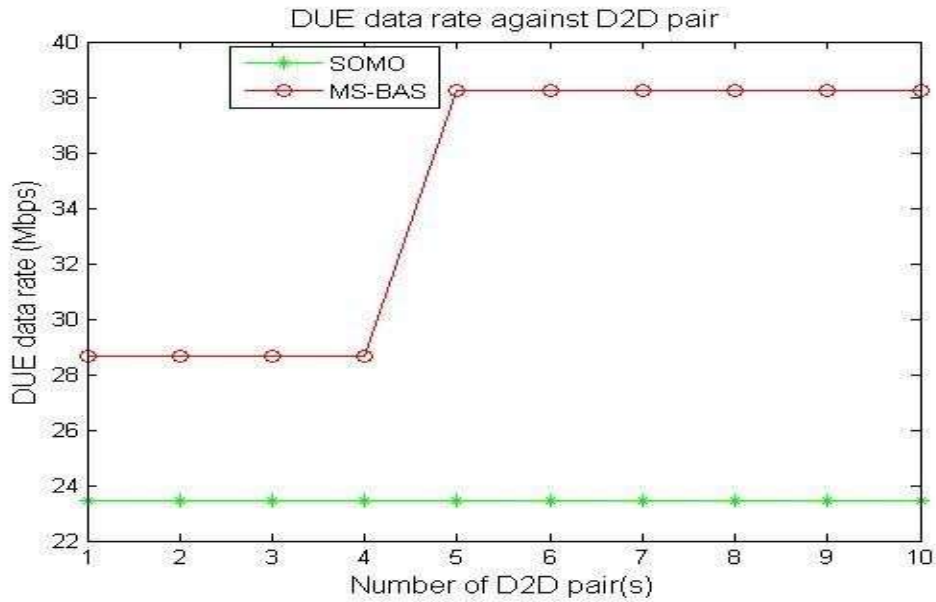
Results presented in Table 4.4, and Figure 4.6a shows that SINR values of MS-BAS and SOMO were constant when number of D2D pair was varied. MS-BAS and SOMO DUE SINR was 2.02 and 1.47 respectively. The DUE SINR performance of MS-BAS was better than that of SOMO at each number of D2D pair by 37.41%.

The data rate performance of MS- BAS scheme when number of D2D pairs was altered from 1 – 10 pairs in terms of DUE, CUE and UE data rate are presented in Table 4.5

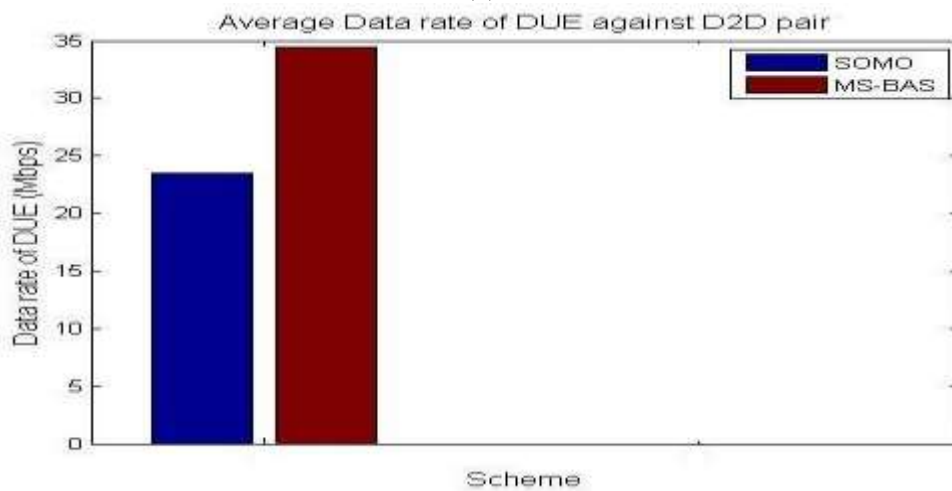
Table 4.5: Data rates of MS-BAS with varied number of D2D pairs

No. of D2D Pairs	DUE data rate (Mbps)		CUE data rate (Mbps)		UE data rate (Mbps)	
	SOMO	MS-BAS	SOMO	MS-BAS	SOMO	MS-BAS
1	23.45	28.68	3.45	3.45	26.89	32.13
2	23.45	28.68	3.89	3.89	27.34	32.57
3	23.45	28.68	4.47	4.47	27.91	33.15
4	23.45	28.68	5.24	5.24	28.68	33.92
5	23.45	38.24	6.33	5.43	29.78	43.67
6	23.45	38.24	8.01	6.87	31.46	45.11
7	23.45	38.24	10.90	9.34	34.35	47.59
8	23.45	38.24	17.07	14.63	40.51	52.87
9	23.45	38.24	39.88	34.18	63.33	72.43
10	23.45	38.24	0.00	0.00	23.45	38.24
Average	23.45	34.42	9.92	8.75	33.37	43.17

The performance of MS-BAS when number of D2D pairs varies in terms of DUE data rate is presented in Figure 4.7.



(a)



(b)

Figure 4.7: MS-BAS DUE data rate based on varied D2D pairs.

(a) MS-BAS performance of DUE data rate when D2D pair was varied

(b) Average MS-BAS performance of DUE data rate with varied D2D pairs

The DUE data rate when number of D2D pairs was varied from 1 – 10 as presented in

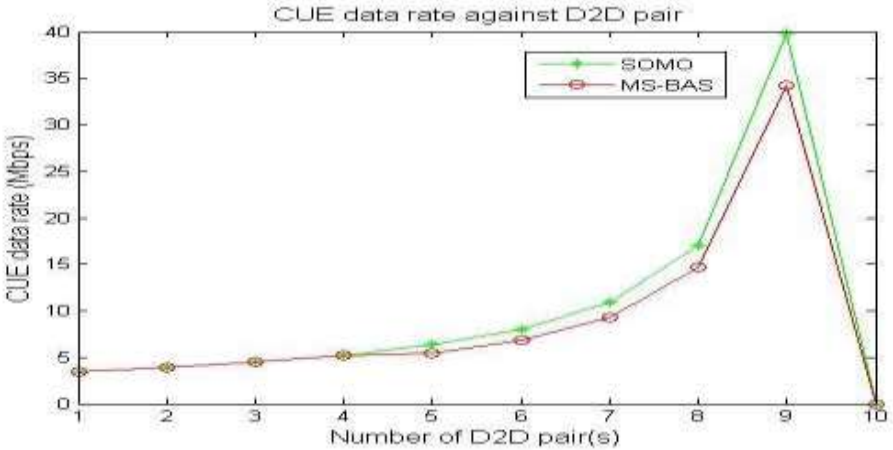
Table 4.5 and Figure 4.7, shows that MS-BAS DUE data rate was better than that of SOMO. At D2D pairs varying from 1 – 4 pairs, DUE data rate of MS-BAS and SOMO was constant at 28.68 Mbps and 23.45 Mbps respectively. The constant data rate is attributed to same bandwidth allocated to DUE, path loss did not change due to same DUE position, and same SINR. Hence, MS-BAS DUE data rate outperformed that of SOMO by 22.30%.

At D2D pair ranging from 5 – 10, the number of DUE increases from 10 – 20, while the number of CUE decreased from 10 – 0. In MS-BAS, when the number of DUE is equal to or greater than the number of CUEs, more bandwidth will be allocated to DUE tier.

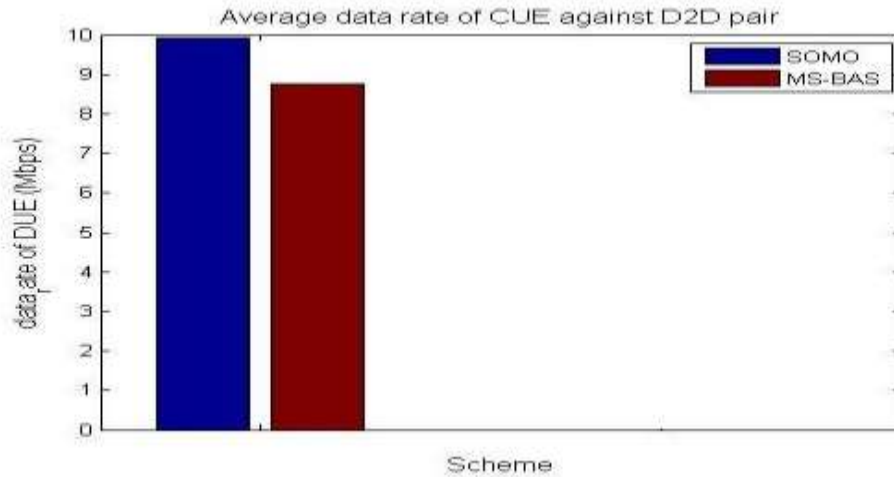
This accounts for the sharp rise in DUE data rate within the range of 5 – 10 D2D pairs.

When number of D2D pairs is equal to 10 and above, MS-BAS DUE data rate outperformed SOMO by 63.07%. In Figure 4.7b, the average DUE data rate of MS-BAS outperformed that of SOMO by 46.78%.

MS-BAS CUE data rate performance with varied D2D pairs is presented in Figure 4.8.



(a)



(b)

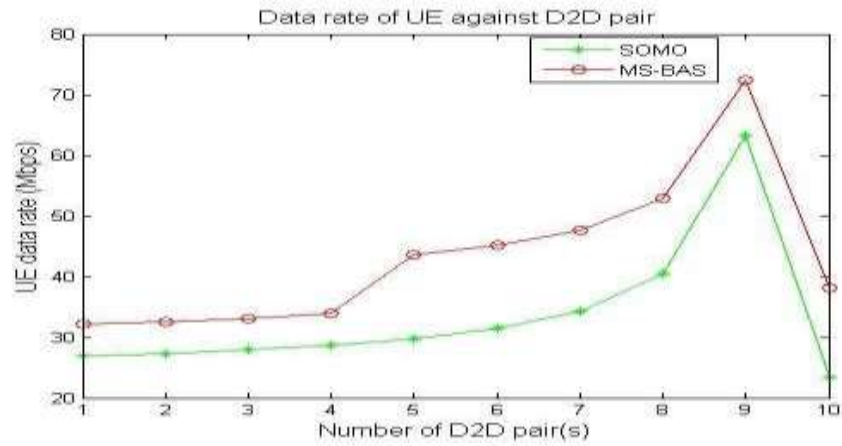
Figure 4.8: MS-BAS CUE data rate based on varied D2D pairs.

(a) MS-BAS performance of CUE data rate with varied D2D pair

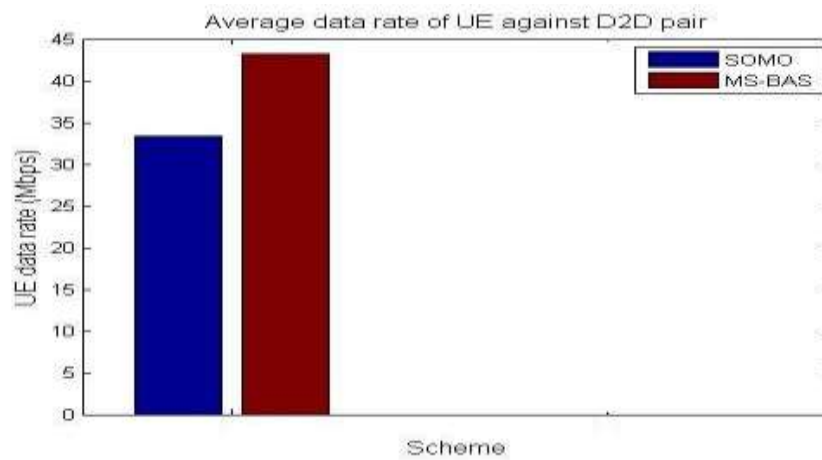
(b) Average MS-BAS performance of CUE data rate with varied D2D pair

From Figure 4.8a, the CUE data rate of SOMO when compared to MS-BAS at D2D pairs ranging from 1 – 4 was the same. While from 5 – 9 D2D pairs the CUE data rate of SOMO outperformed that of MS-BAS from equation (3.18). At 10 D2D pairs, there is no CUE in the simulated network, only 20 DUEs, hence the CUE data rate of both SOMO and MS -BAS at 10 D2D pair was 0.00 Mbps. The SOMO and MS-BAS average CUE data rate as captured in Figure 4.8b was 9.92 Mbps and 8.75 Mbps respectively. SOMO average CUE data rate was better than that of MS-BAS by 13.37%.

MS-BAS UE data rate performance with varied D2D pairs was presented in Figure 4.9.



(a)



(b)

Figure 4.9: MS-BAS UE data rate with varied D2D pairs.

(a) Benchmarked MS-BAS performance of UE data rate varied D2D pair

(b) Average MS-BAS performance of UE data rate with varied D2D pair

The results of SOMO and MS-BAS UE data rate performance when number of D2D pairs was varied as presented in Figure 4.9 and Table 4.5 shows that at number of D2D pairs ranging from 1 – 10, MS-BAS UE data rate was better than that of SOMO by 19.38%, 18.99%, 18.85%, 18.23%, 46.60%, 43.18%, 38.51%, 30.38%, 14.34%, and 63.13% respectively, from equation (3.18), with MS-BAS averagely outperforming SOMO by 29.37%. The average UE data rate of SOMO and MS-BAS when number of D2D pairs increased from 1 – 10 as captured in Figure 4.9b was 33.37 Mbps and 43.17 Mbps respectively.

4.1.2 Results of power control scheme

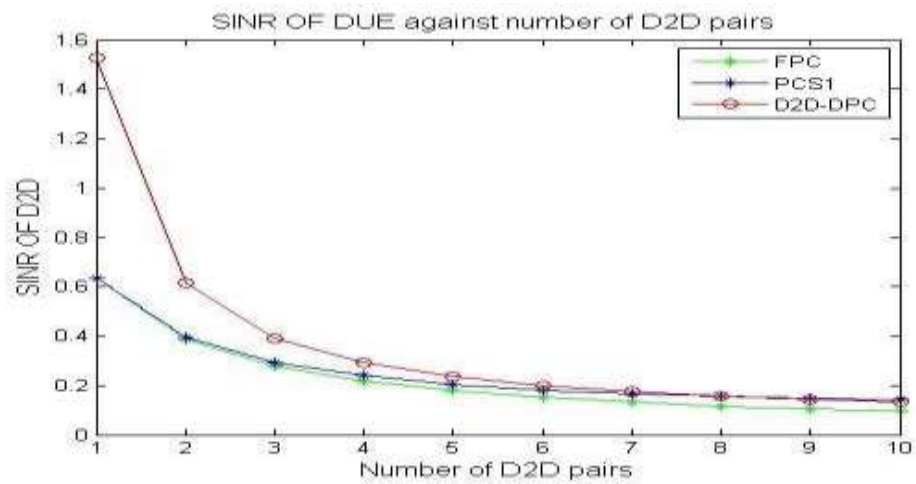
The D2D power control scheme (D2D-PCS) for co-tier interference mitigation in D2D communication was simulated and the performances are presented in Figures 4.10 – 4.22.

The performance of D2D-PCS in terms of SINR when DUE distance was varied from 1 – 10m is as captured in Table 4.6.

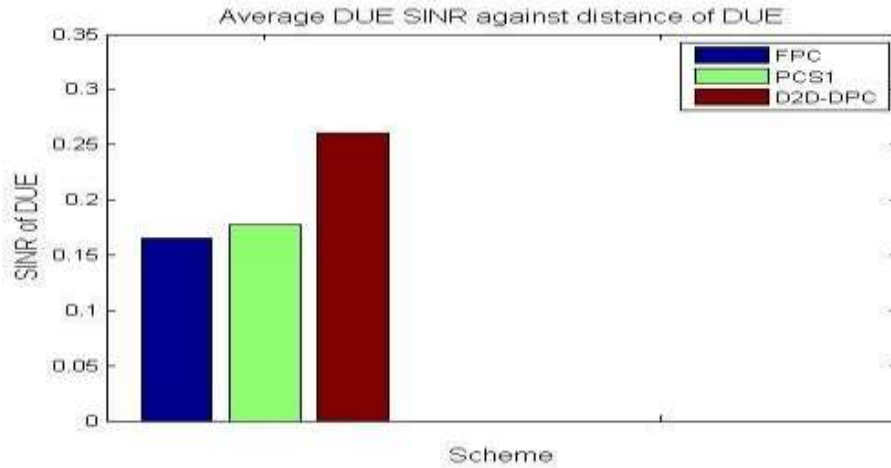
Table 4.6: SINR of D2D-PCS with varied DUE distance

Distance of DUE (m)	DUE SINR		
	FPC	PCS1	D2D-PCS
1	0.19	0.19	0.43
2	0.18	0.18	0.31
3	0.17	0.18	0.27
4	0.17	0.17	0.25
5	0.16	0.17	0.24
6	0.16	0.17	0.23
7	0.16	0.17	0.22
8	0.15	0.18	0.22
9	0.15	0.18	0.22
10	0.15	0.18	0.22
Average	0.16	0.18	0.26

The SINR performance of D2D-PCS when DUE was varied as presented in Table 4.6 was plotted and presented in Figure 4.10.



(a)



(b)

Figure 4.10: SINR of PCS1 based on varied DUE distance.

(a) D2D-PCS performance of DUE SINR with varied DUE distance

(b) Average D2D-PCS performance of DUE SINR with varied DUE distance

The DUE SINR performance of FPC, PCS1 and D2D-PCS when DUE distance was varied as presented in Table 4.6 and Figure 4.10a indicates that D2D-PCS had better DUE SINR. At DUE distance ranging from 1 – 10 m D2D-PCS DUE data rate was better than that of FPC by 126.32%, 72.22%, 58.82%, 47.06%, 50.00%, 43.75%, 37.50%, 46.67%, 46.67%, and 46.67%,

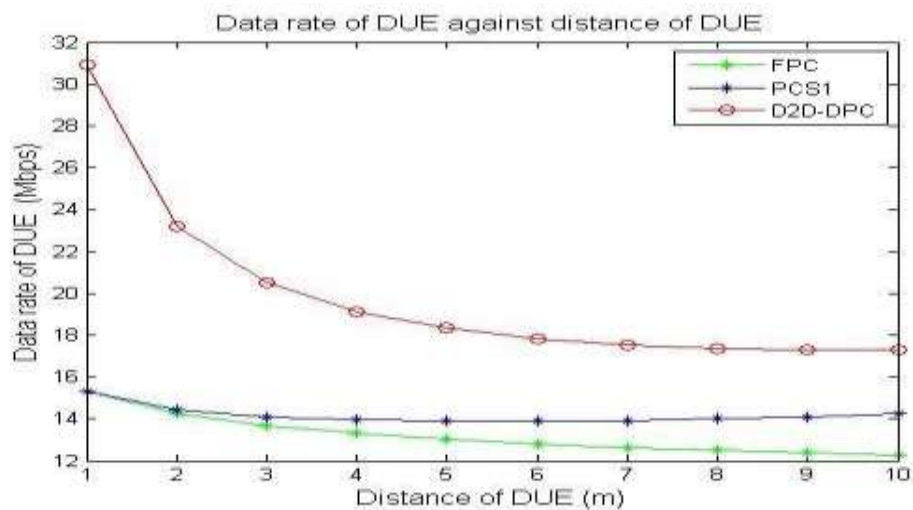
respectively, from equation (3.19), and better than PCS1 at DUE distance of 1 – 10 m by 126.32%, 72.22%, 50.00%, 47.06%, 41.18%, 35.29%, 29.41%, 22.22%, 22.22%, and 22.22% respectively, from equation (3.20)

The average DUE SINR of FPC, PCS1 and D2D-PCS when DUE distance was varied as presented in Figure 4.10b stood at 0.16, 0.18 and 0.26 respectively. Hence, D2D-PCS DUE SINR when DUE distance varied, was better than that of FPC and PCS1 by 62.50% and 44.44% respectively.

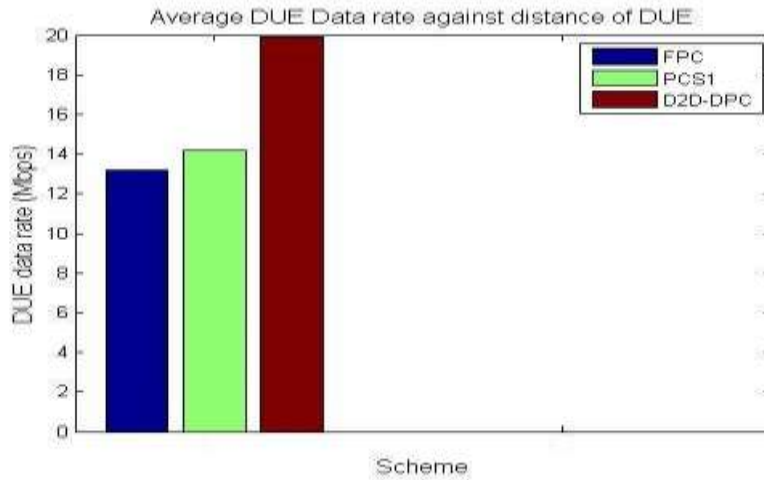
Table 4.7: Data rate of D2D- PCS with varied DUE distance

DUE (m)	FPC		PCS1		D2D- FPC		D2D- PCS		Average	
	PCS	D2D-	PCS	D2D-	PCS	D2D-	PCS	D2D-	PCS	D2D-
1	15.29	15.29	30.93	18.64	18.64	20.42	33.93	33.93	51.35	
2	14.23	14.45	23.18	18.64	19.20	20.75	32.88	33.65	43.93	
3	13.67	14.10	20.50	18.64	19.79	21.09	32.32	33.90	41.59	
4	13.30	13.95	19.13	18.64	20.42	21.81	31.95	34.37	40.57	
5	13.03	13.88	18.32	18.64	21.09	19.13	31.68	34.98	40.13	
6	12.82	13.88	17.82	18.64	21.81	22.19	31.46	35.70	40.01	
7	12.64	13.93	17.52	18.64	22.58		22.58	31.29	36.51	
8	12.49	14.00	17.34	18.64	23.40	22.98	31.14	37.41	40.34	
9	12.37	14.10	17.27	18.64	24.29	23.40	31.01	38.40	40.67	
10	12.25	14.23	17.26	18.64	25.25	23.84	30.90	39.48	41.10	<u>Average</u>
	13.21	14.18	19.93	18.64	21.65	21.82	31.86	35.83	41.98	

The DUE data rate performance of D2D- PCS when DUE distance was varied as in Table 4.7 was plotted and presented in Figure 4.11.



(a)



(b)

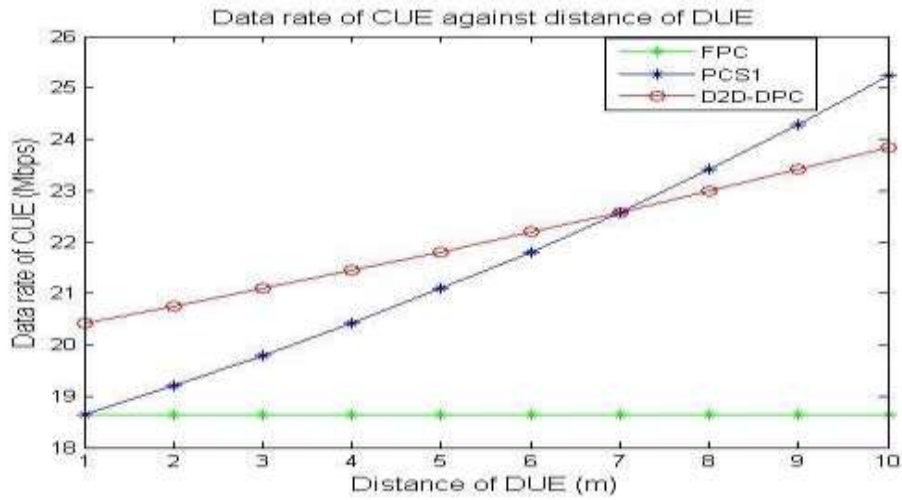
Figure 4.11: D2D-PCS DUE data rate based on varied DUE distance.

(a) Benchmarked D2D-PCS DUE data rate when DUE distance was varied

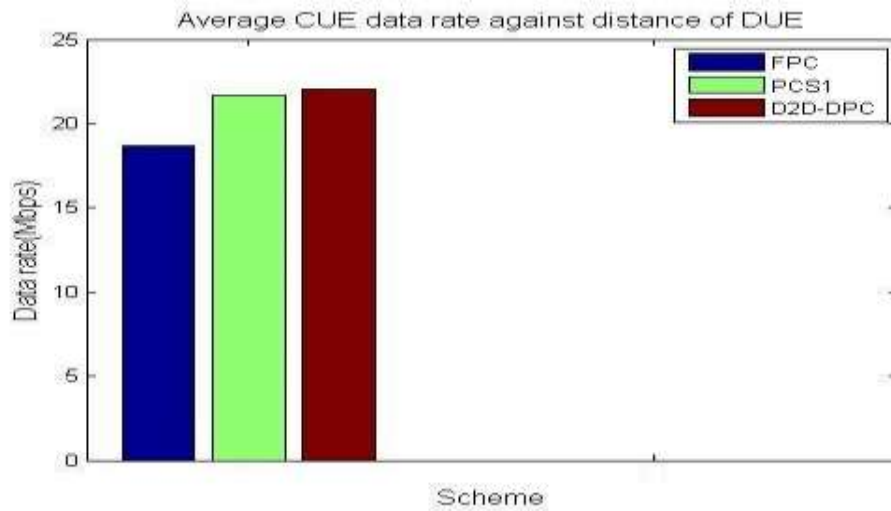
(b) Benchmarked D2D- PCS DUE data rate when DUE distance was varied

From Table 4.7 and Figure 4.11, D2D- PCS had better DUE data rate at different DUE distances. At DUE distance ranging from 1 – 10 m, D2D- PCS had DUE data rate that outperformed that of FPC by 102.07%, 62.88%, 49.92%, 43.89%, 40.37%, 39.02%, 38.61%, 38.98%, 39.77%, and 40.98%, respectively, according to equation (3.19), and that of PCS1 by 102.07%, 60.00%, 45.39%, 37.08%, 31.84%, 28.33%, 25.85%, 23.86%, 22.55%, and 21.27% respectively, according to equation (3.20). As shown in Figure 4.11b, the average DUE data rate of FPC, PSC1 and D2D- PCS when DUE distance was varied stood at 13.21 Mbps, 14.1 Mbps, and 19.93 Mbps respectively. When DUE distance was varied, D2D- PCS had an average DUE data rate which was better than that of FPC and PCS1 by 51.01% and 40.57% respectively.

The plotted performance of D2D- PCS scheme when DUE distance was varied as seen in Table 4.7, in terms of CUE data rate is presented in Figure 4.12.



(a)



(b)

Figure 4.12: D2D-PCS CUE data rate based on varied DUE distance.

(a) Benchmarked D2D- PCS CUE data rate when DUE distance was varied

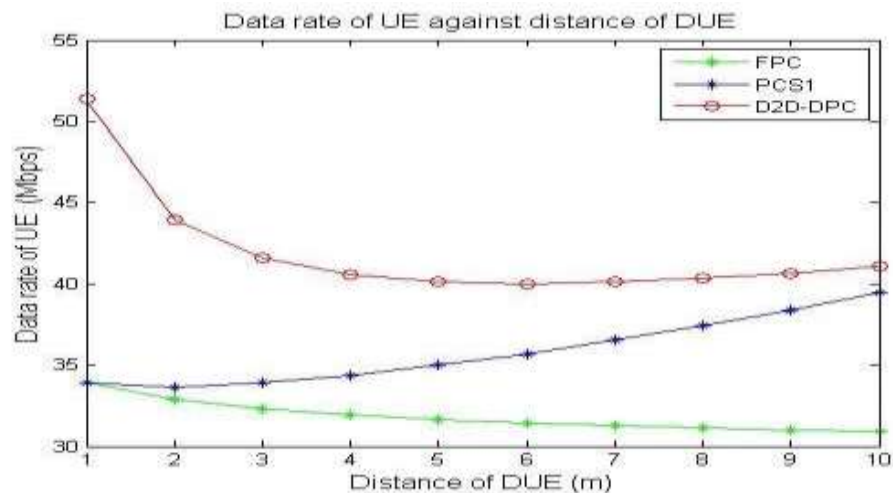
(b) Benchmarked average D2D- PCS CUE data rate when DUE distance was varied

From Table 4.7 and Figure 4.12 D2D- PCS had the best CUE data rate at DUE distance of 1 – 6 m. While at DUE distance of 8 – 10 m, PCS1 had the best CUE data rate. PCS1 and D2D- PCS had same DUE data rate at DUE distance of 7m. But when DUE distance was varied from 1 - 6 m, D2D- PCS had CUE data rate that outperformed that of FPC by

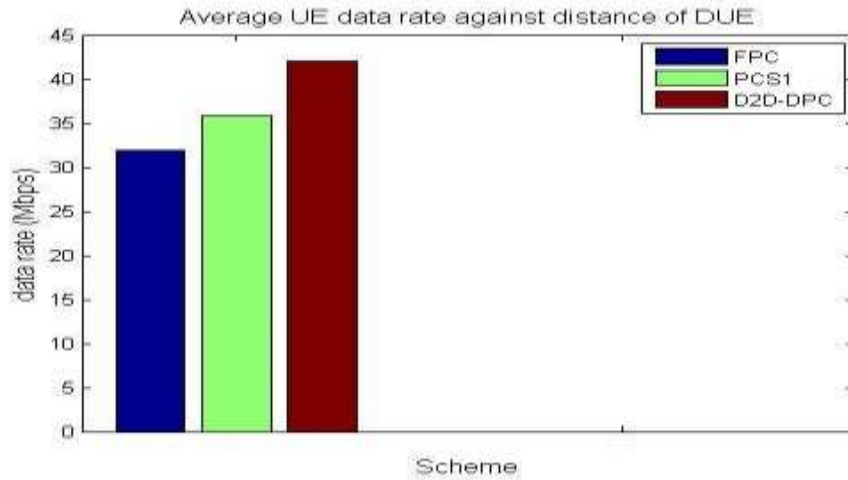
9.54%, 11.84%, 13.10%, 17.04%, 2.78%, and 18.67% respectively in accordance with equation (3.19), while D2D- PCS had CUE data rate that outperformed that of PCS1 by 9.55%, 8.07%, 6.57%, and 6.81% respectively, from equation (3.20). At DUE distance of 8 – 10 m, PCS1 CUE data rate outperformed that of FPC by 20.34 %, 23.26 %, and 26.18 % respectively, and outperformed D2D-PCS by 1.79%, 3.66%, and 5.58% respectively.

The result of average CUE data rate of FPC, PCS1 and D2D- PCS when DUE distance was varied as presented in Figure 4.12b gave 18.64 Mbps, 21.65 Mbps, and 22.09 Mbps respectively. D2D- PCS CUE data rate considering DUE distance was better than that of FPC and PCS1 by 17.06% and 0.80% respectively.

The plot of D2D-PCS UE data rate performance when DUE distance was varied is presented in Figure 4.13. Where Figure 4.13a gives the UE data performance at each DUE distance and Figure 4.13b gives the average UE data rate performance.



(a)



(b)

Figure 4.13: D2D-PCS UE data rate with varied DUE distance

(a) Benchmarked D2D- PCS UE data rate when DUE distance was varied

(b) Average D2D- PCS UE data rate when DUE distance was varied

According to results presented in Table 4.7 and Figure 4.13a, D2D- PCS had the best UE data rate when DUE distance was within 1 – 10 m.

At DUE distance ranging from 1 – 10 m, D2D- PCS had UE data rate that outperformed that of FPC by 51.37%, 33.62%, 28.64%, 26.94%, 26.69%, 27.12%, 28.17%, 29.56%, 31.14%, and 33.36% respectively, and outperformed PCS1 by 51.27%, 30.62%, 22.73%, 18.03%, 16.44%, 12.12%, 10.0%, 7.84%, 5.26%, and 4.1%, respectively, in accordance with equations (3.19) and (3.20) respectively.

The average UE data rate of FPC, PCS1 and D2D- PCS stood at 31.86 Mbps, 35.83 Mbps and 41.98 Mbps respectively.

FPC, PCS1 and D2D- PCS average power consumption of DUE at varying DUE distance was computed; and the result presented in Figure 4.14.

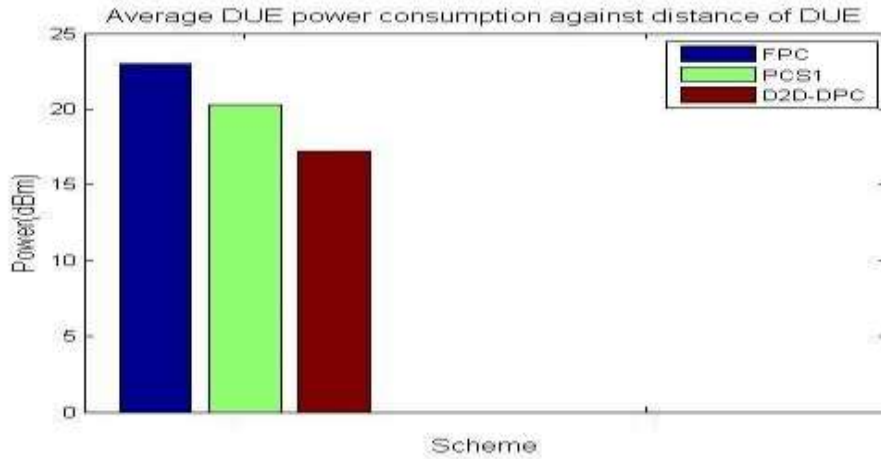


Figure 4.14: D2D-PCS Average DUE power against DUE distance.

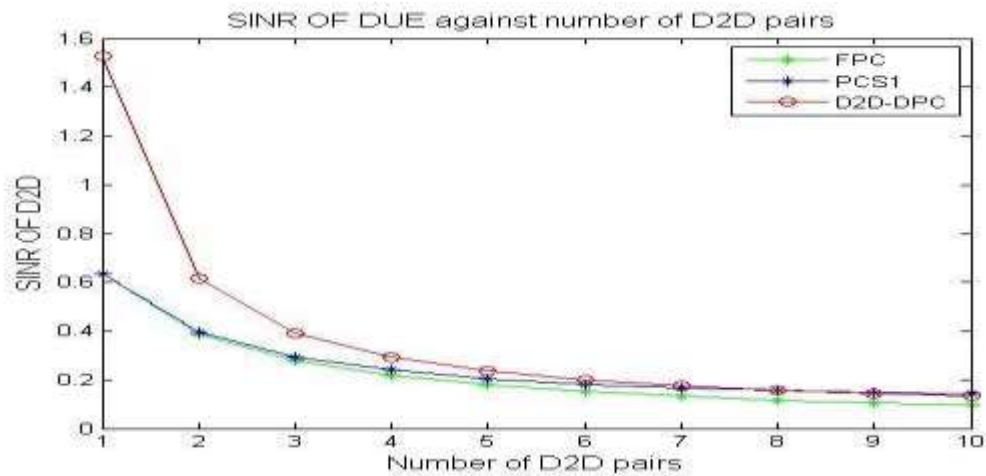
The average UE power consumption of FPC, PSC1 and D2D-PCS stood at 23.00 dB, 20.25 dB and 17.25 dB respectively.

The D2D- PCS performance when number of D2D pairs was altered, in terms of DUE SINR is presented in Table 4.8.

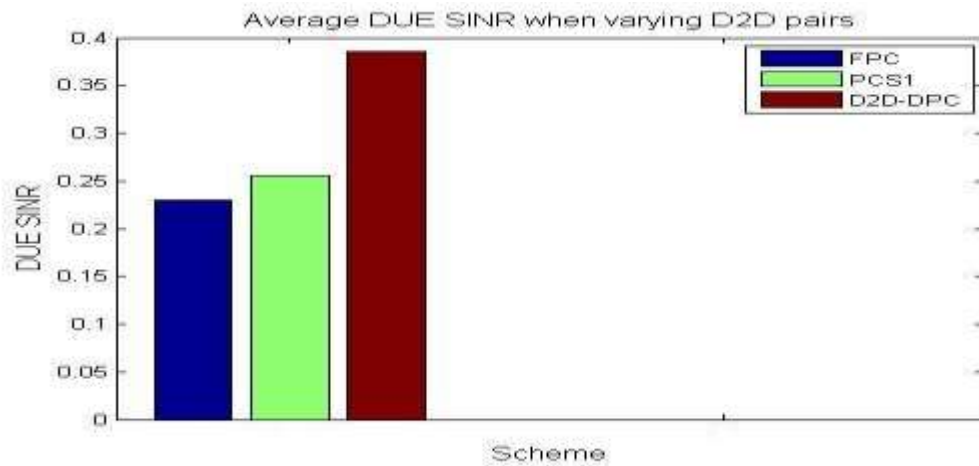
Table 4.8: SINR of D2D- PCS with varied number of D2D pairs

No. of D2D pairs.	DUE SINR		
	FPC	PCS1	D2D-PCS
1	0.63	0.63	1.53
2	0.39	0.39	0.61
3	0.28	0.29	0.39
4	0.22	0.24	0.29
5	0.18	0.20	0.24
6	0.15	0.18	0.20
7	0.13	0.17	0.17
8	0.12	0.16	0.16
9	0.10	0.15	0.14
10	0.09	0.14	0.13
Average	0.23	0.26	0.39

The D2D- PCS performance in terms of DUE SINR when number of D2D pairs was varied is presented in Figure 4.15.



(a)



(b)

Figure 4.15: D2D-PCS DUE SINR on varied D2D Pairs

- (a) Benchmarked D2D- PCS SINR of DUE when number of D2D pair was varied
- (b) An average D2D- PCS SINR of DUE when number of D2D pair was varied

From Table 4.7 and Figure 4.15, when number of D2D was varied from 1 – 8 pairs, D2D- PCS had the best DUE SINR when compared to FPC and PCS1. At 9 and 10 D2D pairs, PCS1 had the best DUE SINR compared to that of FPC and D2D- PCS.

At 1 – 8 D2D pairs, D2D- PCS have DUE SINR that outperformed that of FPC by

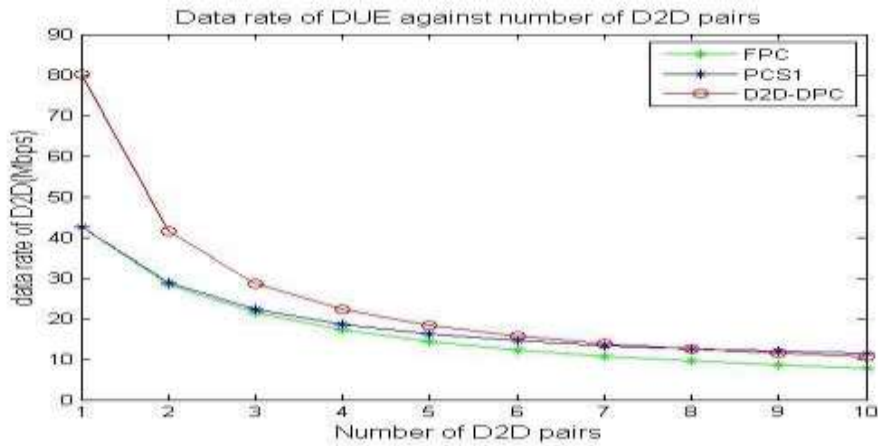
142.86%, 56.41%, 39.29%, 31.82%, 33.33%, 33.33%, 30.77%, and 33.33%. At 1 – 6 D2D pairs, D2D- PCS DUE SINR outperformed that of PCS1 by 142.86%, 56.41%, 34.48%, 20.83%, 20.00%, and 11.11% respectively, according to equations (3.19) and (3.20). At 7 and 8 D2D pairs, D2D- PCS and PCS1 had the same DUE SINR of 0.17 and 0.16 respectively. At 8 and 9 D2D pairs, PCS1 DUE SINR outperformed that of FPC by 33.33%, 35.71% respectively; and that of D2D- PCS by 6.67% and 7.14% respectively.

Results of average DUE SINR of FPC, PCS1 and D2D- PCS when DUE was varied as presented in Figure 4.15b, gave 0.23, 0.26 and 0.39. Hence, the average DUE SINR of D2D- PCS was higher compared to that of FPC and PCS1 by 69.57% and 50.00% respectively.

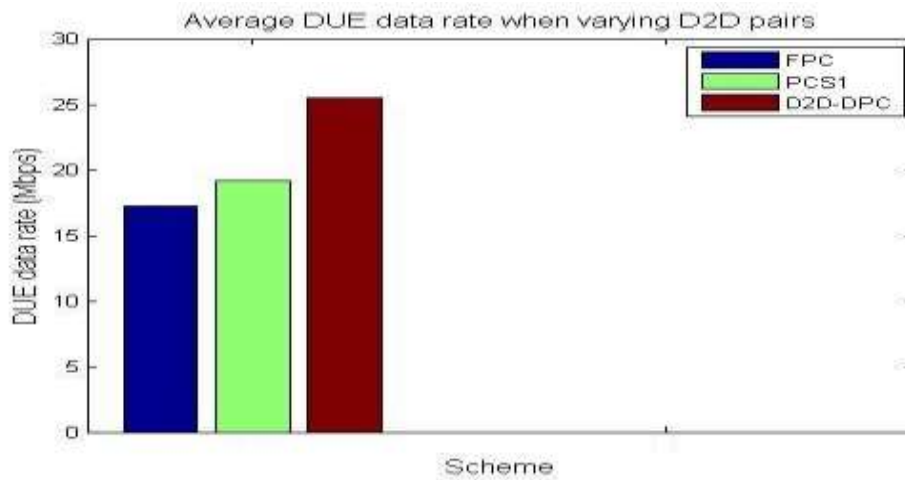
Table 4.9: Data rates of D2D- PCS with varied number of D2D pairs

No. of D2D	DUE data rate (Mbps)			CUE data rate (Mbps)			UE data rate (Mbps)					
	FPC	PCS1	D2D-	FPC	PCS1	D2D-	FPC	PCS1	D2Dpairs	PCS	PCS	PCS
1	42.53	42.53	80.19	8.96	8.96	8.80	51.49	51.49	89.00			
2	28.39	28.81	41.40	10.00	10.36	10.00	38.39	39.17	51.40			
3	21.34	22.31	28.59	11.30	12.13	11.49	32.65	34.44	40.08			
4	17.11	18.55	22.14	13.01	14.42	13.41	30.12	32.97	35.55			
5	14.23	16.14	18.27	15.31	17.47	15.95	29.59	33.60	34.22			
6	12.25	14.49	15.69	18.62	21.67	19.46	30.87	36.16	35.15			
7	10.73	13.32	13.87	23.75	27.75	24.60	34.48	41.07	38.46			
8	9.55	12.48	12.51	32.83	37.19	32.83	42.38	49.67	45.34			
9	8.60	11.89	11.47	53.54	53.54	48.17	62.14	65.43	59.65			
10	7.82	11.48	10.66	0.00	0.00	0.00	07.82	11.48	10.66	Average	17.26	19.20
	25.48	18.73	20.35	18.47	35.99	39.55	43.95					

Figure 4.16 is the DUE data rate performance at different number of D2D pairs.



(a)



(b)

Figure 4.16: D2D-PCS DUE data rate based on varied D2D pairs.

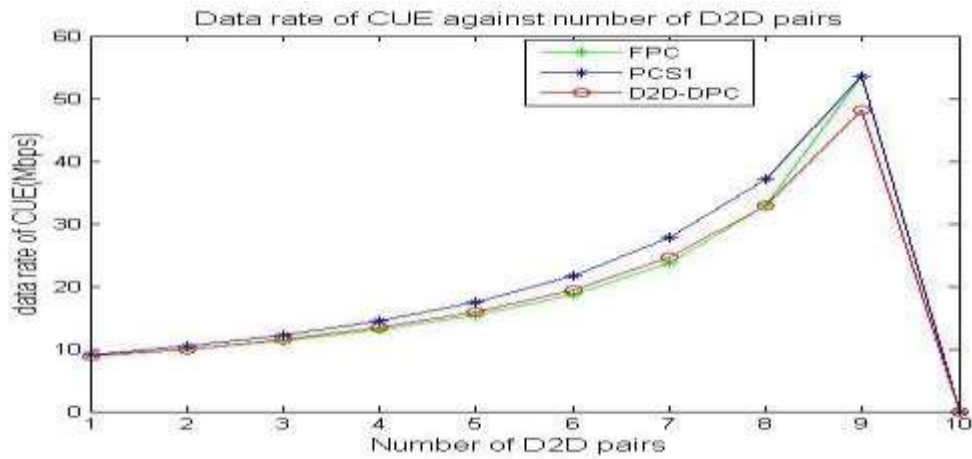
(a) Benchmarked D2D- PCS DUE data rate when number of D2D pairs was varied

(b) Average D2D- PCS DUE data rate when number of D2D pairs was varied

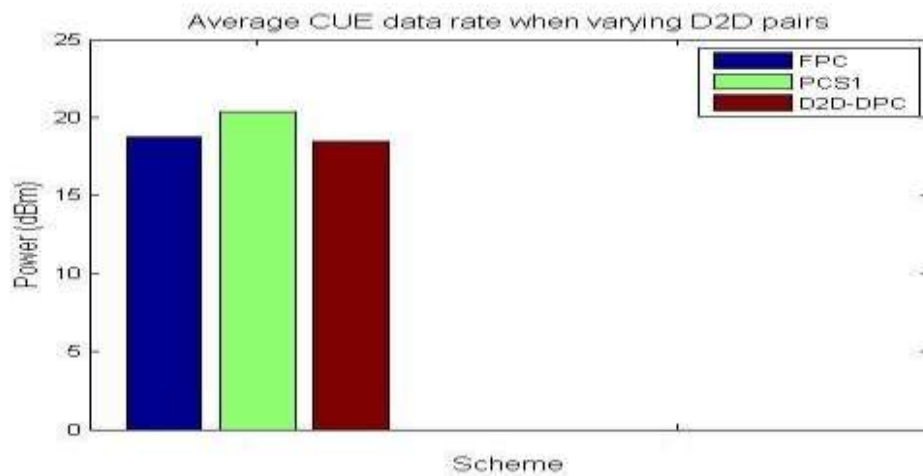
From Table 4.9 and Figure 4.16, at 1 – 8 D2D pairs, DUE data rate of D2D- PCS was better than that of FPC by 88.65%, 45.78%, 34.01%, 29.39%, 28.32%, 28.12%, 29.18%, and 31.08% respectively, according to equation (3.19), and better than that of PCS1 by 88.73%, 43.46%, 28.17%, 19.36%, 13.20%, 8.28%, 4.13%, and 0.24% respectively, from equation (3.20). At 9 and 10 D2D pairs, PCS1 had DUE data rate that outperformed that of FPC by 25.02% and 31.88% respectively; and higher than that of D2D- PCS by 3.53% and 7.14% respectively.

The result of average DUE data rate of FPC, PCS1 and D2D-PCS at varying number of D2D pairs gave 17.26 Mbps, 19.20 Mbps and 25.48 Mbps respectively. The average DUE data rate of D2D- PCS is better than that of FPC and PCS1 by 47.62%, and 32.71% respectively.

The CUE data rate performance at different D2D pairs is presented in Figure 4.17.



(a)



(b)

Figure 4.17: D2D- PCS CUE data rate with varied D2D pairs

(a) D2D-PCS CUE data rate with varied number of D2D pairs

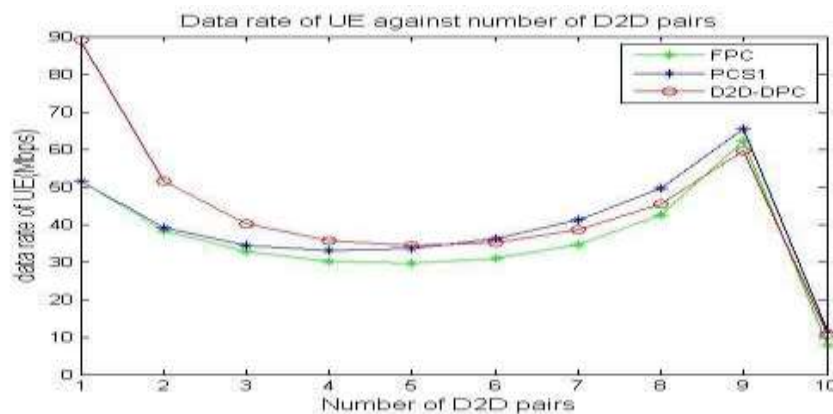
(b) Average D2D-PCS CUE data rate with varied number of D2D pairs

From Table 4.9 and Figure 4.17, when number of D2D pairs was 10, CUE data rate of FPC, PCS1 and D2D- PCS were all 0.0 Mbps, because all UEs were in D2D mode. And when number of D2D pair was varied from 2 – 8 pairs, the CUE data rate of PCS1 was better than that of FPC by 3.47%, 6.84%, 9.78%, 12.36%, 14.07%, 14.41%, and 11.72% respectively. At 1 and 9 D2D pairs, D2D- PCS and FPC had same data rate of 8.96 Mbps, and 53.54 Mbps.

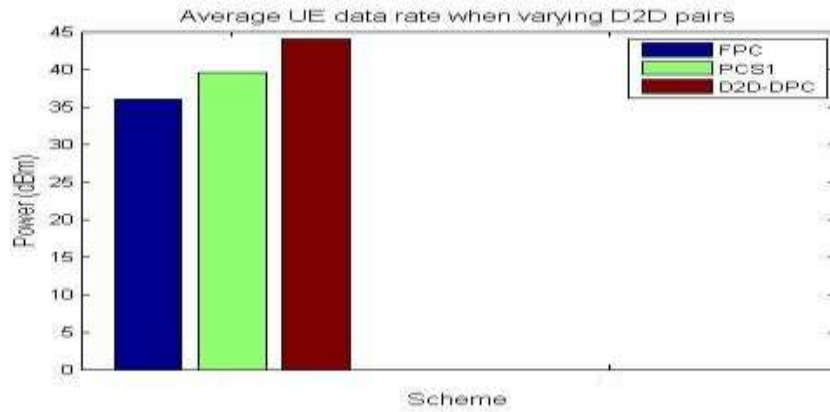
The CUE data rate of PCS1 at varying number of D2D pairs ranging from 1 – 9, was better than that of D2D- PCS by 1.79%, 3.47%, and 5.28%, 7.00%, 3.47%, 10.20 %, 11.35%, 11.72% and 10.03% respectively, in accordance with equation (3.20).

The average DUE data rate of FPC, PCS1 and D2D-PCS at varying number of D2D pairs in Figure 4.17b stood at 18.73 Mbps, 20.35 Mbps and 18.47 Mbps respectively. The average PCS1 average DUE data rate at varying number of D2D pairs outperformed that of FPC and D2D-PCS by 8.64% and 10.18% respectively.

D2D- PCS UE data rate performance with varied D2D pairs is presented in Figure 4.18.



(a)



(b)

Figure 4.18: D2D-PCS UE data rate with varied D2D pairs

(a) D2D- PCS UE data rate with varied number of D2D pairs

(b) Average D2D-PCS UE data rate with varied D2D pairs

From Table 4.9 and Figure 4.18, when number of D2D pairs varied from 1 – 5, D2D-PCS UE data rate outperformed that of FPC by 72.7%, 33.9%, 22.7%, 18%, and 15.7%, and performed better than PCS1 UE data rate by 72.72%, 31.19%, 16.36%, 7.83%, and 1.85% respectively, in accordance with equations (3.19) and (3.20).

The average UE data rate of FPC, PCS1 and D2D-PCS when number of D2D pairs was varied as seen in Figure 4.18b gave 35.99 Mbps, 39.55 Mbps and 43.95 Mbps respectively. Average UE data rate of D2D-PCS at varied number of D2D pairs performed better than that of FPC and PCS1 by 22.12% and 11.13% respectively. The average DUE power consumption at different number of D2D pairs is presented in Figure 4.19.

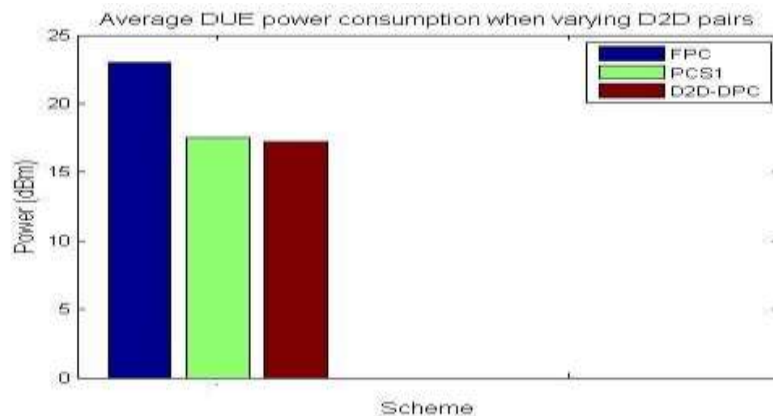


Figure 4.19: D2D- PCS average power consumption with varied D2D pairs.

From Figure 4.19, the average power consumed by DUEs based on Fixed Power Control (FPC), PCS1 and D2D-PCS schemes was 23.00 dBm, 17.50 dBm and 17.25 dBm respectively, which indicates a 1.43% and 25% power efficiency of the D2D-PCS over the PCS1 and FPC schemes respectively.

CHAPTER 5

5.0 CONCLUSION AND RECOMMENDATIONS

5.1 Conclusion

In this work, Mode Selection and Bandwidth Allocation techniques were integrated into a scheme (MS-BAS) to mitigate cross-tier interference, while the D2D Power Control Scheme (D2D-PCS) was developed to mitigate the incidence of co-tier interference in the D2D tier of the network.

The mode selection sub-scheme focused on the UE separation distance and the receiver's SINR to assign communication mode to UEs, while the bandwidth allocation sub-scheme allocated a fixed fraction of 60% of the spectrum to CUEs, and 30% for D2D connections, while dynamically allocating the remainder 10% to deserving communication tier based on the number of UEs in that mode, to maximize data rate, and limit spectrum wastage. The D2D-PCS starts with a low initial transmit power by UEs, thereby conserving energy and reducing interference.

The MS-BAS delivered an average data rate of 43.17 Mbps across the network, indicating a 29.37% improvement when compared with the existing SOMO, and an average SINR of 2.02 representing a 37.41% improvement. The energy efficient D2DPCS recorded an

SINR of 0.39, indicating a 69.57% and 50.00% improvement over the FPC and PCS1 schemes respectively, an average data rate of 25.48 Mbps, indicating a 47.62% and 32.71% performance improvement over the FPC and PCS1 schemes respectively, and a 17.25 dBm DUE average power utilization against 23.00 dBm and 17.50 dBm for the FPC and PCS1 schemes respectively.

The integration of the Mode Selection and Bandwidth Allocation Schemes (MS-BAS), coupled with the D2D-PCS lead to the attainment of better system performance compared with the previous works of Swetha and Murthy, (2017), and Rana *et al.*, (2021). Therefore, the MS-BAS and D2D- PCS addressed the problem of both cross-tier and cotier interference, while improving system throughput, increasing energy conservation, and avoiding spectrum wastage.

5.2 Recommendations

From the algorithmic performance and system behaviour as evidenced in the simulation results, it is seen that the joint usage of the MS-BAS and D2D-PCS schemes have the potential to mitigate the cross-tier and co-tier interferences in the macro-D2D network, and it is recommended for researchers as well as design experts to explore its usage, both as-is, and in combination with other schemes for the mitigation of interference. And for the furtherance of research, future work is recommended in the application of the schemes to multi-cell network scenarios, while considering a larger number of UEs over a longer distance.

5.3 Contribution to Knowledge

The main contributions of this work to the body of knowledge are the development, and validation through simulations, of new methodologies, namely MS-BAS and D2D-PCS, for the mitigation of cross-tier and co-tier interference scenarios respectively, while

improving both energy and spectral efficiency, SINR, and throughput of macro-D2D networks. The 29.37% and 37.41% improvement in data rates and SINR respectively achieved by the MS-BAS, and the 25% improvement in power efficiency achieved by the D2D-PCS translates into improved service quality to subscribers thereby boosting productivity and Return on Investment (ROI) to service providers, which would, of course, boost the national economy.

REFERENCE

- 3GPP Release 8.0 (2014): Overview of 3GPP Release 8. Retrieved on 24th May 2022 from <http://www.3gpp.org/specifications/releases/72-release-8>.
- 5GPPP (2015): The next generation of communication networks and services, European Commission, (2015). Retrieved on 24th May 2022 from <http://5g-ppp.eu/wpcontent/uploads/2015/02/5G-Vision-Brochure-v1.pdf>.
- Adejo, A., Asaka, O., Bello-Salau, H., & Alenoghena, C. (2020). New framework for interference and energy analysis of soft frequency reuse in 5G networks. *Bulletin of Electrical Engineering and Informatics*, 9(5), 1941–1949.
- Adejo A., Said, B., & Jeffrey, N. (2017a). Interference Modelling for Soft Frequency Reuse in Irregular Heterogeneous Cellular Networks. *International Conference on Ubiquitous and Future Networks (ICUFN)*, 9, 381 -386.
- Adejo, A., Hussein, J., & Boussakta, S. (2017b). Optimal transmit power configuration for soft frequency reuse in irregular cellular networks. *International Conference on Ubiquitous and Future Networks*. 711 - 713.
- Adnan, M.H, and Zuriati A.Z. (2020). Device-to-device communication in 5G environment: Issues, solutions, and challenges. *Symmetry* 12, no. 11 (2020): 1762. 1 – 22.
- Agyapong PK, Iwamura M, Staehle D, Kiess W, and Benjebbour A, (2014). Design considerations for a 5G network architecture, *IEEE Communications Magazine*, 52(11), 65 – 75.
- Alquhali, A. H., Roslee, M., Alias, M. Y., & Mohamed, K. S. (2020). D2D communication for spectral efficiency improvement and interference reduction: A survey. *Bulletin of Electrical Engineering and Informatics*, 9(3), 1085–1094.
- Alsharif, M.H., Nordin, R., (2017). Evolution towards fifth generation (5G) wireless networks: current trends and challenges in the deployment of millimetre wave, massive MIMO, and small cells. *Telecommun. Syst.* 64, 617–637.

- Alzubaidi, O.T.H.; Hindia, M.N.; Dimiyati, K.; Noordin, K.A.; Wahab, A.N.A.; Qamar, F.; Hassan, R. (2022) Interference Challenges and Management in B5G Network Design: A Comprehensive Review. *Electronics*, 11, 2842. 1 – 21.
- Andreev S, Galinina O, Pyattaev A, Hosek J, Masek P, Yanikomeroğlu H, and Koucheryavy Y., (2016). Exploring synergy between communications, caching, and computing in 5G-grade deployments, *IEEE Communications Magazine*, 54(8), 60–69.
- Andrews, J.G, Buzzi, S., Choi, W., Hanly, S.V, Lozano, A., Soong, A.C., and Zhang, J.C. (2014) What will 5G be? *IEEE Journal on selected areas in communications*, 32(6). 1065–1082.
- Ansari, R. I., Chrysostomou, C., Hassan, S. A., Guizani, M., Mumtaz, S., Rodriguez, J., & Rodrigues, J. J. P. C. (2018). 5G D2D Networks: Techniques, Challenges, and Future Prospects. *IEEE Systems Journal*, 1–15.
- Asadi, A, Wang Q, and Mancuso V, (2014). A survey on device-to-device communication in cellular networks, *IEEE Communications Surveys & Tutorials*, 16(4), 1801–1819.
- Attia, E. S., El-Dolil, S. A., & Abd-Elnaby, M. (2017). Performance enhancement-based resource allocation scheme using soft frequency reuse for LTE femtocell networks. *National Radio Science Conference, NRSC, Proceedings*, 246–255.
- Atzori, L., Iera, A., & Morabito, G. (2010). The Internet of Things: A survey. *Computer Networks*, 54(15), 2787–2805.
- Barik P.K., Shukla A, Datta R., and Singhal C., (2020). A Resource Sharing Scheme for Intercell D2D Communication in Cellular Networks: A Repeated Game Theoretic Approach. *IEEE Transactions on Vehicular Technology*. 1(1). 1 – 15.
- Bastug E, Bennis M, Médard M, and Debbah M, (2017) Toward Interconnected Virtual Reality: Opportunities, Challenges, and Enablers, *IEEE Communications Magazine*, 55(6), 110–117.
- Bhandari N., Devra S., & Singh K., (2017). Evolution of Cellular Network: From 1G to 5G. *International Journal of Engineering and Techniques – 3(5)*. 1 – 12.
- Binkley P.F, (2003) Predicting the potential of wearable technology, *IEEE engineering in medicine and biology magazine*, 22(3), 23–27.
- Budhiraja, I., Tyagi, S., Tanwar, S., Kumar, N., & Guizani, M. (2018). Cross Layer NOMA Interference Mitigation for Femtocell Users in 5G Environment. *Global Communications Conference, (GLOBECOM)*, 112 -125.
- Chai, Yingqi, Qinghe Du, and Pinyi Ren (2013) Partial time-frequency resource allocation for device-to-device communications underlying cellular networks.

Communications (ICC), IEEE International Conference on Communication. 6055 – 6059.

- Chen, H., Deng, X., Gao, M., Yang, L., Guo, L., & Chi, M. (2018). Location Related Communication Mode Selection and Spectrum Sharing for D2D Communications in Cellular Networks. *International Conference on Intelligent Transportation, Big Data & Smart City.* 169-173.
- Cheng, X., Hu, Y. and Varga, L. (2022). 5G network deployment and the associated energy consumption in the UK: A complex systems' exploration. *Technological Forecasting and Social Change.* 180 (2022) 121672. 1-24.
- Cho B, Koufos K, and Jantti J, (2013) Interference control in cognitive wireless networks by tuning the carrier sensing threshold, *IEEE International Conference on Cognitive Radio Oriented Networks*, 282-287.
- Chou, H.J.; Chang, R.Y. (2017) Joint Mode Selection and Interference Management in Device-to-Device Communications Underlaid MIMO Cellular Networks: *IEEE Trans. Wireless Communication*, 16, 1120–1134.
- Chih-Lin, I., Han, S., Bian, S., (2020). Energy-efficient 5G for a greener future. *Nature Electronics.* 3(4), 182–184.
- Cisco (2017): Cisco Visual Networking Index: Global Mobile Data Traffic Forecast Update, 2015–2020 White Paper, *Cisco Public Information.*
- Cisco, (2020). Cisco Annual Internet Report (2018–2023) White Paper. Retrieved on 16th March 2021 from <https://www.cisco.com/c/en/us/solutions/collateral/executiveperspectives/annual-internet-report/white-paper-c11-741490.html>
- Dawar, K. P., Usman, A. U., & Salihu, B. A. (2021). An Enhanced Active Power Control Technique for Interference Mitigation in 5G Uplink Macro-Femto Cellular Network. *IEEE International Conference on cyberspace (CYBER NIGERIA)*, 2, 85-90.
- DCMS, (2017). Next Generation Mobile Technologies: A 5G Strategy for the UK. Retrieved on May 24th, 2022 from [Microsoft Word - 07.03.17 5G strategy - for publication.docx \(publishing.service.gov.uk\)](#)
- Doppler K, Yu C.H, Ribeiro C.B, and Jänis P, (2010) Mode selection for device-to-device communication underlaying an LTE-Advanced network,” *IEEE Wirel. Commun. Netw. Conf. WCNC.* 1 – 6.
- Dunne L.E, Profita H, Zeagler C, Clawson J, Gilliland S, Do E.Y, and Budd J, (2014) The social comfort of wearable technology and gestural interaction, *36th annual international Conference of the IEEE Engineering in medicine and biology society (EMBC)*, 4159–4162.

- Ericsson Mobility Report (2015): On the Pulse of the Networked Society, Retrieved on 6th June 2017 from <http://www.ericsson.com/res/docs/2015/ericsson-mobilityreport-june-2015.pdf>.
- Ericsson White Paper (2011): More than 50 billion connected devices, Retrieved on 6th June 2017 from http://www.akos-rs.si/files/Telekomunikacije/Digitalna_agenda/Internetni_protokol_Ipv6/Morethan-50-billion-connected-devices.pdf
- Fodor G., and Reider N. (2011) A distributed power control scheme for cellular network assisted D2D communications. *IEEE Global Telecommunications Conference (GLOBECOM)*. 1 – 6.
- Gandotra, P., & Jha, R. K. (2016). Device-to-Device Communication in Cellular Networks: A Survey. *Journal of Network and Computer Applications*, 71, 99–117.
- Gao, X.; Yang, K.; Yang, N.; Wu, J. (2019) Energy-efficient resource block assignment and power control for underlay Device-to-Device communications in multi-cell networks. *Computer Networks*, 149, 240–251.
- Ge X, Cheng H, Guizani M, and Han. T (2014) 5G Wireless Backhaul Networks: Challenges and Research Advances. *IEEE Network*, 28(6):6–11.
- Ghavimi F and Chen H, (2015) M2M communications in 3GPP LTE/LTE-A networks: architectures, service requirements, challenges, and applications, *IEEE Communications Surveys & Tutorials*, 17(2), 525–549.
- GSMA Intelligence (2014) Understanding 5G: Perspectives on future technological advancements in mobile. Retrieved on July 2nd, 2017 from <https://gsmaintelligence.com/research/?file=141208-5g.pdf&download>.
- Gu J, Bae S.J, Choi B.G, and Chung M.Y, (2011) Dynamic power control mechanism for interference coordination of device-to-device communication in cellular networks, *Third International Conference on Ubiquitous Future Networks*, 71–75.
- Guo, B., Sun, S., & Gao, Q. (2015) Interference Management for D2D Communications Underlying Cellular Networks at Cell Edge, *The Tenth International Conference on Wireless and Mobile Communications (ICWMC)*. 118 – 123.
- Gupta, S., Kumar, S., Zhang, R., Kalyani, S., Giridhar, K., & Hanzo, L. (2016). Resource Allocation for D2D Links in the FFR and SFR Aided Cellular Downlink. *IEEE Transactions on Communications*, 64(10), 4434 – 4448.
- Hao, J., Zhang, H., Song, L., & Han, Z. (2015). Graph-based resource allocation for device-to-device communications aided cellular network. *IEEE/CIC International Conference on Communications in China, ICCIC*, 256–260.

- Hassan, M.Y., Hussain, F., Hossen, M.S., Choudhury, S., & Alam, M.M. (2017). Interference Minimization in D2D Communication Underlying Cellular Networks. *IEEE Access*, 5, 22471–22484.
- Hassan, T. U., & Gao, F. (2019). An Active Power Control Technique for Downlink Interference Management in a Two-Tier Macro–Femto Network. *Journal of Sensors*, 19(9), 504 - 528.
- Hassan, T. U., Gao, F., Jalal, B., & Arif, S. (2018). Interference Management in Femtocells by the Adaptive Network Sensing Power Control Technique. *Journal of Future Internet*, 10(3), 2015 -2028.
- Hwang I, Song B, and Soliman S.S., (2013). A holistic view on hyper-dense heterogeneous and small cell networks, *IEEE Communications Magazine*, 51(6) 20–27.
- Iskandar, and Nuraini, H. (2016). Inter-cell interference coordination with soft frequency reuse method for LTE network. *International Conference on Wireless and Telematics*. 57 – 61.
- Jameel, F., Hamid, Z., Jabeen, F., Zeadally, S., & Javed, M. A. (2018). A survey of device-to-device communications: Research issues and challenges. *IEEE Communications Surveys and Tutorials*, 20(3), 2133–2168.
- Jänis, & Pekka, (2009) Interference-avoiding MIMO schemes for device-to-device radio underlying cellular networks. *IEEE 20th International Symposium on Personal, Indoor and Mobile Radio Communications*. 2385 – 2389.
- Jo M, Maksymyuk T, Batista, R.L, Maciel T.F, De Almeida A.L, and Klymash M, (2014) A survey of converging solutions for heterogeneous mobile networks, *IEEE Wireless Communications*, (21)6, 54–62.
- Junjie Tan, Ying-Chang Liang, & Gang Feng (2021). Deep Reinforcement Learning for Joint Channel Selection and Power Control in D2D Networks. *IEEE Transactions on Wireless Communications*, (20)2, 1363 – 1378.
- Kamruzzaman, M.; Sarkar, N.I.; Gutierrez, J.; Ray, S.K. (2019). A mode selection algorithm for mitigating interference in D2D enabled next-generation heterogeneous cellular networks. *Proceedings of the 2019 International Conference on Information Networking*, Kuala Lumpur, Malaysia, 131–135.
- Kar, U.N., & Sanyal, D.K. (2017). An overview of device-to-device communication in cellular networks. *ICT Express*. Vol 4 (4), 203 – 208.
- Khan F, Pi Z, and Rajagopal S, (2012). Millimeter-wave mobile broadband with large scale spatial processing for 5G mobile communication, in *50th Annual Allerton Conference on Communication, Control, and Computing (Allerton)*, 2012, 1517–1523.

- Koushik, M. & Shahedur, R. (2021); Multi-cell Interference Management in In-band D2D communication under LTE-A Network. *4th International Conference on Computing, Electronics and Communications Engineering*, University of Essex, Southend, UK. 16 – 17.
- Kujur, U. and Shukla, R. (2018); Features Analysis and Comparison of 5G Technology: A Review. *International Journal of Advanced Research in Computer Engineering & Technology* 7(5), 2278 – 1323.
- Kushalnagar N, Montenegro G, and Schumacher C, (2007) IPv6 over low-power wireless personal area networks (6LoWPANs): overview, assumptions, problem statement, and goals, *Wireless Personal Area Networks*. (n.d.). *Wireless Broadband Networks*, 429–462.
- Lee, W, Kim J, and Choi S. (2016) New D2D Peer Discovery Scheme based on Spatial Correlation of Wireless Channel, *IEEE Transaction on Vehicular Technology*. 65(12), 10120–10125.
- Lei, L., Shen, X.S, Dohler, M., Lin, C., & Zhong, Z (2014) Queuing Models with Applications to Mode Selection in Device-to-Device Communications Underlying Cellular Networks, *IEEE Transactions on Wireless Communication*, 13(12), 6697–6715.
- Li, C., Yongacoglu, A., & D’Amours, C. (2016). Heterogeneous cellular network user distribution model. *IEEE Latin-American Conference on Communications*. 1 – 6.
- Li, M. (2019). Soft Frequency Reuse-Based Resource Allocation for D2D Communications Using Both Licensed and Unlicensed Bands. *International Conference on Ubiquitous and Future Networks*, 384–386.
- Li, Y, Song, W. Su, Z, Huang, L, Gao, Z, (2018) A distributed mode selection approach based on evolutionary game for Device-to-Device communications. *IEEE Access 2018*, (6) 60045–60058.
- Librino, F., & Quer, G. (2018). Distributed Mode and Power Selection for NonOrthogonal D2D Communications: A Stochastic Approach. *IEEE Transactions on Cognitive Communications and Networking*, 4(2), 232–243.
- Lindner, S., Elsner, R., Tran, P. N., & Timm-Giel, A. (2019). A two-game algorithm for device-to-device resource allocation with frequency reuse. *IEEE Vehicular Technology Conference*, 1–5.
- Ma C, Liu J, Tian X, Yu H, Cui Y, and Wang X, (2015) Interference exploitation in D2D-enabled cellular networks: A secrecy perspective, *IEEE Trans. Commun.*, 63(1), 229–242.

- Masek P, Hosek J, Zeman K, Stusek M, Kovac D, Cika P, and Kropfl F, (2016) Implementation of true IoT vision: Survey on enabling protocols and hands-on experience, *International Journal of Distributed Sensor Networks*. 12 (4), 2 – 18.
- Masek, P., (2017) Heterogeneous Connectivity of Mobile Devices in 5g Wireless Systems, *Doctoral Thesis Submitted to the Department of Telecommunications, Faculty of Electrical Engineering and Communication, BRNO University of Technology, BRNO, Czech Republic*. 9 – 41.
- Melki, L. (2017). Radio Resource Management for Device-to-Device Communications Underlying Network (*Doctoral dissertation, Telecom SudParis, France*).
- METIS final project report, Deliverable D8.4, METIS, (2015). Retrieved on July 19th, 2022 from https://www.metis2020.com/wpcontent/uploads/deliverables/METIS_D8.4_v1.pdf
- Mumtaz, S., Huq, K. M. S., Radwan, A., Rodriguez, J., & Aguiar, R. L. (2014). Energy efficient interference-aware resource allocation in LTE-D2D communication. *IEEE International Conference on Communications (ICC)*. 282 – 287.
- Nasser, A., Muta, O., Elsabrouty, M., & Gacanin, H. (2019). Interference Mitigation and Power Allocation Scheme for Downlink MIMO-NOMA HetNet. *IEEE Transactions on Vehicular Technology*, 1–1. 6805 – 6816.
- Ningombam, D. D., Pyun, J., Hwang, S., & Shin, S. (2017). Fractional Frequency Reuse Scheme for Interference Mitigation in Device-to-Device Communication Underlying LTE-A Networks. *51st Asilomar Conference on Signals, Systems, and Computers*. 1402–1406.
- Ningombam, D.D., & Shin, S. (2019). Resource-sharing optimization for multicast D2D communications underlying LTE-a uplink cellular networks. *Proceedings of the ACM Symposium on Applied Computing, Part F1477*, 2001–2007.
- Nokia Networks White Paper (2016): 5G Use cases and requirements. Retrieved on September 12th 2018 from http://www.techdigest.tv/wp-content/uploads/2016/02/5g_requirements_white_paper-2.pdf
- Noura M and Nordin R (2016). A Survey on Interference Management for Device-to-Device (D2D) Communication and its Challenges in 5G Networks, *Journal of Network and Computer Applications*, Vol. 71, 130 – 150.
- Oleshchuk V and Fensli R, (2011) Remote patient monitoring within a future 5G infrastructure, *Wireless Personal Communications*, 57(3), 431–439.
- Onu, C., Bala. S., & Abolarinwa J. (2018). Enhanced Fractional Frequency Reuse in LTE A Heterogeneous OFDMA Network. *ATBU, Journal of Science, Technology & Education (JOSTE)*, 6 (2), 18 – 27.

- Osanaiye, Opeyemi, Choo K.R, and Dlodlo M. (2016) Distributed Denial of Service (DDoS) Resilience in Cloud: Review and Conceptual Cloud DDoS Mitigation Framework. *Journal of Network and Computer Applications*. Vol. 67, 147 – 165.
- Qian, M., Hardjawana, W., Li, Y., Vucetic, B., Shi, J., & Yang, X. (2012). Inter-cell Interference Coordination Through Adaptive Soft Frequency Reuse in LTE Networks. 1618 – 1623.
- Rana, Z.A., Abdul, R.J., Shakir, M., Mohammad, Z.K., Abdulfattah, N. & Muhammad, R. (2021). Interference Mitigation in D2D Communication Underlying Cellular Networks: Towards Green Energy. *Computers, Materials & Continua*, 68(1), 45 – 58.
- Ratasuk R, Prasad A, Li Z, Ghosh A, and Uusitalo M.A, (2015) Recent advancements in M2M communications in 4G networks and evolution towards 5G, *18th International Conference on Intelligence in Next Generation Networks (ICIN)*, 52–57.
- Ravindra S, and Siddesh G, (2019) Interference Mitigation and Mobility Management for D2D Communication in LTE-A Networks, *International Journal of Wireless and Microwave Technologies*, 2, 20-31.
- Safaei, B, Mahdi, A, Monazzahy, H, Milad B and Ejlali, A., (2017). Reliability SideEffects in Internet of Things Application Layer Protocols. *International Conference on System Reliability and Safety; At: Milan, Italy*. 207 – 212.
- Salihu, B. A., Yang, D., Zhang, X., Zubair, S., & Olawoyin, L. (2014). Scheduling in Interference-Limited Environment for LTE-A Systems. *International Journal of Future Generation Communication and Networking*, 7(5), 179–190.
- Shafi M, Molisch A.F, Smith P.J, Haustein T, Zhu P, De Silva P, and Wunder G, (2017) 5G: A Tutorial Overview of Standards, Trials, Challenges, Deployment, and Practice, *IEEE Journal on Selected Areas in Communications*, 35(6), 1201–1221.
- Shami T.M, Grace D., Burr1 A., and Vardakas J.S. (2019). Load balancing and control with interference mitigation in 5G heterogeneous networks. *EURASIP Journal on Wireless Communications and Networking:177 (1)*. 1 – 12.
- Shuminoski T., and Janevski, T., (2013) Radio network aggregation for 5G mobile terminals in heterogeneous wireless networks, *11th International Conference on Telecommunication in Modern Satellite, Cable and Broadcasting Services (TELSIKS)*, 1, 225–228, IEEE.
- Sihan, L., Yucheng, W., Liang, L., Xiaocui, L., & Weiyang X. (2019). A Two-Stage Energy-Efficient Approach for Joint Power Control and Channel Allocation in D2D Communication. *IEEE ACCESS*, 7, 16940 – 16951.

- Simsek, M., Aijaz, A., Dohler, M., Sachs, J., & Fettweis, G. (2016). The 5G-Enabled Tactile Internet: Applications, requirements, and architecture. 2016 IEEE Wireless Communications and Networking Conference Workshops (WCNCW). 1 – 6.
- Song, X., Han, X., Ni, Y., Dong, L., & Qin, L. (2019). Joint uplink and downlink resource allocation for D2D communications system. *Future Internet*, 11(1), 1–6.
- Swetha, G.D., & Murthy, G.R. (2017). Selective Overlay Mode Operation for D2D communication in dense 5G cellular networks. *IEEE Symposium on Computers and Communications*. 704 – 709.
- Talwar S, Yeh S, Himayat N, Johnsson K, Wu G, and Hu R.Q., (2013). Capacity and Coverage Enhancement in Heterogeneous Networks, *Heterogeneous Cellular Networks*, 51–65.
- Tehrani M, Uysal M, and Yanikomeroglu H, (2014). Device-to-device communication in 5G cellular networks: Challenges, solutions, and future directions, *IEEE Communications Magazine*, 52(5), 86–92.
- UK Government, (2017). UK Digital Strategy [WWW Document]. Retrieved on 16th December 2022 from <https://www.gov.uk/government/publications/uk-digitalstrategy..>
- Wang, Dongyu, Wang X, and Zhao Y. (2012) An interference coordination scheme for device-to-device multicast in cellular networks. *IEEE Vehicular Technology Conference (VTC)*. 1 – 5.
- Wang, H., Fapojuwo, A. O. (2017). A Survey of Enabling Technologies of Low Power and Long-Range Machine-to-Machine Communications. *IEEE Communications Surveys & Tutorials*, 19(4), 2621–2639.
- Wubben D, Rost P, Bartelt J.S, Lalam M, Savin V, Gorgoglione M, and Fettweis G, (2014) Benefits and impact of cloud computing on 5G signal processing: Flexible centralization through cloud-RAN, *IEEE signal processing magazine*, 31(6), 35–44.
- Xiaoqin, L., Yang, X. (2018). Mode Selection and Resource Allocation Algorithm Based on Interference Control for D2D Communication. *International Conference on Communications, Circuits and Systems*, 10(1), 286 – 290
- Xing H and Hakola S (2010) The investigation of power control schemes for a device - To-device communication integrated into OFDMA cellular system, *IEEE International Symposium on Personal, Indoor, and Mobile Radio Communication*, 1775–1780.
- Xu B, Da Xu L, Cai H, Xie C, Hu J, and Bu F, (2014) Ubiquitous data accessing method in IoT-based information system for emergency medical services, *IEEE Transactions on Industrial Informatics*, 10(2), 1578–1586.

- Yang, C. Li, J, Semasinghe, P, Hossain, E, Perlaza, S.M, Han, Z, (2017) Distributed interference and energy-aware power control for ultra-dense D2D networks: A mean field game. *IEEE Trans. Wireless Communication*.16, 1205–1217.
- Yu, C.H, Doppler, K., Ribeiro, C.B., & Tirkkonen, O, (2011) Resource sharing optimization for device-to-device communication underlaying cellular networks, *IEEE Transactions on Wireless Communication*, 10(8), 2752–2763.
- Zhai, D Sheng, M. Wang, X. Sun, Z. Xu, C. Li, J. (2017) Energy-saving resource management for D2D and cellular coexisting networks enhanced by hybrid multiple access technologies. *IEEE Trans. Wireless Communication*. 16, (1), 2678 – 2692.
- Zhang Y, Yu R, Nekovee M, Liu Y, Xie S, and Gjessing S, (2012) Cognitive machine-to-machine communications: visions and potentials for the smart grid, *IEEE network*, vol. 26 (3). 6 – 13.
- Zhao, J., Li, S., Dan, M., & Xiaomin, M. (2018). Research on Joint Mode Selection and Resource Allocation Scheme in D2D Networks. *International Conference on Cyber-Enabled Distributed Computing and Knowledge Discovery*. 429 – 432.
- Zhou L, Ruttik K, and Tirkkonen O. (2015) Interference Canceling Power Optimization for Device-to-Device Communication. *IEEE 81st Vehicular Technology Conference (VTC)*. 1 – 5.

APPENDIX A (Publications)

- i. Ameh A. I., Usman A. U., Mohammed A. S., Salihu B. A., (2018) Interference Management Techniques for Device-to-Device (D2D) Communication in 5G Networks; *8th International Interdisciplinary Conference, Multimedia University of Kenya, Nairobi. (Published)*.
- ii. Ameh A. I., Usman A. U., Mohammed A. S., Salihu B. A., (2023) Integrated Mode Selection and Bandwidth Allocation Scheme for Interference Mitigation in

D2D Networks; *Nigeria Journal of Engineering and Applied Sciences (NJEAS)*:
7(9), 101-104. **(Published)**.

- iii. Ameh A. I., Usman A. U., Mohammed A. S., Salihu B. A., (2023) Interference Mitigation in Macro-D2D HetNets: A Survey; *4th International Engineering Conference, Federal University of Technology, Minna, Nigeria (Published)*. iv. Ameh A. I., Usman A. U., Mohammed A. S., Salihu B. A., An Improved Power Control Scheme for Interference Mitigation in D2D (2022); Networks. *Academy Journal of Science and Engineering (AJSE)*: **(Review ongoing)**.

APPENDIX B (MATLAB Codes)

```
clc; clear all; close all;  
% Benchmark with Zhao et al., 2018 research on joint mode selection and  
% Resource allocation Scheme for D2D Networks  
  
% POWER OF CUE  
CUE_Min_P = 0; % min transmit power of CUE  
CUE_MAX_P = 23; % max transmit power of CUE  
SPEC_DIS_CUE_P = CUE_MAX_P;
```

```

% POWER OF D2D
D2D_MAX_P = 23;
SPEC_DIS_D2DT_P_SOMO = D2D_MAX_P;

D2DT_PB_INI = 20;

D2DT_P_S= D2DT_PB_INI; % initial transmit power of D2DT in our scheme

SPEC_DIS_d_d2dt_d2dr = 1; % DISTANCE BETWEEN D2D PAIR

SPEC_DIS_d_AG_d2d = 8; % DISTANCE BETWEEN D2D AG AND VT D2DRd
SPEC_DIS_CUE = 1000; % fixed distance of CUE from base station
SPEC_DIS_AG_CUE = 800; % fixed distance of VT_CUE from AG_base station

% BANDWIDTH SIZE FOR DIFFERENCE RESOURCES BLOCK
BW_A = 60; % 5G BANDWIDTH IN MHZ
F_DUE_BW_SOMO = 30*BW_A/100 ;
F_CUE_BW_SOMO = 70*BW_A/100 ;
F_CUE_BW = 60*BW_A/100; % fixed bandwidth Reserved to CUE
F_DUE_BW = 30*BW_A/100; % fixed bandwidth reserved to DUE
Variable_BW = 10*BW_A/100;

N = 19.28;

SPEC_DIS_SINR_D2DR_Array = cell(1,10);
SPEC_DIS_A_SINR_D2DR_Array = cell(1,10);
SPEC_DIS_Data_rate_Array = cell(1,10);
SPEC_DIS_A_Data_rate_Array = cell(1,10);
SPEC_DIS_Data_rate_Array_CUE = cell(1,10);
SPEC_DIS_A_Data_rate_Array_CUE = cell(1,10);

% 22 UEs: 8 CUEs AND 14 DUEs
SPEC_DIS_Number_D2D_Pair = 12;
SPEC_DIS_Number_CUE_Pair = 8;
SPEC_DIS_NUM_DUE = SPEC_DIS_Number_D2D_Pair*2;
SPEC_DIS_NUM_CUE = SPEC_DIS_Number_CUE_Pair*2; % NUMBER OF CUE
Number_of_PL = 10; sh = 0;

for x=1:Number_of_PL

% PATHLOSS BETWEEN D2DT AND D2DR USING OUR SCHEME 28 +
40LOG10(d(M))
SPEC_DIS_PLoss_AD2D_D2DT_D2DR = 10*log10(65 +
21*log10(SPEC_DIS_d_d2dt_d2dr));
SPEC_DIS_PLoss_AG_AD2DR = 10*log10(65 +

```

```

    21*log10(SPEC_DIS_d_AG_d2d));
% PATHLOSS BETWEEN D2DT AND D2DR USING SOMO 65 + 21log10[d]dB
SPEC_DIS_PLoss_SOMOD2D_D2DT_D2DR = 10*log10(65 +
    21*log10(SPEC_DIS_d_d2dt_d2dr));
SPEC_DIS_PLoss_AG_SOMOD2DR = 10*log10(65 +
    21*log10(SPEC_DIS_d_AG_d2d));

% PATH LOSS BETWEEN BASE STATION AND CUE

SPEC_DIS_path_loss_BS_CUE = 10*log10(37.6*log10(SPEC_DIS_CUE) + 15.3);
% path loss of AG_BS - VT_CUE

SPEC_DIS_path_loss_BS_AG_VT_CUE =
    10*log10(37.6*log10(SPEC_DIS_AG_CUE) + 15.3);

% D2D CHANNEL GAIN

SPEC_DIS_G_D2DT_P_SOMO = 10^((-SPEC_DIS_PLoss_SOMOD2D_D2DT_D2DR - sh)/10)*(10^2);
SPEC_DIS_G_AG_SOMODDR = 10^((-SPEC_DIS_PLoss_AG_SOMOD2DR - sh)/10)*(10^2);

SPEC_DIS_G_D2DT_P_S = 10^((-SPEC_DIS_PLoss_AD2D_D2DT_D2DR - sh)/10)*(10^2);
SPEC_DIS_G_AG_AD2DR_P_S = 10^((-SPEC_DIS_PLoss_AG_AD2DR - sh)/10)*(10^2);

% CUE CHANNEL GAIN
SPEC_DIS_G_CUE = 10^((-SPEC_DIS_path_loss_BS_CUE - sh)/10)*(10^2);
SPEC_DIS_G_VT_CUE = 10^((-SPEC_DIS_path_loss_BS_AG_VT_CUE - sh)/10)*(10^2);

% D2D SINR of D2DR
SPEC_DIS_SINR_D2DR = (D2D_MAX_P*SPEC_DIS_G_D2DT_P_SOMO)/(((SPEC_DIS_Number_D2D_Pair-1)*SPEC_DIS_D2DT_P_SOMO*SPEC_DIS_G_AG_SOMODDR)+N);
SPEC_DIS_A_SINR_D2DR = (D2DT_PB_INI*SPEC_DIS_G_D2DT_P_S)/(((SPEC_DIS_Number_D2D_Pair-1)*D2DT_P_S*SPEC_DIS_G_AG_AD2DR_P_S)+N);
% CUE SINR
SPEC_DIS_SINR_CUE = (CUE_MAX_P*SPEC_DIS_G_CUE)/(((SPEC_DIS_NUM_CUE-2)*SPEC_DIS_CUE_P*SPEC_DIS_G_CUE)+N);
SPEC_DIS_SINR_VT_CUE = (CUE_MAX_P*SPEC_DIS_G_VT_CUE)/(((SPEC_DIS_NUM_CUE-

```

```

2)*SPEC_DIS_CUE_P*SPEC_DIS_G_VT_CUE)+ N);

% CONDITION FOR ALLOCATING BANDWIDTH FOR DUE BASED ON MODE
AND USER TRAFFIC
% bandwidth alllocation for D2D1 pair
if (SPEC_DIS_NUM_DUE>=SPEC_DIS_NUM_CUE)
SPEC_DIS_BW_DUE = F_DUE_BW +Variable_BW ;
else % allocate 40% bandwidth to DUE
SPEC_DIS_BW_DUE = F_DUE_BW ; end

if (SPEC_DIS_NUM_DUE<SPEC_DIS_NUM_CUE)
SPEC_DIS_BW_CUE = F_CUE_BW +Variable_BW ;
else % allocate 40% bandwidth to
DUE SPEC_DIS_BW_CUE =
F_CUE_BW ; end

% DATA RATE OF D2D
% Data rate of D2DR USING SOMO = BW_D2D_SOMO*log2(1 + SINR_D2DR1)
SPEC_DIS_Data_rate_D2DR = F_DUE_BW_SOMO*log2(1
+SPEC_DIS_SINR_D2DR);
% Data rate of D2DR1 USING OUR SCHEME = BW_DUE*log2(1 + SINR_D2DR1)
SPEC_DIS_A_Data_rate_D2DR = SPEC_DIS_BW_DUE*log2(1
+SPEC_DIS_A_SINR_D2DR);

SPEC_DIS_Data_rate_D2D= SPEC_DIS_Data_rate_D2DR;
SPEC_DIS_A_Data_rate_D2D= SPEC_DIS_A_Data_rate_D2DR;

% DATA RATE OF CUE
% Data rate of CUE USING SOMO = F_CUE_BW_SOMO*log2(1 + SINR_CUE)
SPEC_DIS_Data_rate_CUE = F_CUE_BW_SOMO*log2(1
+SPEC_DIS_SINR_CUE);
% Data rate of CUE USING OUR SCHEME = BW_CUE*log2(1 + SINR_CUE)
SPEC_DIS_A_Data_rate_CUE = SPEC_DIS_BW_CUE*log2(1
+SPEC_DIS_SINR_CUE);

% ARRAY OF SINR

SPEC_DIS_SINR_D2DR_Array{x}= SPEC_DIS_SINR_D2DR;
SPEC_DIS_A_SINR_D2DR_Array{x}= SPEC_DIS_A_SINR_D2DR;
% ARRAY OF DATA RATE
% ARRAY OF D2D DATA RATE
SPEC_DIS_Data_rate_Array{x}= SPEC_DIS_Data_rate_D2D;
SPEC_DIS_A_Data_rate_Array{x}= SPEC_DIS_A_Data_rate_D2D;

% ARRAY OF CUE DATA RATE
SPEC_DIS_Data_rate_Array_CUE{x}= SPEC_DIS_Data_rate_CUE;
SPEC_DIS_A_Data_rate_Array_CUE{x}= SPEC_DIS_A_Data_rate_CUE;

```

```

SPEC_DIS_d_d2dt_d2dr = SPEC_DIS_d_d2dt_d2dr +1; % increment distance by
interval of 5m

end

% ARRAY OF SINR BAR
% array of eNB SINR

% array of D2D SINR

SPEC_DIS_SINR_D2DR_AVG_array =
    [SPEC_DIS_SINR_D2DR_Array{1},SPEC_DIS_SINR_D2DR_Array{2},SPE
    C_DIS_SINR_D2DR_Array{3},SPEC_DIS_SINR_D2DR_Array{4},SPEC_DI
    S_SINR_D2DR_Array{5},SPEC_DIS_SINR_D2DR_Array{6},SPEC_DIS_SI
    NR_D2DR_Array{7},SPEC_DIS_SINR_D2DR_Array{8},SPEC_DIS_SINR_
    D2DR_Array{9},SPEC_DIS_SINR_D2DR_Array{10}]
SPEC_DIS_A_SINR_D2DR_AVG_array =
    [SPEC_DIS_A_SINR_D2DR_Array{1},SPEC_DIS_A_SINR_D2DR_Array{2
    },SPEC_DIS_A_SINR_D2DR_Array{3},SPEC_DIS_A_SINR_D2DR_Array{
    4},SPEC_DIS_A_SINR_D2DR_Array{5},SPEC_DIS_A_SINR_D2DR_Array
    {6},SPEC_DIS_A_SINR_D2DR_Array{7},SPEC_DIS_A_SINR_D2DR_Arra
    y{8},SPEC_DIS_A_SINR_D2DR_Array{9},SPEC_DIS_A_SINR_D2DR_Arr
    ay{10}]

% AVERAGE SINR

SPEC_DIS_SINR_D2DR_AVG =
    [sum(SPEC_DIS_SINR_D2DR_AVG_array)/Number_of_PL;0];
SPEC_DIS_A_SINR_D2DR_AVG =
    [sum(SPEC_DIS_A_SINR_D2DR_AVG_array)/Number_of_PL;0];
% average DUE SINR bar
SPEC_DIS_SINR_D2DR_bar =
    [SPEC_DIS_SINR_D2DR_AVG,SPEC_DIS_A_SINR_D2DR_AVG];
% ARRAY OF DATA RATE BAR
% d2d data rate array collections
SPEC_DIS_D2DR_Data_rate_array =
    [SPEC_DIS_Data_rate_Array{1},SPEC_DIS_Data_rate_Array{2},SPEC_DIS_
    Data_rate_Array{3},SPEC_DIS_Data_rate_Array{4},SPEC_DIS_Data_rate_A
    rray{5},SPEC_DIS_Data_rate_Array{6},SPEC_DIS_Data_rate_Array{7},SPE
    C_DIS_Data_rate_Array{8},SPEC_DIS_Data_rate_Array{9},SPEC_DIS_Data
    _rate_Array{10}]
SPEC_DIS_A_D2DR_Data_rate_array =
    [SPEC_DIS_A_Data_rate_Array{1},SPEC_DIS_A_Data_rate_Array{2},SPEC
    _DIS_A_Data_rate_Array{3},SPEC_DIS_A_Data_rate_Array{4},SPEC_DIS_
    A_Data_rate_Array{5},SPEC_DIS_A_Data_rate_Array{6},SPEC_DIS_A_Dat
    a_rate_Array{7},SPEC_DIS_A_Data_rate_Array{8},SPEC_DIS_A_Data_rate
    _Array{9},SPEC_DIS_A_Data_rate_Array{10}]

```

```

% cue data rate array collections
SPEC_DIS_CUE_Data_rate_array =
    [SPEC_DIS_Data_rate_Array_CUE{1},SPEC_DIS_Data_rate_Array_CUE{2},
    SPEC_DIS_Data_rate_Array_CUE{3},SPEC_DIS_Data_rate_Array_CUE{4},
    SPEC_DIS_Data_rate_Array_CUE{5},SPEC_DIS_Data_rate_Array_CUE{6},
    SPEC_DIS_Data_rate_Array_CUE{7},SPEC_DIS_Data_rate_Array_CUE{8},
    SPEC_DIS_Data_rate_Array_CUE{9},SPEC_DIS_Data_rate_Array_CUE{10}
    ]
SPEC_DIS_A_CUE_Data_rate_array =
    [SPEC_DIS_A_Data_rate_Array_CUE{1},SPEC_DIS_A_Data_rate_Array_C
    UE{2},SPEC_DIS_A_Data_rate_Array_CUE{3},SPEC_DIS_A_Data_rate_Arr
    ay_CUE{4},SPEC_DIS_A_Data_rate_Array_CUE{5},SPEC_DIS_A_Data_rat
    e_Array_CUE{6},SPEC_DIS_A_Data_rate_Array_CUE{7},SPEC_DIS_A_Da
    ta_rate_Array_CUE{8},SPEC_DIS_A_Data_rate_Array_CUE{9},SPEC_DIS_
    A_Data_rate_Array_CUE{10}]

% Average CUE data rate array
SPEC_DIS_data_rate_CUE_AVG =
    [sum(SPEC_DIS_CUE_Data_rate_array)/Number_of_PL;0];
SPEC_DIS_A_data_rate_CUE_AVG =
    [sum(SPEC_DIS_A_CUE_Data_rate_array)/Number_of_PL;0];

% Average CUE data rate barchart
SPEC_DIS_data_rate_CUE_bar =
    [SPEC_DIS_data_rate_CUE_AVG,SPEC_DIS_A_data_rate_CUE_AVG]
% sum of D2D data rate
% D2D SUM OF DATA RATE
SPEC_DIS_SUM_D2DR_Data_rate =sum(SPEC_DIS_D2DR_Data_rate_array);
SPEC_DIS_SUM_A_D2DR_Data_rate =
    sum(SPEC_DIS_A_D2DR_Data_rate_array);
% Average D2D data rate
SPEC_DIS_Avg_D2DR_Data_rate =
    [SPEC_DIS_SUM_D2DR_Data_rate/Number_of_PL;0];
SPEC_DIS_Avg_A_D2DR_Data_rate =
    [SPEC_DIS_SUM_A_D2DR_Data_rate/Number_of_PL;0];
% Average DUE data rate bar analysis
SPEC_DIS_Avg_D2DR_Data_rate_bar =
    [SPEC_DIS_Avg_D2DR_Data_rate,SPEC_DIS_Avg_A_D2DR_Data_rate]
% cue sum of data rate
SPEC_DIS_SUM_CUE_Data_rate_array = sum(SPEC_DIS_CUE_Data_rate_array);
SPEC_DIS_SUM_A_CUE_Data_rate_array =
    sum(SPEC_DIS_A_CUE_Data_rate_array);

% SUM OF ENTIRE NETWORK DATA RATE
SPEC_DIS_ENTIRE_DATA_RATE_ARRAY =
    [(SPEC_DIS_Data_rate_Array{1}+SPEC_DIS_Data_rate_Array_CUE{1}),(SP
    EC_DIS_Data_rate_Array{2}+SPEC_DIS_Data_rate_Array_CUE{2}),(SPEC_

```

```

DIS_Data_rate_Array{3}+SPEC_DIS_Data_rate_Array_CUE{3}),(SPEC_DIS
_Data_rate_Array{4}+SPEC_DIS_Data_rate_Array_CUE{4}),(SPEC_DIS_Da
ta_rate_Array{5}+SPEC_DIS_Data_rate_Array_CUE{5}),(SPEC_DIS_Data_r
ate_Array{6}+SPEC_DIS_Data_rate_Array_CUE{6}),(SPEC_DIS_Data_rate_
Array{7}+SPEC_DIS_Data_rate_Array_CUE{7}),(SPEC_DIS_Data_rate_Arra
y{8}+SPEC_DIS_Data_rate_Array_CUE{8}),(SPEC_DIS_Data_rate_Array{9
}+SPEC_DIS_Data_rate_Array_CUE{9}),(SPEC_DIS_Data_rate_Array{10}+
SPEC_DIS_Data_rate_Array_CUE{10})]
SPEC_DIS_A_ENTIRE_DATA_RATE_ARRAY =
[(SPEC_DIS_A_Data_rate_Array{1}+SPEC_DIS_A_Data_rate_Array_CUE{1
}),(SPEC_DIS_A_Data_rate_Array{2}+SPEC_DIS_A_Data_rate_Array_CUE
{2}),(SPEC_DIS_A_Data_rate_Array{3}+SPEC_DIS_A_Data_rate_Array_CU
E{3}),(SPEC_DIS_A_Data_rate_Array{4}+SPEC_DIS_A_Data_rate_Array_C
UE{4}),(SPEC_DIS_A_Data_rate_Array{5}+SPEC_DIS_A_Data_rate_Array_
CUE{5}),(SPEC_DIS_A_Data_rate_Array{6}+SPEC_DIS_A_Data_rate_Arra
y_CUE{6}),(SPEC_DIS_A_Data_rate_Array{7}+SPEC_DIS_A_Data_rate_Ar
ray_CUE{7}),(SPEC_DIS_A_Data_rate_Array{8}+SPEC_DIS_A_Data_rate_
Array_CUE{8}),(SPEC_DIS_A_Data_rate_Array{9}+SPEC_DIS_A_Data_rat
e_Array_CUE{9}),(SPEC_DIS_A_Data_rate_Array{10}+SPEC_DIS_A_Data
_rate_Array_CUE{10}]]

% average data rate of entire network
SPEC_DIS_Avg_data_rate= [(SPEC_DIS_SUM_D2DR_Data_rate +
SPEC_DIS_SUM_CUE_Data_rate_array)/(Number_of_PL);0];
SPEC_DIS_A_Avg_D2DR_data_rate_avg= [(SPEC_DIS_SUM_A_D2DR_Data_rate
+ SPEC_DIS_SUM_A_CUE_Data_rate_array)/(Number_of_PL);0];

% AVERAGE DATA RATE BAR CHART
SPEC_DIS_DATA_RATE_BAR_CHART =
[SPEC_DIS_Avg_data_rate,SPEC_DIS_A_Avg_D2DR_data_rate_avg]

X_axis= 1:1:10;

figure(1)

J1= plot(X_axis,SPEC_DIS_SINR_D2DR_AVG_array,'-*g');
hold on;
J2= plot(X_axis,SPEC_DIS_A_SINR_D2DR_AVG_array,'-or');

title('SINR OF DUE against varying
distance','FontSize',12) xlabel ('DISTANCE OF DUE
(m)','FontSize',12) ylabel ('SINR OF D2DR','FontSize',12)
legend ([J1 J2],'SOMO','MS-BAS')
hold off

figure(2)
bar(SPEC_DIS_SINR_D2DR_bar)

```

```

    title('Average DUE SINR against DUE
distance','FontSize',12) ylabel('DUE SINR') xlabel
('Scheme')
    legend('SOMO','MS-BAS') figure(3)
    J3= plot(X_axis,SPEC_DIS_D2DR_Data_rate_array,'-*g');
hold on;
    J4= plot(X_axis,SPEC_DIS_A_D2DR_Data_rate_array,'-or');

```

```

    title('DUE data rate against DUE
distance','FontSize',12) xlabel ('DUE distance
(m)','FontSize',12) ylabel ('DUE data rate
(Mbps)','FontSize',12) legend ([J3 J4],'SOMO','MS-
BAS')
    hold off

```

```

figure (4)
bar(SPEC_DIS_Avg_D2DR_Data_rate_bar)
    title('Average DUE data rate against DUE
distance','FontSize',12) ylabel('DUE Data rate (Mbps)') xlabel
('Scheme')
    legend('SOMO','MS-BAS') figure

```

```

(5)
    J5= plot(X_axis,SPEC_DIS_CUE_Data_rate_array,'-*g');
hold on;
    J6= plot(X_axis,SPEC_DIS_A_CUE_Data_rate_array,'-or');

```

```

    title('CUE data rate against DUE
distance','FontSize',12) xlabel ('DUE distance
(m)','FontSize',12) ylabel ('CUE data rate
(Mbps)','FontSize',12) legend ([J5 J6],'SOMO','MS-
BAS')
    hold off

```

```

figure (6)
bar(SPEC_DIS_data_rate_CUE_bar) title('Average CUE data
rate against DUE distance','FontSize',12) ylabel('CUE Data rate
(Mbps)') xlabel ('Scheme')
    legend('SOMO','MS-BAS')

```

```

figure(7)
    J7= plot(X_axis,SPEC_DIS_ENTIRE_DATA_RATE_ARRAY,'-*g');
hold on;
    J8= plot(X_axis,SPEC_DIS_A_ENTIRE_DATA_RATE_ARRAY,'-or');

```

```

    title('UE data rate against DUE
distance','FontSize',12) xlabel ('distance of DUE
(m)','FontSize',12) ylabel ('UE data rate

```

```
(Mbps)',FontSize',12) legend ([J7 J8],'SOMO','MS-
BAS')
hold off
figure (8)
```

```
bar(SPEC_DIS_DATA_RATE_BAR_CHART)
title('Average UE data rate against DUE
distance',FontSize',12) ylabel('UE Data rate (Mbps)') xlabel
('Scheme')
legend('SOMO','MS-BAS')
```

```
%%%%%%%%%%%%%%%%%%%%%%%%%%%%%%%%%%%%%%%%%%%%%%%%%%%%%%%%%%%%%%%%%%%%%%%%
%%%%%%%%%%%%%%%%%%%%%%%%%%%%%%%%%%%%%%%%%%%%%%%%%%%%%%%%%%%%%%%%%%%%%%%%
%%%%%%%%%%%%%%%%%%%%%%%%%%%%%%%%%%%%%%%%%%%%%%%%%%%%%%%%%%%%%%%%%%%%%%%%SPEC_DUE_PAIR%%%%%%%%
%%%%%%%%%%%%%%%%%%%%%%%%%%%%%%%%%%%%%%%%%%%%%%%%%%%%%%%%%%%%%%%%%%%%%%%%
```

```
CUE_Min_P = 0; % min transmit power of CUE
CUE_MAX_P= 23; % max transmit power of CUE
SPEC_UE_CUE_P = CUE_MAX_P;
CUE_P_INI = 20;
SPEC_UE_CUE_P_S = CUE_P_INI;
```

```
% 0 UEs
SPEC_UE_Number_D2D_Pair = 1;
SPEC_UE_Number_CUE_Pair = 19;
SPEC_UE_NUM_DUE = SPEC_UE_Number_D2D_Pair*2; % 2 initial DUE
SPEC_UE_NUM_CUE = SPEC_UE_Number_CUE_Pair*2; % 18 initial CUE
```

```
% POWER OF D2D
D2D_MIN_P = 0;
D2D_MAX_P = 23;
SPEC_UE_D2DT_P_SOMO = D2D_MAX_P;
```

```
D2DT_PB_INI = 23;
```

```
SPEC_UE_D2DT_P_S= D2DT_PB_INI; % initial transmit power of D2DT in our scheme
```

```
SINR_eNB_TARGET = 0; % Susanto eta al, 2017;
SINR_D2DR_TARGET = 0;
```

```
% distances
d_d2d_target = 10; % TARGET DISTANCE FOR D2D MODE SPEC_UE_d_eNB_cue
= 2000; % distance between CUE and eNB
SPEC_UE_d_d2dt_d2dr = 6; % DISTANCE BETWEEN D2D PAIR
```

```
SPEC_UE_d_AG_d2d = 14; % DISTANCE BETWEEN D2D AG AND VT D2DR
SPEC_UE_D_CUE = 1000; % fixed distance of CUE from base station
```

```

SPEC_UE_D_AG_CUE = 800;    % fixed distance of VT_CUE from AG_base station N
= 19.28;    % THERMAL NOISE in dBm/Hz, 1 Hz= -174 dBm, 100Hz and 60Hz = -
96dBm,
SPEC_UE_AVG_SINR_D2DR_Array = cell(1,10);
SPEC_UE_AVG_A_SINR_D2DR_Array = cell(1,10);
SPEC_UE_Data_rate_Array = cell(1,10);
SPEC_UE_A_Data_rate_Array = cell(1,10);
SPEC_UE_Data_rate_Array_CUE = cell(1,10);
SPEC_UE_A_Data_rate_Array_CUE = cell(1,10);

sh = 0;

% PATHLOSS BETWEEN D2DT AND D2DR USING OUR SCHEME 28 +
40LOG10(d(M))
SPEC_UE_PLoss_AD2D_D2DT_D2DR = 10*log10(65 +
21*log10(SPEC_UE_d_d2dt_d2dr));
SPEC_UE_PLoss_AG_AD2DR = abs(10*log10(65 +
21*log10(SPEC_UE_d_AG_d2d)));

% PATHLOSS BETWEEN D2DT AND D2DR USING SOMO 65 + 21log10[d]dB
SPEC_UE_PLoss_SOMOD2D_D2DT_D2DR = 10*log10(65 +
21*log10(SPEC_UE_d_d2dt_d2dr));
SPEC_UE_PLoss_AG_SOMOD2DR = 10*log10(65 +
21*log10(SPEC_UE_d_AG_d2d));

% PATH LOSS BETWEEN BASE STATION AND CUE

SPEC_UE_path_loss_BS_CUE= 10*log10(37.6*log10(SPEC_UE_D_CUE) + 15.3);

% path loss of AG_BS - VT_CUE
SPEC_UE_path_loss_BS_AG_VT_CUE=
10*log10(37.6*log10(SPEC_UE_D_AG_CUE) + 15.3);

% CHANNEL GAIN OF D2D

SPEC_UE_G_D2DT_P_SOMO = 10^((-
SPEC_UE_PLoss_SOMOD2D_D2DT_D2DR -sh)/10)*(10^2);
SPEC_UE_G_AG_SOMOD2DR = 10^((-SPEC_UE_PLoss_AG_SOMOD2DR -
sh)/10)*(10^2);

SPEC_UE_G_D2DT_P_S = 10^((-SPEC_UE_PLoss_AD2D_D2DT_D2DR-
sh)/10)*(10^2);
SPEC_UE_G_AG_AD2DR_P_S = 10^((-SPEC_UE_PLoss_AG_AD2DR-
sh)/10)*(10^2);

% CUE CHANNEL GAIN
SPEC_UE_G_CUE = 10^((-SPEC_UE_path_loss_BS_CUE - sh)/10)*(10^2);

```

```

SPEC_UE_G_VT_CUE = 10^((-SPEC_UE_path_loss_BS_AG_VT_CUE -
sh)/10)*(10^2);

% BANDWIDTH SIZE FOR DIFFERENCE RESOURCES BLOCK
BW_A = 60; % 5G BANDWIDTH IN MHz
F_DUE_BW_SOMO = 30*BW_A/100 ;
F_CUE_BW_SOMO = 70*BW_A/100 ;
F_CUE_BW = 60*BW_A/100; % fixed bandwidth Reserved to CUE
F_DUE_BW = 30*BW_A/100; % fixed bandwidth reserved to DUE
Variable_BW = 10*BW_A/100;

SPEC_PAIR_Number_of_PL = 20;
for X=1:SPEC_PAIR_Number_of_PL

% D2D SINR of D2DR USING SOMO
SPEC_UE_SINR_D2DR =
(D2D_MAX_P*SPEC_UE_G_D2DT_P_SOMO)/(((SPEC_UE_Number_D2D_Pair-1)*SPEC_UE_D2DT_P_SOMO*SPEC_UE_G_AG_SOMOD2DR)+ N);

% D2D SINR of D2DR USING OUR SCHEME
SPEC_UE_A_SINR_D2DR =
(D2DT_PB_INI*SPEC_UE_G_D2DT_P_S)/(((SPEC_UE_Number_D2D_Pair-1)*SPEC_UE_D2DT_P_S*SPEC_UE_G_AG_AD2DR_P_S)+ N);

% CUE SINR
SPEC_UE_SINR_CUE =
(CUE_MAX_P*SPEC_UE_G_CUE)/(((SPEC_UE_NUM_CUE-2)*SPEC_UE_CUE_P*SPEC_UE_G_CUE)+ N);

SPEC_UE_SINR_VT_CUE =
(CUE_MAX_P*SPEC_UE_G_VT_CUE)/(((SPEC_UE_NUM_CUE-2)*SPEC_UE_CUE_P*SPEC_UE_G_VT_CUE)+ N);

% CONDITION FOR ALLOCATING BANDWIDTH FOR DUE BASED ON MODE
AND USER TRAFFIC
% bandwidth alllocation for D2D1 pair
if (SPEC_UE_NUM_DUE>=SPEC_UE_NUM_CUE)
SPEC_UE_BW_DUE = F_DUE_BW +Variable_BW;
else % allocate 40% bandwidth to DUE
SPEC_UE_BW_DUE = F_DUE_BW ; end

if (SPEC_UE_NUM_DUE<SPEC_UE_NUM_CUE)
SPEC_UE_BW_CUE = F_CUE_BW +Variable_BW;
else % allocate 40% bandwidth to DUE
SPEC_UE_BW_CUE = F_CUE_BW ; end

% DATA RATE OF D2D

```

```

% Data rate of D2DR USING SOMO = BW_D2D_SOMO*log2(1 + SINR_D2DR)
SPEC_UE_Data_rate_D2DR          =          F_DUE_BW_SOMO*log2(1
+SPEC_UE_SINR_D2DR);

% Data rate of D2DR USING OUR SCHEME = BW_DUE*log2(1 + SINR_D2DR)
SPEC_UE_A_Data_rate_D2DR        =          SPEC_UE_BW_DUE*log2(1
+SPEC_UE_A_SINR_D2DR);

% DATA RATE OF CUE
% Data rate of CUE USING SOMO = F_CUE_BW_SOMO*log2(1 + SINR_CUE)
SPEC_UE_Data_rate_CUE          =          F_CUE_BW_SOMO*log2(1
+SPEC_UE_SINR_CUE);
% Data rate of CUE USING OUR SCHEME = BW_CUE*log2(1 + SINR_CUE)
SPEC_UE_A_Data_rate_CUE        =          SPEC_UE_BW_CUE*log2(1
+SPEC_UE_SINR_CUE);

% ARRAY OF SINR

SPEC_UE_AVG_SINR_D2DR_Array{X}= abs(SPEC_UE_SINR_D2DR);
SPEC_UE_AVG_A_SINR_D2DR_Array{X}= abs(SPEC_UE_A_SINR_D2DR);

% ARRAY OF DATA RATE

SPEC_UE_Data_rate_Array{X}= abs(SPEC_UE_Data_rate_D2DR);
SPEC_UE_A_Data_rate_Array{X}= abs(SPEC_UE_A_Data_rate_D2DR);

% ARRAY OF CUE DATA RATE
SPEC_UE_Data_rate_Array_CUE{X}= abs(SPEC_UE_Data_rate_CUE);
SPEC_UE_A_Data_rate_Array_CUE{X}= abs(SPEC_UE_A_Data_rate_CUE);

SPEC_UE_NUM_DUE = SPEC_UE_NUM_DUE+2;
SPEC_UE_NUM_CUE = SPEC_UE_NUM_CUE-2;

end

% ARRAY OF SINR BAR
% array of eNB SINR

% array of D2D SINR
SPEC_UE_SINR_D2DR_Array_BAR          =
[SPEC_UE_AVG_SINR_D2DR_Array{1},SPEC_UE_AVG_SINR_D2DR_Ar
array{2},SPEC_UE_AVG_SINR_D2DR_Array{3},SPEC_UE_AVG_SINR_D2
DR_Array{4},SPEC_UE_AVG_SINR_D2DR_Array{5},SPEC_UE_AVG_SI
NR_D2DR_Array{6},SPEC_UE_AVG_SINR_D2DR_Array{7},SPEC_UE_A
VG_SINR_D2DR_Array{8},SPEC_UE_AVG_SINR_D2DR_Array{9},SPEC_
UE_AVG_SINR_D2DR_Array{10},SPEC_UE_AVG_SINR_D2DR_Array{11

```

```

    },SPEC_UE_AVG_SINR_D2DR_Array{12},SPEC_UE_AVG_SINR_D2DR_
    Array{13},SPEC_UE_AVG_SINR_D2DR_Array{14},SPEC_UE_AVG_SINR
    _D2DR_Array{15},SPEC_UE_AVG_SINR_D2DR_Array{16},SPEC_UE_AV
    G_SINR_D2DR_Array{17},SPEC_UE_AVG_SINR_D2DR_Array{18},SPEC
    _UE_AVG_SINR_D2DR_Array{19},SPEC_UE_AVG_SINR_D2DR_Array{2
    0}]
SPEC_UE_A_SINR_D2DR_Array_BAR =
    [SPEC_UE_AVG_A_SINR_D2DR_Array{1},SPEC_UE_AVG_A_SINR_D2D
    R_Array{2},SPEC_UE_AVG_A_SINR_D2DR_Array{3},SPEC_UE_AVG_A
    _SINR_D2DR_Array{4},SPEC_UE_AVG_A_SINR_D2DR_Array{5},SPEC_
    UE_AVG_A_SINR_D2DR_Array{6},SPEC_UE_AVG_A_SINR_D2DR_Arra
    y{7},SPEC_UE_AVG_A_SINR_D2DR_Array{8},SPEC_UE_AVG_A_SINR_
    D2DR_Array{9},SPEC_UE_AVG_A_SINR_D2DR_Array{10},SPEC_UE_A
    VG_A_SINR_D2DR_Array{11},SPEC_UE_AVG_A_SINR_D2DR_Array{12
    },SPEC_UE_AVG_A_SINR_D2DR_Array{13},SPEC_UE_AVG_A_SINR_D
    2DR_Array{14},SPEC_UE_AVG_A_SINR_D2DR_Array{15},SPEC_UE_AV
    G_A_SINR_D2DR_Array{16},SPEC_UE_AVG_A_SINR_D2DR_Array{17},
    SPEC_UE_AVG_A_SINR_D2DR_Array{18},SPEC_UE_AVG_A_SINR_D2
    DR_Array{19},SPEC_UE_AVG_A_SINR_D2DR_Array{20}]

% cue data rate array collections
SPEC_UE_CUE_Data_rate_array =
    [(SPEC_UE_Data_rate_Array_CUE{1});(SPEC_UE_Data_rate_Array_CUE{2
    });(SPEC_UE_Data_rate_Array_CUE{3});(SPEC_UE_Data_rate_Array_CUE{
    4});(SPEC_UE_Data_rate_Array_CUE{5});(SPEC_UE_Data_rate_Array_CUE
    {6});(SPEC_UE_Data_rate_Array_CUE{7});(SPEC_UE_Data_rate_Array_CU
    E{8});(SPEC_UE_Data_rate_Array_CUE{9});(SPEC_UE_Data_rate_Array_C
    UE{10});(SPEC_UE_Data_rate_Array_CUE{11});(SPEC_UE_Data_rate_Arra
    y_CUE{12});(SPEC_UE_Data_rate_Array_CUE{13});(SPEC_UE_Data_rate_
    Array_CUE{14});(SPEC_UE_Data_rate_Array_CUE{15});(SPEC_UE_Data_r
    ate_Array_CUE{16});(SPEC_UE_Data_rate_Array_CUE{17});(SPEC_UE_Da
    ta_rate_Array_CUE{18});(SPEC_UE_Data_rate_Array_CUE{19});(SPEC_UE
    _Data_rate_Array_CUE{20})]
SPEC_UE_A_CUE_Data_rate_array =
    [(SPEC_UE_A_Data_rate_Array_CUE{1});(SPEC_UE_A_Data_rate_Array_C
    UE{2});(SPEC_UE_A_Data_rate_Array_CUE{3});(SPEC_UE_A_Data_rate_
    Array_CUE{4});(SPEC_UE_A_Data_rate_Array_CUE{5});(SPEC_UE_A_Dat
    a_rate_Array_CUE{6});(SPEC_UE_A_Data_rate_Array_CUE{7});(SPEC_UE
    _A_Data_rate_Array_CUE{8});(SPEC_UE_A_Data_rate_Array_CUE{9});(SP
    EC_UE_A_Data_rate_Array_CUE{10});(SPEC_UE_A_Data_rate_Array_CUE
    {11});(SPEC_UE_A_Data_rate_Array_CUE{12});(SPEC_UE_A_Data_rate_A
    rray_CUE{13});(SPEC_UE_A_Data_rate_Array_CUE{14});(SPEC_UE_A_Da
    ta_rate_Array_CUE{15});(SPEC_UE_A_Data_rate_Array_CUE{16});(SPEC_
    UE_A_Data_rate_Array_CUE{17});(SPEC_UE_A_Data_rate_Array_CUE{18
    });(SPEC_UE_A_Data_rate_Array_CUE{19});(SPEC_UE_A_Data_rate_Array
    _CUE{20})]

SPEC_UE_CUE_Analysis_bar =

```

```
[SPEC_UE_CUE_Data_rate_array,SPEC_UE_A_CUE_Data_rate_array]
```

```
% Average of SINR
```

```
SPEC_UE_SINR_D2DR_AVG =  
[sum(SPEC_UE_SINR_D2DR_Array_BAR)/SPEC_PAIR_Number_of_PL;0];  
SPEC_UE_A_SINR_D2DR_AVG =  
[sum(SPEC_UE_A_SINR_D2DR_Array_BAR)/SPEC_PAIR_Number_of_PL;  
0]
```

```
% bar chart of SINR of DUE
```

```
SPEC_UE_SINR_D2DR_bar =  
[SPEC_UE_SINR_D2DR_AVG,SPEC_UE_A_SINR_D2DR_AVG]
```

```
% Average of CUE data rate
```

```
SPEC_UE_CUE_A_D2DR_data_rate_AVG =  
[sum(SPEC_UE_A_CUE_Data_rate_array)/SPEC_PAIR_Number_of_PL;0];  
SPEC_UE_CUE_D2DR_data_rate_AVG =  
[sum(SPEC_UE_CUE_Data_rate_array)/SPEC_PAIR_Number_of_PL;0];
```

```
% bar chart of SINR of DUE
```

```
SPEC_UE_CUE_D2DR_data_rate_bar =  
[SPEC_UE_CUE_D2DR_data_rate_AVG,SPEC_UE_CUE_A_D2DR_data_rate_AVG]
```

```
% ARRAY OF DATA RATE BAR
```

```
% data rate of D2D
```

```
SPEC_UE_Data_rate_D2DR_Array_BAR =  
[SPEC_UE_Data_rate_Array{1};SPEC_UE_Data_rate_Array{2};SPEC_UE_Data_rate_Array{3};SPEC_UE_Data_rate_Array{4};SPEC_UE_Data_rate_Array{5};SPEC_UE_Data_rate_Array{6};SPEC_UE_Data_rate_Array{7};SPEC_UE_Data_rate_Array{8};SPEC_UE_Data_rate_Array{9};SPEC_UE_Data_rate_Array{10};SPEC_UE_Data_rate_Array{11};SPEC_UE_Data_rate_Array{12};SPEC_UE_Data_rate_Array{13};SPEC_UE_Data_rate_Array{14};SPEC_UE_Data_rate_Array{15};SPEC_UE_Data_rate_Array{16};SPEC_UE_Data_rate_Array{17};SPEC_UE_Data_rate_Array{18};SPEC_UE_Data_rate_Array{19};SPEC_UE_Data_rate_Array{20}]
```

```
SPEC_UE_A_Data_rate_D2DR_Array_BAR =  
[SPEC_UE_A_Data_rate_Array{1};SPEC_UE_A_Data_rate_Array{2};SPEC_UE_A_Data_rate_Array{3};SPEC_UE_A_Data_rate_Array{4};SPEC_UE_A_Data_rate_Array{5};SPEC_UE_A_Data_rate_Array{6};SPEC_UE_A_Data_rate_Array{7};SPEC_UE_A_Data_rate_Array{8};SPEC_UE_A_Data_rate_Array{9};SPEC_UE_A_Data_rate_Array{10};SPEC_UE_A_Data_rate_Array{11};SPEC_UE_A_Data_rate_Array{12};SPEC_UE_A_Data_rate_Array{13};SPEC_UE_A_Data_rate_Array{14};SPEC_UE_A_Data_rate_Array{15};SPEC_UE_A_Data_rate_Array{16};SPEC_UE_A_Data_rate_Array{17};SPEC_UE_A_Data_rate_Array{18};SPEC_UE_A_Data_rate_Array{19};SPEC_UE_A_Data_rate_Array{20}]
```

```

% Average of DUE data rate array
SPEC_UE_Avg_D2DR_Data_rate_array =
    [sum(SPEC_UE_Data_rate_D2DR_Array_BAR)/SPEC_PAIR_Number_of_PL
    ;0];
SPEC_UE_Avg_A_D2DR_Data_rate_array =
    [sum(SPEC_UE_A_Data_rate_D2DR_Array_BAR)/SPEC_PAIR_Number_of_
    PL;0];
% Average DUE data rate bar
SPEC_UE_D2DR_Data_rate_bar =
    [SPEC_UE_Avg_D2DR_Data_rate_array,SPEC_UE_Avg_A_D2DR_Data_rat
    e_array]
% cue sum of data rate
SPEC_UE_SUM_CUE_Data_rate_array =
    [SPEC_UE_Data_rate_Array_CUE{1}+SPEC_UE_Data_rate_Array_CUE{2}
    +SPEC_UE_Data_rate_Array_CUE{3}+SPEC_UE_Data_rate_Array_CUE{4}
    +SPEC_UE_Data_rate_Array_CUE{5}+SPEC_UE_Data_rate_Array_CUE{6}
    +SPEC_UE_Data_rate_Array_CUE{7}+SPEC_UE_Data_rate_Array_CUE{8}
    +SPEC_UE_Data_rate_Array_CUE{9}+SPEC_UE_Data_rate_Array_CUE{10}
    ]+SPEC_UE_Data_rate_Array_CUE{11}+SPEC_UE_Data_rate_Array_CUE{
    12}+SPEC_UE_Data_rate_Array_CUE{13}+SPEC_UE_Data_rate_Array_CU
    E{14}+SPEC_UE_Data_rate_Array_CUE{15}+SPEC_UE_Data_rate_Array_C
    UE{16}+SPEC_UE_Data_rate_Array_CUE{17}+SPEC_UE_Data_rate_Array
    _CUE{18}+SPEC_UE_Data_rate_Array_CUE{19}+SPEC_UE_Data_rate_Arr
    ay_CUE{20}];
SPEC_UE_SUM_A_CUE_Data_rate_array =
    [SPEC_UE_A_Data_rate_Array_CUE{1}+SPEC_UE_A_Data_rate_Array_CU
    E{2}+SPEC_UE_A_Data_rate_Array_CUE{3}+SPEC_UE_A_Data_rate_Arra
    y_CUE{4}+SPEC_UE_A_Data_rate_Array_CUE{5}+SPEC_UE_A_Data_rate
    _Array_CUE{6}+SPEC_UE_A_Data_rate_Array_CUE{7}+SPEC_UE_A_Dat
    a_rate_Array_CUE{8}+SPEC_UE_A_Data_rate_Array_CUE{9}+SPEC_UE_
    A_Data_rate_Array_CUE{10}+SPEC_UE_A_Data_rate_Array_CUE{11}+SP
    EC_UE_A_Data_rate_Array_CUE{12}+SPEC_UE_A_Data_rate_Array_CUE
    {13}+SPEC_UE_A_Data_rate_Array_CUE{14}+SPEC_UE_A_Data_rate_Arr
    ay_CUE{15}+SPEC_UE_A_Data_rate_Array_CUE{16}+SPEC_UE_A_Data_
    rate_Array_CUE{17}+SPEC_UE_A_Data_rate_Array_CUE{18}+SPEC_UE_
    A_Data_rate_Array_CUE{19}+SPEC_UE_A_Data_rate_Array_CUE{20}];

% SUM OF ENTIRE NETWORK DATA RATE
SPEC_UE_ENTIRE_DATA_RATE_ARRAY =
    [(SPEC_UE_Data_rate_Array{1}+SPEC_UE_Data_rate_Array_CUE{1}),(SPE
    C_UE_Data_rate_Array{2}+SPEC_UE_Data_rate_Array_CUE{2}),(SPEC_U
    E_Data_rate_Array{3}+SPEC_UE_Data_rate_Array_CUE{3}),(SPEC_UE_Da
    ta_rate_Array{4}+SPEC_UE_Data_rate_Array_CUE{4}),(SPEC_UE_Data_rat
    e_Array{5}+SPEC_UE_Data_rate_Array_CUE{5}),(SPEC_UE_Data_rate_Arr
    ay{6}+SPEC_UE_Data_rate_Array_CUE{6}),(SPEC_UE_Data_rate_Array{7}
    +SPEC_UE_Data_rate_Array_CUE{7}),(SPEC_UE_Data_rate_Array{8}+SPE

```

```

C_UE_Data_rate_Array_CUE{8}),(SPEC_UE_Data_rate_Array{9}+SPEC_U
E_Data_rate_Array_CUE{9}),(SPEC_UE_Data_rate_Array{10}+SPEC_UE_D
ata_rate_Array_CUE{10}),(SPEC_UE_Data_rate_Array{11}+SPEC_UE_Data
_rate_Array_CUE{11}),(SPEC_UE_Data_rate_Array{12}+SPEC_UE_Data_ra
te_Array_CUE{12}),(SPEC_UE_Data_rate_Array{13}+SPEC_UE_Data_rate_
Array_CUE{13}),(SPEC_UE_Data_rate_Array{14}+SPEC_UE_Data_rate_Arr
ay_CUE{14}),(SPEC_UE_Data_rate_Array{15}+SPEC_UE_Data_rate_Array_
CUE{15}),(SPEC_UE_Data_rate_Array{16}+SPEC_UE_Data_rate_Array_C
UE{16}),(SPEC_UE_Data_rate_Array{17}+SPEC_UE_Data_rate_Array_CUE
{17}),(SPEC_UE_Data_rate_Array{19}+SPEC_UE_Data_rate_Array_CUE{1
8}),(SPEC_UE_Data_rate_Array{19}+SPEC_UE_Data_rate_Array_CUE{19})
,(SPEC_UE_Data_rate_Array{20}+SPEC_UE_Data_rate_Array_CUE{20}));
SPEC_UE_A_ENTIRE_DATA_RATE_ARRAY =
[(SPEC_UE_A_Data_rate_Array{1}+SPEC_UE_A_Data_rate_Array_CUE{1}
),(SPEC_UE_A_Data_rate_Array{2}+SPEC_UE_A_Data_rate_Array_CUE{2
}),(SPEC_UE_A_Data_rate_Array{3}+SPEC_UE_A_Data_rate_Array_CUE{
3}),(SPEC_UE_A_Data_rate_Array{4}+SPEC_UE_A_Data_rate_Array_CUE
{4}),(SPEC_UE_A_Data_rate_Array{5}+SPEC_UE_A_Data_rate_Array_CU
E{5}),(SPEC_UE_A_Data_rate_Array{6}+SPEC_UE_A_Data_rate_Array_C
UE{6}),(SPEC_UE_A_Data_rate_Array{7}+SPEC_UE_A_Data_rate_Array_
CUE{7}),(SPEC_UE_A_Data_rate_Array{8}+SPEC_UE_A_Data_rate_Array_
_CUE{8}),(SPEC_UE_A_Data_rate_Array{9}+SPEC_UE_A_Data_rate_Arra
y_CUE{9}),(SPEC_UE_A_Data_rate_Array{10}+SPEC_UE_A_Data_rate_Ar
ray_CUE{10}),(SPEC_UE_A_Data_rate_Array{11}+SPEC_UE_A_Data_rate_
Array_CUE{11}),(SPEC_UE_A_Data_rate_Array{12}+SPEC_UE_A_Data_ra
te_Array_CUE{12}),(SPEC_UE_A_Data_rate_Array{13}+SPEC_UE_A_Data
_rate_Array_CUE{13}),(SPEC_UE_A_Data_rate_Array{14}+SPEC_UE_A_D
ata_rate_Array_CUE{14}),(SPEC_UE_A_Data_rate_Array{15}+SPEC_UE_A
_Data_rate_Array_CUE{15}),(SPEC_UE_A_Data_rate_Array{16}+SPEC_UE
_A_Data_rate_Array_CUE{16}),(SPEC_UE_A_Data_rate_Array{17}+SPEC_
UE_A_Data_rate_Array_CUE{17}),(SPEC_UE_A_Data_rate_Array{18}+SPE
C_UE_A_Data_rate_Array_CUE{18}),(SPEC_UE_A_Data_rate_Array{19}+S
PEC_UE_A_Data_rate_Array_CUE{19}),(SPEC_UE_A_Data_rate_Array{20}
+SPEC_UE_A_Data_rate_Array_CUE{20}));

```

% average data rate of entire network

```

SPEC_UE_data_rate_avg=
[((SPEC_UE_Data_rate_Array{1}+SPEC_UE_Data_rate_Array_CUE{1}))+
(SPEC_UE_Data_rate_Array{2}+SPEC_UE_Data_rate_Array_CUE{2}))+
(SPEC_UE_Data_rate_Array{3}+SPEC_UE_Data_rate_Array_CUE{3}))+
(SPEC_UE_Data_rate_Array{4}+SPEC_UE_Data_rate_Array_CUE{4}))+
(SPEC_UE_Data_rate_Array{5}+SPEC_UE_Data_rate_Array_CUE{5}))+
(SPEC_UE_Data_rate_Array{6}+SPEC_UE_Data_rate_Array_CUE{6}))+
(SPEC_UE_Data_rate_Array{7}+SPEC_UE_Data_rate_Array_CUE{7}))+
(SPEC_UE_Data_rate_Array{8}+SPEC_UE_Data_rate_Array_CUE{8}))+
(SPEC_UE_Data_rate_Array{9}+SPEC_UE_Data_rate_Array_CUE{9}))+
(SPEC_UE_Data_rate_Array{10}+SPEC_UE_Data_rate_Array_CUE{10}))+
(SPEC_UE_Data_rate_Array{11}+SPEC_UE_Data_rate_Array_CUE{11}))+
(SPEC_UE_Data_rate_Array{12}+SPEC_

```

```

UE_Data_rate_Array_CUE{12}))+ (SPEC_UE_Data_rate_Array{13}+SPEC_UE_Data_rate_Array_CUE{13}))+ (SPEC_UE_Data_rate_Array{14}+SPEC_UE_Data_rate_Array_CUE{14}))+ (SPEC_UE_Data_rate_Array{15}+SPEC_UE_Data_rate_Array_CUE{15}))+ (SPEC_UE_Data_rate_Array{16}+SPEC_UE_Data_rate_Array_CUE{16}))+ (SPEC_UE_Data_rate_Array{17}+SPEC_UE_Data_rate_Array_CUE{17}))+ (SPEC_UE_Data_rate_Array{18}+SPEC_UE_Data_rate_Array_CUE{18}))+ (SPEC_UE_Data_rate_Array{19}+SPEC_UE_Data_rate_Array_CUE{19}))+ (SPEC_UE_Data_rate_Array{20}+SPEC_UE_Data_rate_Array_CUE{20}))/SPEC_PAIR_Number_of_PL;0];
SPEC_A_UE_data_rate_avg=
[ ((SPEC_UE_A_Data_rate_Array{1}+SPEC_UE_A_Data_rate_Array_CUE{1}))+ (SPEC_UE_A_Data_rate_Array{2}+SPEC_UE_A_Data_rate_Array_CUE{2}))+ (SPEC_UE_A_Data_rate_Array{3}+SPEC_UE_A_Data_rate_Array_CUE{3}))+ (SPEC_UE_A_Data_rate_Array{4}+SPEC_UE_A_Data_rate_Array_CUE{4}))+ (SPEC_UE_A_Data_rate_Array{5}+SPEC_UE_A_Data_rate_Array_CUE{5}))+ (SPEC_UE_A_Data_rate_Array{6}+SPEC_UE_A_Data_rate_Array_CUE{6}))+ (SPEC_UE_A_Data_rate_Array{7}+SPEC_UE_A_Data_rate_Array_CUE{7}))+ (SPEC_UE_A_Data_rate_Array{8}+SPEC_UE_A_Data_rate_Array_CUE{8}))+ (SPEC_UE_A_Data_rate_Array{9}+SPEC_UE_A_Data_rate_Array_CUE{9}))+ (SPEC_UE_A_Data_rate_Array{10}+SPEC_UE_A_Data_rate_Array_CUE{10}))/Number_of_PL;0];

% AVERAGE DATA RATE BAR CHART OF DUE
SPEC_UE_DATA_RATE_BAR_CHART =
[abs(SPEC_UE_data_rate_avg),abs(SPEC_A_UE_data_rate_avg)]

```

```

SPEC_PAIR_X_axis= 1:1:20;

```

figure(9)

```

J1= plot(SPEC_PAIR_X_axis,SPEC_UE_SINR_D2DR_Array_BAR,'-*g');
hold on;
J2= plot(SPEC_PAIR_X_axis,SPEC_UE_A_SINR_D2DR_Array_BAR,'-or');

title(' SINR of DUE against D2D
pair','FontSize',12) xlabel ('Number of D2D
pair(s)','FontSize',12) ylabel ('SINR of
DUE','FontSize',12) legend ([J1 J2], 'SOMO','MS-
BAS')
hold off

```

figure(10)

```

bar(SPEC_UE_SINR_D2DR_bar)
title('Average SINR of DUE against D2D
pair','FontSize',12) xlabel('Scheme','fontsize',12)
ylabel('SINR of DUE', 'fontsize',12)
legend('SOMO','MS-BAS')

```

figure(11)

```
J3= plot(SPEC_PAIR_X_axis,SPEC_UE_Data_rate_D2DR_Array_BAR,'-*g');
hold on
J4= plot(SPEC_PAIR_X_axis,SPEC_UE_A_Data_rate_D2DR_Array_BAR,'-or');

title(' DUE data rate against D2D
pair','FontSize',12) xlabel ('Number of D2D
pair(s)','FontSize',12) ylabel ('DUE data rate
(Mbps)','FontSize',12) legend ([J3 J4],'SOMO','MS-
BAS')
hold off
```

figure(12)

```
bar(SPEC_UE_D2DR_Data_rate_bar)
title('Average Data rate of DUE against D2D pair','FontSize',12)
xlabel('Scheme','fontSize',12)
ylabel('Data rate of DUE (Mbps)', 'fontSize',12)
legend('SOMO','MS-BAS')
```

figure(13)

```
J5= plot(SPEC_PAIR_X_axis,SPEC_UE_CUE_Data_rate_array,'-*g');
hold on;
J6= plot(SPEC_PAIR_X_axis,SPEC_UE_A_CUE_Data_rate_array,'-or');

title(' CUE data rate against D2D
pair','FontSize',12) xlabel ('Number of D2D
pair(s)','FontSize',12) ylabel ('CUE data rate
(Mbps)','FontSize',12) legend ([J5 J6],'SOMO','MS-
BAS')
hold off
```

figure(14)

```
bar(SPEC_UE_CUE_D2DR_data_rate_bar)
title('Average data rate of CUE against D2D pair','FontSize',12)
xlabel('Scheme','fontSize',12)
ylabel('data_rate of DUE (Mbps)', 'fontSize',12)
legend('SOMO','MS-BAS')
```

figure(15)

```
J7= plot(SPEC_PAIR_X_axis,SPEC_UE_ENTIRE_DATA_RATE_ARRAY,'-*g');
hold on;
J8= plot(SPEC_PAIR_X_axis,SPEC_UE_A_ENTIRE_DATA_RATE_ARRAY,'or');

title(' Data rate of UE against D2D
pair','FontSize',12) xlabel ('Number of D2D
pair(s)','FontSize',12) ylabel ('UE data rate
```



```
POWER_DIS_PC_SINR_CUE_Array = cell(1,10);
POWER_DIS_Fixed_SINR_CUE_Array = cell(1,10);
POWER_DIS_AP_SINR_CUE_Array = cell(1,10);
POWER_DIS_PC_SINR_D2DR_Array = cell(1,10);
POWER_DIS_Fixed_SINR_D2DR_Array = cell(1,10);
POWER_DIS_AP_SINR_D2DR_Array = cell(1,10);
```

```
POWER_DIS_PC_Data_rate_CUE_Array = cell(1,10);
POWER_DIS_Fixed_Data_rate_CUE_Array = cell(1,10);
```

```
POWER_DIS_PC_Data_rate_D2DR_Array = cell(1,10);
POWER_DIS_Fixed_Data_rate_D2DR_Array = cell(1,10);
POWER_DIS_AP_Data_rate_D2DR_Array = cell(1,10);
```

```
POWER_DIS_AP_CUE_P_S_ARRAY = cell(1,10);
POWER_DIS_AP_D2DT_P_S_ARRAY = cell(1,10);
```

```
POWER_DIS_AP_AVG_CUE_P_S_ARRAY = cell(1,10);
POWER_DIS_AP_AVG_D2DT_P_S_ARRAY = cell(1,10);
```

```
POWER_DIS_CUE_P_ARRAY = cell(1,10);
POWER_DIS_D2DT_P_ARRAY = cell(1,10);
POWER_DIS_Fixed_CUE_P_ARRAY = cell(1,10);
POWER_DIS_Fixed_D2DT_P_ARRAY = cell(1,10);
POWER_DIS_AP_Data_rate_CUE_Array = cell(1,10);
POWER_DIS_PC_AVG_SINR_D2DR_Array = cell(1,10);
POWER_DIS_Fixed_AVG_SINR_D2DR_Array = cell(1,10);
POWER_DIS_AP_AVG_SINR_D2DR_Array = cell(1,10);
POWER_DIS_PC_AVG_Data_rate_D2DR_Array = cell(1,10);
POWER_DIS_Fixed_AVG_Data_rate_D2DR_Array = cell(1,10);
POWER_DIS_AP_AVG_Data_rate_D2DR_Array = cell(1,10);
POWER_DIS_PC_SINR_UE_Array = cell(1,10);
POWER_DIS_Fixed_SINR_UE_Array = cell(1,10);
POWER_DIS_AP_SINR_UE_Array = cell(1,10);
POWER_DIS_PC_Data_rate_UE_Array = cell(1,10);
POWER_DIS_Fixed_Data_rate_UE_Array = cell(1,10);
POWER_DIS_AP_Data_rate_UE_Array = cell(1,10);
```

```
Delta_Value = 0.5;
```

```
POWER_DIS_num_d2d_pair = 6;
POWER_DIS_num_cue_pair = 4;
Number_of_PL = 10;
```

```
for x=1:Number_of_PL
```

```
% PATHLOSS BETWEEN D2DT1 AND D2DR1 USING PCS1
```

```

POWER_DIS_PLoss_D2DT_D2DR = 10*log10(148 +
    40*log10(POWER_DIS_d_d2dt_d2dr));
% PATHLOSS BETWEEN D2DT1 AND D2DR1 USING OUR SCHEME 28 +
    40LOG10(d(KM))

POWER_DIS_AP_PLoss_AD2D_D2DT_D2DR = 10*log10(28 +
    40*log10(POWER_DIS_d_d2dt_d2dr));

% PATHLOSS BETWEEN AG D2DT AND VT D2DR USING PCS1
POWER_DIS_PLoss_INT_D2D = (10*log10(148 + 40*log10(d_int_d2dR)));
% PATHLOSS BETWEEN AG D2DT AND VT D2DR USING OUR SCHEME 28 +
    40LOG10(d(KM))
POWER_DIS_AP_PLoss_INT_AD2D = (10*log10(28 + 40*log10(d_int_d2dR)));

% PATHLOSS BETWEEN CUE AND BS USING PCS1
POWER_DIS_PLoss_CUE_BS = 10*log10(128+37.6*(log10(d_eNB_cue/1000)));
POWER_DIS_PLoss_CUE_BS_INT =
    10*log10(128+37.6*(log10(d_eNB_cue_INT/1000)));

% SINR OF eNB AND D2DR
sh =0;
% CUE Gain
POWER_DIS_G_CUE_P = 10^((-POWER_DIS_PLoss_CUE_BS -sh)/10)*(10^2);
POWER_DIS_G_CUE_P_INT = 10^((-POWER_DIS_PLoss_CUE_BS_INT -
    sh)/10)*(10^2);
POWER_DIS_Fixed_G_CUE_P = 10^((-POWER_DIS_PLoss_CUE_BS
    sh)/10)*(10^2);
POWER_DIS_Fixed_G_CUE_P_INT = 10^((-POWER_DIS_PLoss_CUE_BS_INT -
    sh)/10)*(10^2);
% CUE SINR
if POWER_DIS_num_cue_pair >0

POWER_DIS_SINR_CUE =
    (CUE_MAX_P*POWER_DIS_G_CUE_P)/((POWER_DIS_num_cue_pair-
    1)*POWER_DIS_CUE_P*POWER_DIS_G_CUE_P_INT+N);
POWER_DIS_AP_SINR_CUE = (CUE_MAX_P*POWER_DIS_G_CUE_P-
    sh)/((POWER_DIS_num_cue_pair-
    1)*POWER_DIS_AP_CUE_P_S*POWER_DIS_G_CUE_P_INT+N);
POWER_DIS_Fixed_SINR_CUE =
    (Fixed_CUE_P*POWER_DIS_Fixed_G_CUE_P)/((POWER_DIS_num_cue_p
    air-1)*Fixed_CUE_P*POWER_DIS_Fixed_G_CUE_P_INT+N) ;

else
    POWER_DIS_SINR_CUE = 0;
    POWER_DIS_AP_SINR_CUE = 0;
POWER_DIS_Fixed_SINR_CUE = 0; end

```

```

% D2D GAIN

POWER_DIS_G_D2DT_P      = (10^((-POWER_DIS_PLoss_D2DT_D2DR -
sh)/10))*(10^2);
POWER_DIS_G_D2DT_P_INT  = (10^((-POWER_DIS_PLoss_INT_D2D
sh)/10))*(10^2);

POWER_DIS_Fixed_G_D2DT_P = (10^((-POWER_DIS_PLoss_D2DT_D2DR -
sh)/10))*(10^2);
POWER_DIS_Fixed_G_D2DT_P_INT = (10^((-POWER_DIS_PLoss_INT_D2D -
sh)/10))*(10^2);

POWER_DIS_AP_G_D2DT_P_S      = (10^((-
POWER_DIS_AP_PLoss_AD2D_D2DT_D2DR-sh)/10))*(10^2);
POWER_DIS_AP_G_D2DT_INT_P_S  = (10^((-
POWER_DIS_AP_PLoss_INT_AD2D-sh)/10))*(10^2);

% D2D SINR of D2DR if
POWER_DIS_num_d2d_pair>0
    POWER_DIS_Fixed_SINR_D2DR      =
        (Fixed_D2DT_P_MAX*POWER_DIS_Fixed_G_D2DT_P)/(((POWER_DIS_n
um_d2d_pair-
1)*Fixed_D2DT_P_MAX*POWER_DIS_Fixed_G_D2DT_P_INT)+ N);

    POWER_DIS_SINR_D2DR      =
        (D2D_MAX_P*POWER_DIS_G_D2DT_P)/(((POWER_DIS_num_d2d_pair-
1)*(POWER_DIS_D2DT_P)*POWER_DIS_G_D2DT_P_INT)+ N);
    POWER_DIS_AP_SINR_D2DR      =
        (D2DT_P_INI*POWER_DIS_AP_G_D2DT_P_S)/(((POWER_DIS_num_d2d_
pair-
1)*POWER_DIS_AP_D2DT_P_S*POWER_DIS_AP_G_D2DT_INT_P_S)+
N);

else
    POWER_DIS_SINR_D2DR = 0;
    POWER_DIS_Fixed_SINR_D2DR =0;
    POWER_DIS_AP_SINR_D2DR =0; end

% POWER ADJUSTMENT OF OUR SCHEME
% Power control of D2D based on SINR

if      POWER_DIS_AP_SINR_D2DR      >      SINR_TARGET
POWER_DIS_S_D2DT =-1;
elseif POWER_DIS_AP_SINR_D2DR < SINR_TARGET
    POWER_DIS_S_D2DT =+1;
else
    POWER_DIS_S_D2DT = 0;

```

```

end

% CUE power control
if POWER_DIS_AP_SINR_CUE > SINR_TARGET
POWER_DIS_S_CUE = -1;
elseif POWER_DIS_AP_SINR_CUE < SINR_TARGET
POWER_DIS_S_CUE = +1;
else
POWER_DIS_S_CUE = 0;
end

POWER_DIS_CUE_P_S = POWER_DIS_AP_CUE_P_S
+(POWER_DIS_S_CUE*Delta_Value);
POWER_DIS_AP_CUE_P_S =
max((min(POWER_DIS_CUE_P_S,CUE_MAX_P)),CUE_Min_P);

POWER_DIS_D2DT_PS = POWER_DIS_AP_D2DT_P_S
+(POWER_DIS_S_D2DT*Delta_Value);
POWER_DIS_AP_D2DT_P_S =
max((min(POWER_DIS_D2DT_PS,D2D_MAX_P)),D2D_MIN_P);

% POWER ADJUSTMENT OF PCS1
% Power control of D2D based on PCS1

if POWER_DIS_SINR_D2DR > SINR_TARGET
POWER_DIS_D2DT = -1;
elseif POWER_DIS_SINR_D2DR < SINR_TARGET
POWER_DIS_D2DT = +1;
else
POWER_DIS_D2DT = 0;
end

% power control of CUE based on PCS1
if POWER_DIS_SINR_CUE > SINR_TARGET
POWER_DIS_CUE = -1;
elseif POWER_DIS_SINR_CUE < SINR_TARGET
POWER_DIS_CUE = +1;
else
POWER_DIS_CUE = 0;
end

POWER_DIS_CUE_P = max((min((POWER_DIS_CUE_P
+POWER_DIS_CUE*1),CUE_MAX_P)),CUE_Min_P);
POWER_DIS_D2DT_P = max((min((POWER_DIS_D2DT_P
+POWER_DIS_D2DT*0.5),D2D_MAX_P)),D2D_MIN_P);

% DATA RATE OF eNB = BW_CUE*log2(1 + SINR_eNB)

```

```

% Data rate of eNB USING PCS1
POWER_DIS_Data_rate_CUE = BW_A*log2(1+POWER_DIS_SINR_CUE);
% Data rate of eNB USING Fixed Power
POWER_DIS_Fixed_Data_rate_CUE =
    BW_A*log2(1+POWER_DIS_Fixed_SINR_CUE);
% Data rate of eNB USING OUR SCHEME
POWER_DIS_AP_Data_rate_CUE =
    BW_A*log2(1+POWER_DIS_AP_SINR_CUE);

% DATA RATE OF D2D
% Data rate of D2DR USING PCS1 = BW_D2D*log2(1 + SINR_D2DR1)
POWER_DIS_Data_rate_D2DR = BW_A*log2(1 + POWER_DIS_SINR_D2DR);
% Data rate of D2DR USING Fixed Power = BW_D2D*log2(1 + SINR_D2DR1)
POWER_DIS_Fixed_Data_rate_D2DR = BW_A*log2(1
    +POWER_DIS_Fixed_SINR_D2DR);
% Data rate of D2DR USING OUR SCHEME = BW_D2D*log2(1 + SINR_D2DR1)
POWER_DIS_AP_Data_rate_D2DR = BW_A*log2(1
    +POWER_DIS_AP_SINR_D2DR);

% ARRAY OF SINR
% array of CUE SINRs
POWER_DIS_PC_SINR_CUE_Array{x} = abs(POWER_DIS_SINR_CUE);
POWER_DIS_Fixed_SINR_CUE_Array{x} = abs(POWER_DIS_Fixed_SINR_CUE);
POWER_DIS_AP_SINR_CUE_Array{x} = abs(POWER_DIS_AP_SINR_CUE);

% array of D2DR SINR
POWER_DIS_PC_SINR_D2DR_Array{x} = abs(POWER_DIS_SINR_D2DR);
POWER_DIS_Fixed_SINR_D2DR_Array{x} =
    abs(POWER_DIS_Fixed_SINR_D2DR);
POWER_DIS_AP_SINR_D2DR_Array{x} = abs(POWER_DIS_AP_SINR_D2DR); %
array of UE SINR
POWER_DIS_PC_SINR_UE_Array{x} =
    abs(POWER_DIS_SINR_D2DR+POWER_DIS_SINR_CUE);
POWER_DIS_Fixed_SINR_UE_Array{x} =
    abs(POWER_DIS_Fixed_SINR_D2DR+POWER_DIS_Fixed_SINR_CUE);
POWER_DIS_AP_SINR_UE_Array{x} =
    abs(POWER_DIS_AP_SINR_D2DR+POWER_DIS_AP_SINR_CUE);

% ARRAY OF DATA RATE
% array of CUE Data rate
POWER_DIS_PC_Data_rate_CUE_Array{x} = abs(POWER_DIS_Data_rate_CUE);
POWER_DIS_Fixed_Data_rate_CUE_Array{x} =
    abs(POWER_DIS_Fixed_Data_rate_CUE);
POWER_DIS_AP_Data_rate_CUE_Array{x} =
    abs(POWER_DIS_AP_Data_rate_CUE);

```

```

% array of D2D data rate
POWER_DIS_PC_Data_rate_D2DR_Array{x}=(POWER_DIS_Data_rate_D2DR);
POWER_DIS_Fixed_Data_rate_D2DR_Array{x}=
    (POWER_DIS_Fixed_Data_rate_D2DR);
POWER_DIS_AP_Data_rate_D2DR_Array{x}=
    (POWER_DIS_AP_Data_rate_D2DR);

% array of UE data rate
POWER_DIS_PC_Data_rate_UE_Array{x}=
    (POWER_DIS_Data_rate_D2DR)+(POWER_DIS_Data_rate_CUE);
POWER_DIS_Fixed_Data_rate_UE_Array{x}=
    abs(POWER_DIS_Fixed_Data_rate_D2DR)+abs(POWER_DIS_Fixed_Data_rate_CUE);
POWER_DIS_AP_Data_rate_UE_Array{x}=
    abs(POWER_DIS_AP_Data_rate_D2DR)+abs(POWER_DIS_AP_Data_rate_CUE);

% POWER ARRAY BASED ON SCHEME
POWER_DIS_AP_CUE_P_S_ARRAY{x}= abs(POWER_DIS_AP_CUE_P_S);
POWER_DIS_AP_D2DT_P_S_ARRAY{x} =abs(POWER_DIS_AP_D2DT_P_S);

% POWER ARRAY BASED ON PCS1
POWER_DIS_CUE_P_ARRAY{x}= abs(POWER_DIS_CUE_P);
POWER_DIS_D2DT_P_ARRAY{x} =abs(POWER_DIS_D2DT_P);
% POWER ARRAY BASED ON Fixed Power
POWER_DIS_Fixed_CUE_P_ARRAY{x}= Fixed_CUE_P;
POWER_DIS_Fixed_D2DT_P_ARRAY{x} = Fixed_D2DT_P_MAX;

% Change the distance between D2D Pair
POWER_DIS_d_d2dt_d2dr = POWER_DIS_d_d2dt_d2dr+1; % distance of DUE
    increase by 1m
end

% POWER COLLECTION OF CUE

```

```

POWER_DIS_CUE_P_ARRAY_BAR
=[POWER_DIS_CUE_P_ARRAY{1},POWER_DIS_CUE_P_ARRAY{2},PO
WER_DIS_CUE_P_ARRAY{3},POWER_DIS_CUE_P_ARRAY{4},POWER
_DIS_CUE_P_ARRAY{5},POWER_DIS_CUE_P_ARRAY{6},POWER_DIS
_CUE_P_ARRAY{7},POWER_DIS_CUE_P_ARRAY{8},POWER_DIS_CU
E_P_ARRAY{9},POWER_DIS_CUE_P_ARRAY{10}]
POWER_DIS_Fixed_CUE_P_ARRAY_BAR
=[POWER_DIS_Fixed_CUE_P_ARRAY{1},POWER_DIS_Fixed_CUE_P_A
RRAY{2},POWER_DIS_Fixed_CUE_P_ARRAY{3},POWER_DIS_Fixed_C
UE_P_ARRAY{4},POWER_DIS_Fixed_CUE_P_ARRAY{5},POWER_DIS_
Fixed_CUE_P_ARRAY{6},POWER_DIS_Fixed_CUE_P_ARRAY{7},POWE
R_DIS_Fixed_CUE_P_ARRAY{8},POWER_DIS_Fixed_CUE_P_ARRAY{9
},POWER_DIS_Fixed_CUE_P_ARRAY{10}]
POWER_DIS_AP_CUE_P_S_ARRAY_BAR
=[POWER_DIS_AP_CUE_P_S_ARRAY{1},POWER_DIS_AP_CUE_P_S_A
RRAY{2},POWER_DIS_AP_CUE_P_S_ARRAY{3},POWER_DIS_AP_CUE
_P_S_ARRAY{4},POWER_DIS_AP_CUE_P_S_ARRAY{5},POWER_DIS_
AP_CUE_P_S_ARRAY{6},POWER_DIS_AP_CUE_P_S_ARRAY{7},POWE
R_DIS_AP_CUE_P_S_ARRAY{8},POWER_DIS_AP_CUE_P_S_ARRAY{9
},POWER_DIS_AP_CUE_P_S_ARRAY{10}]
% Average CUE POWER
POWER_DIS_AVG_CUE_P_ARRAY_BAR2
=[(sum(POWER_DIS_CUE_P_ARRAY_BAR)/(Number_of_PL));0];
POWER_DIS_Fixed_AVG_CUE_P_ARRAY_BAR2
=[(sum(POWER_DIS_Fixed_CUE_P_ARRAY_BAR)/(Number_of_PL));0];
POWER_DIS_AP_AVG_CUE_P_S_ARRAY_BAR2
=[(sum(POWER_DIS_AP_CUE_P_S_ARRAY_BAR)/(Number_of_PL));0];
% barchart of CUE power
POWER_DIS_AVG_CUE_P_S_BAR =
[POWER_DIS_Fixed_AVG_CUE_P_ARRAY_BAR2,POWER_DIS_AVG_C
UE_P_ARRAY_BAR2,POWER_DIS_AP_AVG_CUE_P_S_ARRAY_BAR2]

% POWER COLLECTION OF D2D
POWER_DIS_AVG_D2DT_ARRAY_BAR =
[POWER_DIS_D2DT_P_ARRAY{1},POWER_DIS_D2DT_P_ARRAY{2},
POWER_DIS_D2DT_P_ARRAY{3},POWER_DIS_D2DT_P_ARRAY{4},PO
WER_DIS_D2DT_P_ARRAY{5},POWER_DIS_D2DT_P_ARRAY{6},POW
ER_DIS_D2DT_P_ARRAY{7},POWER_DIS_D2DT_P_ARRAY{8},POWER
_DIS_D2DT_P_ARRAY{9},POWER_DIS_D2DT_P_ARRAY{10}];
POWER_DIS_Fixed_AVG_D2DT_ARRAY_BAR =
[POWER_DIS_Fixed_D2DT_P_ARRAY{1},POWER_DIS_Fixed_D2DT_P_
ARRAY{2},
POWER_DIS_Fixed_D2DT_P_ARRAY{3},POWER_DIS_Fixed_D2DT_P_A
RRAY{4},POWER_DIS_Fixed_D2DT_P_ARRAY{5},POWER_DIS_Fixed_
=

```

```

D2DT_P_ARRAY{6},POWER_DIS_Fixed_D2DT_P_ARRAY{7},POWER_
DIS_Fixed_D2DT_P_ARRAY{8},POWER_DIS_Fixed_D2DT_P_ARRAY{9}
,POWER_DIS_Fixed_D2DT_P_ARRAY{10}];
POWER_DIS_AP_AVG_D2DT_P_S_ARRAY_BAR
[POWER_DIS_AP_D2DT_P_S_ARRAY{1},POWER_DIS_AP_D2DT_P_S_
ARRAY{2},POWER_DIS_AP_D2DT_P_S_ARRAY{3},POWER_DIS_AP_D
2DT_P_S_ARRAY{4},POWER_DIS_AP_D2DT_P_S_ARRAY{5},POWER_
DIS_AP_D2DT_P_S_ARRAY{6},POWER_DIS_AP_D2DT_P_S_ARRAY{7
},POWER_DIS_AP_D2DT_P_S_ARRAY{8},POWER_DIS_AP_D2DT_P_S_
ARRAY{9},POWER_DIS_AP_D2DT_P_S_ARRAY{10}];
% Average DUE power
POWER_DIS_AVG_D2D_P_S_ARRAY =
[(sum(POWER_DIS_AVG_D2DT_ARRAY_BAR)/Number_of_PL);0];
POWER_DIS_Fixed_AVG_D2D_P_S_ARRAY =
[(sum(POWER_DIS_Fixed_AVG_D2DT_ARRAY_BAR)/Number_of_PL);0];
POWER_DIS_AP_AVG_D2D_P_S_ARRAY =
[(sum(POWER_DIS_AP_AVG_D2DT_P_S_ARRAY_BAR)/Number_of_PL);
0];
% Barchart of DUE
POWER_DIS_D2D_P_S_BAR =
[POWER_DIS_Fixed_AVG_D2D_P_S_ARRAY,POWER_DIS_AVG_D2D_P
_S_ARRAY,POWER_DIS_AP_AVG_D2D_P_S_ARRAY]
% ARRAY OF SINR BAR
% array of eNB SINR
POWER_DIS_PC_SINR_CUE_Array_BAR =
[POWER_DIS_PC_SINR_CUE_Array{1},POWER_DIS_PC_SINR_CUE_Arr
ay{2},POWER_DIS_PC_SINR_CUE_Array{3},POWER_DIS_PC_SINR_CU
E_Array{4},POWER_DIS_PC_SINR_CUE_Array{5},POWER_DIS_PC_SIN
R_CUE_Array{6},POWER_DIS_PC_SINR_CUE_Array{7},POWER_DIS_PC
_SINR_CUE_Array{8},POWER_DIS_PC_SINR_CUE_Array{9},POWER_DI
S_PC_SINR_CUE_Array{10}]
POWER_DIS_Fixed_SINR_CUE_Array_BAR =
[POWER_DIS_Fixed_SINR_CUE_Array{1},POWER_DIS_Fixed_SINR_CUE
_Array{2},POWER_DIS_Fixed_SINR_CUE_Array{3},POWER_DIS_Fixed_S
INR_CUE_Array{4},POWER_DIS_Fixed_SINR_CUE_Array{5},POWER_DI
S_Fixed_SINR_CUE_Array{6},POWER_DIS_Fixed_SINR_CUE_Array{7},P
OWER_DIS_Fixed_SINR_CUE_Array{8},POWER_DIS_Fixed_SINR_CUE_
Array{9},POWER_DIS_Fixed_SINR_CUE_Array{10}]
POWER_DIS_AP_SINR_CUE_Array_BAR =
[POWER_DIS_AP_SINR_CUE_Array{1},POWER_DIS_AP_SINR_CUE_Arr
ay{2},POWER_DIS_AP_SINR_CUE_Array{3},POWER_DIS_AP_SINR_CU
E_Array{4},POWER_DIS_AP_SINR_CUE_Array{5},POWER_DIS_AP_SIN
R_CUE_Array{6},POWER_DIS_AP_SINR_CUE_Array{7},POWER_DIS_A
=

```

```

P_SINR_CUE_Array{8},POWER_DIS_AP_SINR_CUE_Array{9},POWER_
DIS_AP_SINR_CUE_Array{10}]
% Average eNB SINR
POWER_DIS_PC_SINR_CUE_AVG =
[(sum(POWER_DIS_PC_SINR_CUE_Array_BAR)/(Number_of_PL));0];
POWER_DIS_Fixed_SINR_CUE_AVG =
[(sum(POWER_DIS_Fixed_SINR_CUE_Array_BAR)/(Number_of_PL));0];
POWER_DIS_AP_SINR_CUE_AVG =
[(sum(POWER_DIS_AP_SINR_CUE_Array_BAR)/(Number_of_PL));0];
% barchart of AVERAGE CUE SINR
POWER_DIS_Average_CUE_SINR
[POWER_DIS_Fixed_SINR_CUE_AVG;POWER_DIS_PC_SINR_CUE_AV
G;POWER_DIS_AP_SINR_CUE_AVG]
% array of D2D SINR
POWER_DIS_PC_AVG_SINR_D2DR_Array_BAR =
[POWER_DIS_PC_SINR_D2DR_Array{1},POWER_DIS_PC_SINR_D2DR_
Array{2},POWER_DIS_PC_SINR_D2DR_Array{3},POWER_DIS_PC_SINR
_D2DR_Array{4},POWER_DIS_PC_SINR_D2DR_Array{5},POWER_DIS_P
C_SINR_D2DR_Array{6},POWER_DIS_PC_SINR_D2DR_Array{7},POWE
R_DIS_PC_SINR_D2DR_Array{8},POWER_DIS_PC_SINR_D2DR_Array{9
},POWER_DIS_PC_SINR_D2DR_Array{10}]
POWER_DIS_Fixed_AVG_SINR_D2DR_Array_BAR =
[POWER_DIS_Fixed_SINR_D2DR_Array{1},POWER_DIS_Fixed_SINR_D2
DR_Array{2},POWER_DIS_Fixed_SINR_D2DR_Array{3},POWER_DIS_Fix
ed_SINR_D2DR_Array{4},POWER_DIS_Fixed_SINR_D2DR_Array{5},PO
WER_DIS_Fixed_SINR_D2DR_Array{6},POWER_DIS_Fixed_SINR_D2DR
_Array{7},POWER_DIS_Fixed_SINR_D2DR_Array{8},POWER_DIS_Fixed
_SINR_D2DR_Array{9},POWER_DIS_Fixed_SINR_D2DR_Array{10}]
POWER_DIS_AP_AVG_SINR_D2DR_Array_BAR =
[POWER_DIS_AP_SINR_D2DR_Array{1},POWER_DIS_AP_SINR_D2DR_
Array{2},POWER_DIS_AP_SINR_D2DR_Array{3},POWER_DIS_AP_SINR
_D2DR_Array{4},POWER_DIS_AP_SINR_D2DR_Array{5},POWER_DIS_
AP_SINR_D2DR_Array{6},POWER_DIS_AP_SINR_D2DR_Array{7},POW
ER_DIS_AP_SINR_D2DR_Array{8},POWER_DIS_AP_SINR_D2DR_Array{
9},POWER_DIS_AP_SINR_D2DR_Array{10}]

% Average D2DR SINR
POWER_DIS_PC_SINR_D2DR_AVG =
[(sum(POWER_DIS_PC_AVG_SINR_D2DR_Array_BAR)/(Number_of_PL));
0];
POWER_DIS_Fixed_SINR_D2DR_AVG =
[(sum(POWER_DIS_Fixed_AVG_SINR_D2DR_Array_BAR)/(Number_of_P
L));0];
POWER_DIS_AP_SINR_D2DR_AVG =

```

```

    [(sum(POWER_DIS_AP_AVG_SINR_D2DR_Array_BAR)/(Number_of_PL));
    0];
% barchart of Average D2DR SINR
POWER_DIS_SINR_D2DR_AVG =
    [POWER_DIS_Fixed_SINR_D2DR_AVG,POWER_DIS_PC_SINR_D2DR_A
    VG,POWER_DIS_AP_SINR_D2DR_AVG]

% UE SINR
% array of UE SINR
POWER_DIS_PC_SINR_UE_Array_BAR =
    [POWER_DIS_PC_SINR_UE_Array{1},POWER_DIS_PC_SINR_UE_Array{
    2},POWER_DIS_PC_SINR_UE_Array{3},POWER_DIS_PC_SINR_UE_Arra
    y{4},POWER_DIS_PC_SINR_UE_Array{5},POWER_DIS_PC_SINR_UE_Ar
    ray{6},POWER_DIS_PC_SINR_UE_Array{7},POWER_DIS_PC_SINR_UE_
    Array{8},POWER_DIS_PC_SINR_UE_Array{9},POWER_DIS_PC_SINR_U
    E_Array{10}]
POWER_DIS_Fixed_SINR_UE_Array_BAR
    [POWER_DIS_Fixed_SINR_UE_Array{1},POWER_DIS_Fixed_SINR_UE_A
    rray{2},POWER_DIS_Fixed_SINR_UE_Array{3},POWER_DIS_Fixed_SINR

```

=

```

    _UE_Array{4},POWER_DIS_Fixed_SINR_UE_Array{5},POWER_DIS_Fixe
    d_SINR_UE_Array{6},POWER_DIS_Fixed_SINR_UE_Array{7},POWER_D
    IS_Fixed_SINR_UE_Array{8},POWER_DIS_Fixed_SINR_UE_Array{9},PO
    WER_DIS_Fixed_SINR_UE_Array{10}]
POWER_DIS_AP_SINR_UE_Array_BAR =
    [POWER_DIS_AP_SINR_UE_Array{1},POWER_DIS_AP_SINR_UE_Array{
    2},POWER_DIS_AP_SINR_UE_Array{3},POWER_DIS_AP_SINR_UE_Arra
    y{4},POWER_DIS_AP_SINR_UE_Array{5},POWER_DIS_AP_SINR_UE_A
    rray{6},POWER_DIS_AP_SINR_UE_Array{7},POWER_DIS_AP_SINR_UE
    _Array{8},POWER_DIS_AP_SINR_UE_Array{9},POWER_DIS_AP_SINR_
    UE_Array{10}]

% Average UE SINR
POWER_DIS_PC_SINR_UE_AVG =
    [(sum(POWER_DIS_PC_SINR_UE_Array_BAR)/(Number_of_PL));0];
POWER_DIS_Fixed_SINR_UE_AVG =
    [(sum(POWER_DIS_Fixed_SINR_UE_Array_BAR)/(Number_of_PL));0];
POWER_DIS_AP_SINR_UE_AVG =
    [(sum(POWER_DIS_AP_SINR_UE_Array_BAR)/(Number_of_PL));0];
% barchart of Average UE SINR
POWER_DIS_SINR_UE_AVG =
    [POWER_DIS_Fixed_SINR_UE_AVG,POWER_DIS_PC_SINR_UE_AVG,P
    OWER_DIS_AP_SINR_UE_AVG]

% ARRAY OF DATA RATE BAR
% data rate of eNB
POWER_DIS_PC_Data_rate_CUE_Array_BAR =
    [POWER_DIS_PC_Data_rate_CUE_Array{1},POWER_DIS_PC_Data_rate_C
    UE_Array{2},POWER_DIS_PC_Data_rate_CUE_Array{3},POWER_DIS_PC
    _Data_rate_CUE_Array{4},POWER_DIS_PC_Data_rate_CUE_Array{5},PO
    WER_DIS_PC_Data_rate_CUE_Array{6},POWER_DIS_PC_Data_rate_CUE_
    Array{7},POWER_DIS_PC_Data_rate_CUE_Array{8},POWER_DIS_PC_Dat
    a_rate_CUE_Array{9},POWER_DIS_PC_Data_rate_CUE_Array{10}]
POWER_DIS_Fixed_Data_rate_CUE_Array_BAR =
    [POWER_DIS_Fixed_Data_rate_CUE_Array{1},POWER_DIS_Fixed_Data_ra
    te_CUE_Array{2},POWER_DIS_Fixed_Data_rate_CUE_Array{3},POWER_
    DIS_Fixed_Data_rate_CUE_Array{4},POWER_DIS_Fixed_Data_rate_CUE_
    Array{5},POWER_DIS_Fixed_Data_rate_CUE_Array{6},POWER_DIS_Fixe
    d_Data_rate_CUE_Array{7},POWER_DIS_Fixed_Data_rate_CUE_Array{8},
    POWER_DIS_Fixed_Data_rate_CUE_Array{9},POWER_DIS_Fixed_Data_rat
    e_CUE_Array{10}]
POWER_DIS_AP_Data_rate_CUE_Array_BAR =
    [POWER_DIS_AP_Data_rate_CUE_Array{1},POWER_DIS_AP_Data_rate_C
    UE_Array{2},POWER_DIS_AP_Data_rate_CUE_Array{3},POWER_DIS_AP
    _Data_rate_CUE_Array{4},POWER_DIS_AP_Data_rate_CUE_Array{5},PO
    WER_DIS_AP_Data_rate_CUE_Array{6},POWER_DIS_AP_Data_rate_CUE
    _Array{7},POWER_DIS_AP_Data_rate_CUE_Array{8},POWER_DIS_AP_D

```

```

ata_rate_CUE_Array{9},POWER_DIS_AP_Data_rate_CUE_Array{10}] %
average eNB data rate POWER_DIS_PC_Data_rate_CUE_AVG_Array_BAR =
[sum(POWER_DIS_PC_Data_rate_CUE_Array_BAR)/Number_of_PL;0];
POWER_DIS_Fixed_Data_rate_CUE_AVG_Array_BAR =
[sum(POWER_DIS_Fixed_Data_rate_CUE_Array_BAR)/Number_of_PL;0];
POWER_DIS_AP_Data_rate_CUE_AVG_Array_BAR =
[sum(POWER_DIS_AP_Data_rate_CUE_Array_BAR)/Number_of_PL;0]; %
Barchart of average eNB data rate
POWER_DIS_Data_Rate_CUE_AVG =
[POWER_DIS_Fixed_Data_rate_CUE_AVG_Array_BAR,POWER_DIS_PC_
Data_rate_CUE_AVG_Array_BAR,POWER_DIS_AP_Data_rate_CUE_AVG_
Array_BAR]

% data rate of D2D
POWER_DIS_PC_Data_rate_D2DR_Array_BAR =
[POWER_DIS_PC_Data_rate_D2DR_Array{1},POWER_DIS_PC_Data_rate_
D2DR_Array{2},POWER_DIS_PC_Data_rate_D2DR_Array{3},POWER_DIS
_PC_Data_rate_D2DR_Array{4},POWER_DIS_PC_Data_rate_D2DR_Array{
5},POWER_DIS_PC_Data_rate_D2DR_Array{6},POWER_DIS_PC_Data_rat
e_D2DR_Array{7},POWER_DIS_PC_Data_rate_D2DR_Array{8},POWER_D
IS_PC_Data_rate_D2DR_Array{9},POWER_DIS_PC_Data_rate_D2DR_Arra
y{10}]
POWER_DIS_Fixed_Data_rate_D2DR_Array_BAR =
[POWER_DIS_Fixed_Data_rate_D2DR_Array{1},POWER_DIS_Fixed_Data_
rate_D2DR_Array{2},POWER_DIS_Fixed_Data_rate_D2DR_Array{3},POW
ER_DIS_Fixed_Data_rate_D2DR_Array{4},POWER_DIS_Fixed_Data_rate_D
2DR_Array{5},POWER_DIS_Fixed_Data_rate_D2DR_Array{6},POWER_DI
S_Fixed_Data_rate_D2DR_Array{7},POWER_DIS_Fixed_Data_rate_D2DR_
Array{8},POWER_DIS_Fixed_Data_rate_D2DR_Array{9},POWER_DIS_Fix
ed_Data_rate_D2DR_Array{10}]
POWER_DIS_AP_Data_rate_D2DR_Array_BAR =
[POWER_DIS_AP_Data_rate_D2DR_Array{1},POWER_DIS_AP_Data_rate_
D2DR_Array{2},POWER_DIS_AP_Data_rate_D2DR_Array{3},POWER_DIS
_AP_Data_rate_D2DR_Array{4},POWER_DIS_AP_Data_rate_D2DR_Array{
5},POWER_DIS_AP_Data_rate_D2DR_Array{6},POWER_DIS_AP_Data_rat
e_D2DR_Array{7},POWER_DIS_AP_Data_rate_D2DR_Array{8},POWER_
DIS_AP_Data_rate_D2DR_Array{9},POWER_DIS_AP_Data_rate_D2DR_Arr
ay{10}]
% average data rate of DUE
POWER_DIS_PC_Data_rate_D2DR_Array_AVG_BAR =
[(sum(POWER_DIS_PC_Data_rate_D2DR_Array_BAR)/Number_of_PL);0];
POWER_DIS_Fixed_Data_rate_D2DR_Array_AVG_BAR =
[(sum(POWER_DIS_Fixed_Data_rate_D2DR_Array_BAR)/Number_of_PL);0
];
POWER_DIS_AP_Data_rate_D2DR_Array_AVG_BAR =
[(sum(POWER_DIS_AP_Data_rate_D2DR_Array_BAR)/Number_of_PL);0];
% Barchart of average DUE data rate
POWER_DIS_Data_Rate_D2D_AVG =

```

```

[POWER_DIS_Fixed_Data_rate_D2DR_Array_AVG_BAR,POWER_DIS_PC
_Data_rate_D2DR_Array_AVG_BAR,POWER_DIS_AP_Data_rate_D2DR_A
rray_AVG_BAR]
% Entire UE data rate
% data rate array of UE
POWER_DIS_PC_Data_rate_UE_Array_BAR =
[POWER_DIS_PC_Data_rate_UE_Array{1},POWER_DIS_PC_Data_rate_UE
_Array{2},POWER_DIS_PC_Data_rate_UE_Array{3},POWER_DIS_PC_Dat
a_rate_UE_Array{4},POWER_DIS_PC_Data_rate_UE_Array{5},POWER_DI
S_PC_Data_rate_UE_Array{6},POWER_DIS_PC_Data_rate_UE_Array{7},P
OWER_DIS_PC_Data_rate_UE_Array{8},POWER_DIS_PC_Data_rate_UE_
Array{9},POWER_DIS_PC_Data_rate_UE_Array{10}]
POWER_DIS_Fixed_Data_rate_UE_Array_BAR =
[POWER_DIS_Fixed_Data_rate_UE_Array{1},POWER_DIS_Fixed_Data_rat
e_UE_Array{2},POWER_DIS_Fixed_Data_rate_UE_Array{3},POWER_DIS_
Fixed_Data_rate_UE_Array{4},POWER_DIS_Fixed_Data_rate_UE_Array{5},
POWER_DIS_Fixed_Data_rate_UE_Array{6},POWER_DIS_Fixed_Data_rate
_UE_Array{7},POWER_DIS_Fixed_Data_rate_UE_Array{8},POWER_DIS_F
ixed_Data_rate_UE_Array{9},POWER_DIS_Fixed_Data_rate_UE_Array{10}
]
POWER_DIS_AP_Data_rate_UE_Array_BAR =
[POWER_DIS_AP_Data_rate_UE_Array{1},POWER_DIS_AP_Data_rate_UE
_Array{2},POWER_DIS_AP_Data_rate_UE_Array{3},POWER_DIS_AP_Dat
a_rate_UE_Array{4},POWER_DIS_AP_Data_rate_UE_Array{5},POWER_DI
S_AP_Data_rate_UE_Array{6},POWER_DIS_AP_Data_rate_UE_Array{7},P
OWER_DIS_AP_Data_rate_UE_Array{8},POWER_DIS_AP_Data_rate_UE_
Array{9},POWER_DIS_AP_Data_rate_UE_Array{10}]
% average data rate of UE
POWER_DIS_PC_Data_rate_UE_Array_AVG_BAR =
[(sum(POWER_DIS_PC_Data_rate_UE_Array_BAR)/Number_of_PL);0];
POWER_DIS_Fixed_Data_rate_UE_Array_AVG_BAR =
[(sum(POWER_DIS_Fixed_Data_rate_UE_Array_BAR)/Number_of_PL);0];
POWER_DIS_AP_Data_rate_UE_Array_AVG_BAR =
[(sum(POWER_DIS_AP_Data_rate_UE_Array_BAR)/Number_of_PL);0];
% Barchart of average UE data rate
POWER_DIS_Data_Rate_UE_AVG =
[POWER_DIS_Fixed_Data_rate_UE_Array_AVG_BAR,POWER_DIS_PC_D
ata_rate_UE_Array_AVG_BAR,POWER_DIS_AP_Data_rate_UE_Array_AV
G_BAR]
X_axis= 1:1:10;

figure (17)
J3= plot(X_axis,POWER_DIS_Fixed_AVG_SINR_D2DR_Array_BAR,'-*g');
hold on;
J4= plot(X_axis,POWER_DIS_PC_AVG_SINR_D2DR_Array_BAR,'-*b');
J5= plot(X_axis,POWER_DIS_AP_AVG_SINR_D2DR_Array_BAR,'-or');

```

```

    title('SINR of DUE against distance of
DUE','FontSize',12) xlabel ('distance of DUE
(m)','FontSize',12) ylabel ('SINR of DUE','FontSize',12)
legend ([J3 J4 J5],'FPC','PCS1','D2D-PCS') hold off

```

figure (18)

```

bar(POWER_DIS_SINR_D2DR_AVG)
    title('Average DUE SINR against distance of
DUE','FontSize',12) xlabel ('Scheme','FontSize',12) ylabel
('SINR of DUE','FontSize',12)
    legend ('FPC','PCS1','D2D-PCS')

```

figure(19)

```

J6= plot(X_axis,POWER_DIS_Fixed_Data_rate_D2DR_Array_BAR,'-*g');
hold on;
J7= plot(X_axis,POWER_DIS_PC_Data_rate_D2DR_Array_BAR,'-*b') ;
J8= plot(X_axis,POWER_DIS_AP_Data_rate_D2DR_Array_BAR,'-or') ;
    title('Data rate of DUE against distance of
DUE','FontSize',12) xlabel('Distance of DUE
(m)','FontSize',12) ylabel('Data rate of DUE
(Mbps)','FontSize',12) legend([J6 J7 J8],'FPC','PCS1','D2D-
PCS') hold off;

```

figure (20)

```

bar(abs(POWER_DIS_Data_Rate_D2D_AVG))
    title('Average DUE Data rate against distance of
DUE','FontSize',12) xlabel ('Scheme','FontSize',12) ylabel ('DUE
data rate (Mbps)','FontSize',12) legend ('FPC','PCS1','D2D-PCS')

```

figure(21)

```

bar(abs(POWER_DIS_D2D_P_S_BAR))
    title('Average DUE power consumption against distance of
DUE','FontSize',12) xlabel ('Scheme','FontSize',12) ylabel
('Power(dBm)','FontSize',12)
    legend ('FPC','PCS1','D2D-PCS')

```

figure (22)

```

J6= plot(X_axis,POWER_DIS_Fixed_Data_rate_CUE_Array_BAR,'-*g');
hold on;
J7= plot(X_axis,POWER_DIS_PC_Data_rate_CUE_Array_BAR,'-*b') ;
J8= plot(X_axis,POWER_DIS_AP_Data_rate_CUE_Array_BAR,'-or');
title('Data rate of CUE against distance of DUE','FontSize',12)
xlabel('Distance of DUE (m)','FontSize',12) ylabel('Data rate of CUE
(Mbps)','FontSize',12) legend([J6 J7 J8],'FPC','PCS1','D2D-PCS') hold
off;

```

figure(23)

```

% average eNB data rate

```

```

bar(POWER_DIS_Data_Rate_CUE_AVG)
    title('Average CUE data rate against distance of DUE','FontSize',12)
xlabel ('Scheme','FontSize',12) ylabel ('Data
rate(Mbps)','FontSize',12) legend ('FPC','PCS1','D2D-PCS')
figure(24)
% UE data rate
J9= plot(X_axis,POWER_DIS_Fixed_Data_rate_UE_Array_BAR,'-*g') ;
hold on;
J10= plot(X_axis,POWER_DIS_PC_Data_rate_UE_Array_BAR,'-*b') ;
J11= plot(X_axis,POWER_DIS_AP_Data_rate_UE_Array_BAR,'-or') ;
    title('Data rate of UE against distance of
DUE','FontSize',12) xlabel('Distance of DUE
(m)','FontSize',12) ylabel('Data rate of UE
(Mbps)','FontSize',12) legend([J9 J10
J11],'FPC','PCS1','D2D-PCS') hold off;

figure(25)
bar(POWER_DIS_Data_Rate_UE_AVG)
    title('Average UE data rate against distance of
DUE','FontSize',12) xlabel ('Scheme','FontSize',12) ylabel ('data
rate (Mbps)','FontSize',12)
    legend ('FPC','PCS1','D2D-PCS')

%%%%%%%%%%
%%%%%%%%%%
%%%%%%%%%%
%%%%%%%%%%D2D_POWER_PAIR%%%%%%%%%%
%%%%%%%%%%

% POWER OF CUE
CUE_Min_P = 0; % min transmit power of CUE
CUE_MAX_P= 23; % max transmit power of CUE
POWER_UE_CUE_P = CUE_MAX_P;
Fixed_CUE_P = CUE_MAX_P;

CUE_P_INI = 20;
POWER_UE_AP_CUE_P_S = CUE_P_INI;

% POWER OF D2D
D2D_MIN_P = 0;
D2D_MAX_P = 23;
POWER_UE_D2DT_P = D2D_MAX_P;
Fixed_D2DT_P = D2D_MAX_P;

D2DT_P_INI = 20;
POWER_UE_AP_D2DT_P_S= D2DT_P_INI; % initial transmit power of D2DT in our
scheme

```

```

SINR_TARGET = 0; % Susanto eta al, 2017;

% distances
d_d2d_target = 10; % TARGET DISTANCE FOR D2D MODE d_d2d_eNB
= 1000; % DISTANCE BETWEEN D2D AND eNB d_eNB_cue = 2000;
% distance between CUE and eNB POWER_UE_d_d2dt_d2dr = 10; %
DISTANCE BETWEEN D2D PAIR
POWER_UE_d_int_d2dR = 10; % DISTANCE BETWEEN D2D AG AND VT D2DR

% BANDWIDTH
BW_A = 60; % 5G BANDWIDTH IN MHZ
N = 19.28; % THERMAL NOISE in dBm/Hz, 1 Hz= -174 dBm, 100Hz and 60Hz
= -96dBm,

POWER_Pair_PC_SINR_eNB_Array = cell(1,20);
POWER_Pair_Fixed_SINR_eNB_Array = cell(1,20);
POWER_Pair_AP_SINR_eNB_Array = cell(1,20);
POWER_Pair_PC_SINR_D2DR_Array = cell(1,20);
POWER_Pair_Fixed_SINR_D2DR_Array = cell(1,20);
POWER_Pair_AP_SINR_D2DR_Array = cell(1,20);

POWER_Pair_PC_Data_rate_eNB_Array = cell(1,20);
POWER_Pair_Fixed_Data_rate_eNB_Array = cell(1,20);
POWER_Pair_AP_Data_rate_eNB_Array = cell(1,20);
POWER_Pair_PC_Data_rate_D2DR_Array = cell(1,20);
POWER_Pair_Fixed_Data_rate_D2DR_Array = cell(1,20);
POWER_Pair_AP_Data_rate_D2DR_Array = cell(1,20);

POWER_UE_AP_CUE_P_S_ARRAY = cell(1,20);
POWER_UE_AP_D2DT_P_S_ARRAY = cell(1,20);

POWER_UE_CUE_ARRAY = cell(1,20);
POWER_UE_D2DT_ARRAY = cell(1,20);
POWER_UE_Fixed_CUE_ARRAY = cell(1,20);
POWER_UE_Fixed_D2DT_ARRAY = cell(1,20);
POWER_Pair_PC_Data_rate_UE_Array = cell(1,20);
POWER_Pair_AP_Data_rate_UE_Array = cell(1,20);
POWER_Pair_Fixed_Data_rate_UE_Array = cell(1,20);
% PATHLOSS MODEL BETWEEN D2D PAIR using OUR SCHEME
% PATHLOSS BETWEEN eNB AND CUE USING PCS1

% PATHLOSS BETWEEN D2DT1 AND D2DR1 USING PCS1
POWER_UE_PLoss_D2DT_D2DR = 10*log10(148 +
40*log10(POWER_UE_d_d2dt_d2dr));
% PATHLOSS BETWEEN D2DT1 AND D2DR1 USING OUR SCHEME 28 +
40LOG10(d(KM))

```

```

POWER_UE_AP_PLoss_AD2D_D2DT_D2DR = 10*log10(28 +
40*log10(POWER_UE_d_d2dt_d2dr));

% PATHLOSS BETWEEN AG D2DT AND VT D2DR USING PCS1
POWER_UE_PLoss_INT_D2D = abs(10*log10(148 +
40*log10(POWER_UE_d_int_d2dR)));
% PATHLOSS BETWEEN AG D2DT AND VT D2DR USING OUR SCHEME 28 +
40LOG10(d(KM))
POWER_UE_AP_PLoss_INT_AD2D = abs(10*log10(28 +
40*log10(POWER_UE_d_int_d2dR)));

% PATHLOSS BETWEEN CUE AND BS USING PCS1
POWER_UE_PLoss_CUE_BS = 10*log10(128+37.6*(log10(d_eNB_cue/1000)));

Delta_Value = 0.5;
POWER_UE_num_d2d_pair = 1;
POWER_UE_num_cue_pair = 19;

POWER_PAIR_Number_of_PL = 20;
for x=1:POWER_PAIR_Number_of_PL

% SINR OF eNB AND D2DR
sh =0;
% CUE SINR of eNB USING PCS1
POWER_UE_G_CUE_P = 10^((-POWER_UE_PLoss_CUE_BS -sh)/10)*(10^2);

POWER_UE_SINR_CUE =
(CUE_MAX_P*POWER_UE_G_CUE_P)/(((POWER_UE_num_cue_pair-
1)*POWER_UE_CUE_P*POWER_UE_G_CUE_P)+ N);

% CUE SINR of eNB USING Power Control
POWER_UE_Fixed_G_CUE_P = 10^((-POWER_UE_PLoss_CUE_BS -
sh)/10)*(10^2);
POWER_UE_Fixed_SINR_CUE =
(Fixed_CUE_P*POWER_UE_Fixed_G_CUE_P)/(((POWER_UE_num_cue_pa
ir-1)*Fixed_CUE_P*POWER_UE_Fixed_G_CUE_P)+ N);

% CUE SINR of eNB USING OUR SCHEME
POWER_UE_AP_G_CUE_P_S = 10^((-POWER_UE_PLoss_CUE_BS-
sh)/10)*(10^2);
POWER_UE_AP_A_SINR_CUE =
(CUE_P_INI*POWER_UE_AP_G_CUE_P_Ssh)/(((POWER_UE_num_cue_pa
ir-
1)*POWER_UE_AP_CUE_P_S*POWER_UE_AP_G_CUE_P_S)+ N);

```

```

% D2D SINR of D2DR USING PCS1

POWER_UE_G_D2DT_P      = 10^((-POWER_UE_PLoss_D2DT_D2DR -
sh)/10)*(10^2);
POWER_UE_G_D2DT_P_INT  = 10^((-POWER_UE_PLoss_INT_D2D -
sh)/10)*(10^2);
if POWER_UE_num_d2d_pair>0
POWER_UE_SINR_D2DR      =
(D2D_MAX_P*POWER_UE_G_D2DT_P)/(((POWER_UE_num_d2d_pair-
1)*POWER_UE_D2DT_P*POWER_UE_G_D2DT_P_INT)+ N);
else
POWER_UE_SINR_D2DR = 0;
end
% D2D SINR of D2DR USING Fixed power

POWER_UE_Fixed_G_D2DT_P = 10^((-POWER_UE_PLoss_D2DT_D2DR -
sh)/10)*(10^2);
POWER_UE_Fixed_G_D2DT_P_INT = 10^((-POWER_UE_PLoss_INT_D2D -
sh)/10)*(10^2);

POWER_UE_Fixed_SINR_D2DR      =
(Fixed_D2DT_P*POWER_UE_Fixed_G_D2DT_P)/(((POWER_UE_num_d2d
_pair-1)*Fixed_D2DT_P*POWER_UE_Fixed_G_D2DT_P_INT)+ N);

% D2D SINR of D2DR USING OUR SCHEME
POWER_UE_AP_G_D2DT_P_S      = 10^((-
POWER_UE_AP_PLoss_AD2D_D2DT_D2DR-sh)/10)*(10^2);
POWER_UE_AP_G_D2DT_INT_P_S  = 10^((-
POWER_UE_AP_PLoss_INT_AD2D-sh)/10)*(10^2);

POWER_UE_AP_SINR_D2DR      =
(D2DT_P_INI*POWER_UE_AP_G_D2DT_P_S)/(((POWER_UE_num_d2d_p
air-1)*POWER_UE_AP_D2DT_P_S*POWER_UE_AP_G_D2DT_INT_P_S)+
N);

% POWER ADJUSTMENT OF OUR SCHEME
% Power control of D2D based on SINR

if POWER_UE_AP_SINR_D2DR      > SINR_TARGET
POWER_UE_S_D2DT =-1;
elseif POWER_UE_AP_SINR_D2DR < SINR_TARGET
POWER_UE_S_D2DT =+1;
else
POWER_UE_S_D2DT = 0;
end
end

```

```

    if POWER_UE_AP_A_SINR_CUE > SINR_TARGET
POWER_UE_CUE =-1;  elseif
POWER_UE_AP_A_SINR_CUE < SINR_TARGET
    POWER_UE_CUE =+1;
    else
        POWER_UE_CUE = 0;
    end

CUE_P_S1=POWER_UE_AP_CUE_P_S +(POWER_UE_CUE*Delta_Value);
POWER_UE_AP_CUE_P_S = max((min(CUE_P_S1,CUE_MAX_P)),CUE_Min_P);

D2DT_PS1=POWER_UE_AP_D2DT_P_S +(POWER_UE_S_D2DT*Delta_Value);
POWER_UE_AP_D2DT_P_S =
    max((min(D2DT_PS1,D2D_MAX_P)),D2D_MIN_P);

% POWER ADJUSTMENT OF PCS1
% Power control of D2D based on SINR

    if    POWER_UE_SINR_D2DR    >    SINR_TARGET
POWER_UE_D2DT =-1;
    elseif POWER_UE_SINR_D2DR < SINR_TARGET
        POWER_UE_D2DT =+1;
    else
        POWER_UE_D2DT = 0;
    end

    if    POWER_UE_SINR_CUE    >    SINR_TARGET
POWER_UE_CUE =-1;
    elseif POWER_UE_SINR_CUE < SINR_TARGET
        POWER_UE_CUE =+1;
    else
        POWER_UE_CUE = 0;
    end

POWER_UE_CUE_P =
    max((min((POWER_UE_CUE_P
+POWER_UE_CUE*1),CUE_MAX_P)),CUE_Min_P);
POWER_UE_D2DT_P =
    max((min((POWER_UE_D2DT_P
+POWER_UE_D2DT*1),D2D_MAX_P)),D2D_MIN_P);

% DATA RATE OF eNB = BW_CUE*log2(1 + SINR_eNB)
% Data rate of eNB USING PCS1
    POWER_UE_Data_rate_CUE = BW_A*log2(1+POWER_UE_SINR_CUE);
% Data rate of eNB USING Fixed control

```

```

POWER_UE_Fixed_Data_rate_CUE =
    BW_A*log2(1+POWER_UE_Fixed_SINR_CUE);
% Data rate of eNB USING OUR SCHEME
POWER_UE_AP_Data_rate_CUE =
    BW_A*log2(1+POWER_UE_AP_A_SINR_CUE);

% DATA RATE OF D2D
% Data rate of D2DR1 USING PCS1 = BW_D2D*log2(1 + SINR_D2DR1)
POWER_UE_Data_rate_D2DR = BW_A*log2(1+POWER_UE_SINR_D2DR);
% Data rate of D2DR1 USING Fixed Control = BW_D2D*log2(1 + SINR_D2DR1)
POWER_UE_Fixed_Data_rate_D2DR =
    BW_A*log2(1+POWER_UE_Fixed_SINR_D2DR);
% Data rate of D2DR1 USING OUR SCHEME = BW_D2D*log2(1 + SINR_D2DR1)
POWER_UE_AP_Data_rate_D2DR =
    BW_A*log2(1+POWER_UE_AP_SINR_D2DR);

% ARRAY OF SINR
% array of eNB SINRs
POWER_Pair_PC_SINR_eNB_Array{x}=      abs(POWER_UE_SINR_CUE);
POWER_Pair_Fixed_SINR_eNB_Array{x}=
abs(POWER_UE_Fixed_SINR_CUE);
POWER_Pair_AP_SINR_eNB_Array{x}= abs(POWER_UE_AP_A_SINR_CUE);

% array of D2DR SINR
POWER_Pair_PC_SINR_D2DR_Array{x}= abs(POWER_UE_SINR_D2DR);
POWER_Pair_Fixed_SINR_D2DR_Array{x}=
    abs(POWER_UE_Fixed_SINR_D2DR);
POWER_Pair_AP_SINR_D2DR_Array{x}= abs(POWER_UE_AP_SINR_D2DR);

% ARRAY OF DATA RATE
% array of eNB Data rate
POWER_Pair_PC_Data_rate_eNB_Array{x}= (POWER_UE_Data_rate_CUE);
POWER_Pair_Fixed_Data_rate_eNB_Array{x}=
    (POWER_UE_Fixed_Data_rate_CUE);
POWER_Pair_AP_Data_rate_eNB_Array{x}= (POWER_UE_AP_Data_rate_CUE);

% array of D2D data rate
POWER_Pair_PC_Data_rate_D2DR_Array{x}=
    abs(POWER_UE_Data_rate_D2DR);
POWER_Pair_Fixed_Data_rate_D2DR_Array{x}=
    abs(POWER_UE_Fixed_Data_rate_D2DR);
POWER_Pair_AP_Data_rate_D2DR_Array{x}=
    abs(POWER_UE_AP_Data_rate_D2DR);
% array of UE data rate
POWER_Pair_PC_Data_rate_UE_Array{x}=
    abs(POWER_UE_Data_rate_D2DR)+abs(POWER_UE_Data_rate_CUE);

```

```

POWER_Pair_Fixed_Data_rate_UE_Array{x}=
    abs(POWER_UE_Fixed_Data_rate_D2DR)+abs(POWER_UE_Fixed_Data_rate_CUE);
POWER_Pair_AP_Data_rate_UE_Array{x}=
    abs(POWER_UE_AP_Data_rate_D2DR)+abs(POWER_UE_AP_Data_rate_CUE);

% POWER ARRAY BASED ON SCHEME
POWER_UE_AP_CUE_P_S_ARRAY{x}= abs(POWER_UE_AP_CUE_P_S);
POWER_UE_AP_D2DT_P_S_ARRAY{x} =abs(POWER_UE_AP_D2DT_P_S);

% POWER ARRAY BASED ON PCS1
POWER_UE_CUE_ARRAY{x}= abs(POWER_UE_CUE_P);
POWER_UE_D2DT_ARRAY{x} =abs(POWER_UE_D2DT_P);
% POWER ARRAY BASED ON Fixed power
POWER_UE_Fixed_CUE_ARRAY{x}= Fixed_CUE_P;
POWER_UE_Fixed_D2DT_ARRAY{x} =Fixed_D2DT_P;

% changes THE NUMBER of D2D Pair
POWER_UE_num_d2d_pair = POWER_UE_num_d2d_pair+1;
POWER_UE_num_cue_pair = POWER_UE_num_cue_pair-1;

end

% POWER COLLECTION OF CUE

POWER_Pair_CUE_ARRAY_BAR
    =[POWER_UE_CUE_ARRAY{1},POWER_UE_CUE_ARRAY{2},POWER_UE_CUE_ARRAY{3},POWER_UE_CUE_ARRAY{4},POWER_UE_CUE_ARRAY{5},POWER_UE_CUE_ARRAY{6},POWER_UE_CUE_ARRAY{7},POWER_UE_CUE_ARRAY{8},POWER_UE_CUE_ARRAY{9},POWER_UE_CUE_ARRAY{10},POWER_UE_CUE_ARRAY{11},POWER_UE_CUE_ARRAY{12},POWER_UE_CUE_ARRAY{13},POWER_UE_CUE_ARRAY{14},POWER_UE_CUE_ARRAY{15},POWER_UE_CUE_ARRAY{16},POWER_UE_CUE_ARRAY{17},POWER_UE_CUE_ARRAY{18},POWER_UE_CUE_ARRAY{19},POWER_UE_CUE_ARRAY{20}]
POWER_Pair_Fixed_CUE_ARRAY_BAR
    =[POWER_UE_Fixed_CUE_ARRAY{1},POWER_UE_Fixed_CUE_ARRAY{2},POWER_UE_Fixed_CUE_ARRAY{3},POWER_UE_Fixed_CUE_ARRAY{4},POWER_UE_Fixed_CUE_ARRAY{5},POWER_UE_Fixed_CUE_ARRAY{6},POWER_UE_Fixed_CUE_ARRAY{7},POWER_UE_Fixed_CUE_ARRAY{8},POWER_UE_Fixed_CUE_ARRAY{9},POWER_UE_Fixed_CUE_ARRAY{10},POWER_UE_Fixed_CUE_ARRAY{11},POWER_UE_Fixed_CUE_ARRAY{12},POWER_UE_Fixed_CUE_ARRAY{13},POWER_UE_Fixed_CUE_ARRAY{14},POWER_UE_Fixed_CUE_ARRAY{15},POWER_UE_Fixed_CUE_ARRAY{16},POWER_UE_Fixed_CUE_ARRAY{17},POWER_UE_Fixed_CUE_ARRAY{18},POWER_UE_Fixed_CUE_ARRAY{19},POWER_UE_Fixed_CUE_ARRAY{20}]

```

E_Fixed_CUE_ARRAY{18},POWER_UE_Fixed_CUE_ARRAY{19},POWER_UE_Fixed_CUE_ARRAY{20}]
 POWER_Pair_AP_CUE_P_S_ARRAY_BAR
 =[POWER_UE_AP_CUE_P_S_ARRAY{1},POWER_UE_AP_CUE_P_S_ARRAY{2},POWER_UE_AP_CUE_P_S_ARRAY{3},POWER_UE_AP_CUE_P_S_ARRAY{4},POWER_UE_AP_CUE_P_S_ARRAY{5},POWER_UE_AP_CUE_P_S_ARRAY{6},POWER_UE_AP_CUE_P_S_ARRAY{7},POWER_UE_AP_CUE_P_S_ARRAY{8},POWER_UE_AP_CUE_P_S_ARRAY{9},POWER_UE_AP_CUE_P_S_ARRAY{10},POWER_UE_AP_CUE_P_S_ARRAY{11},POWER_UE_AP_CUE_P_S_ARRAY{12},POWER_UE_AP_CUE_P_S_ARRAY{13},POWER_UE_AP_CUE_P_S_ARRAY{14},POWER_UE_AP_CUE_P_S_ARRAY{15},POWER_UE_AP_CUE_P_S_ARRAY{16},POWER_UE_AP_CUE_P_S_ARRAY{17},POWER_UE_AP_CUE_P_S_ARRAY{18},POWER_UE_AP_CUE_P_S_ARRAY{19},POWER_UE_AP_CUE_P_S_ARRAY{20}]

POWER_Pair_CUE_ARRAY_BAR2
 =[sum(POWER_Pair_CUE_ARRAY_BAR)/POWER_PAIR_Number_of_PL];

POWER_Pair_Fixed_CUE_ARRAY_BAR2
 =[sum(POWER_Pair_Fixed_CUE_ARRAY_BAR)/POWER_PAIR_Number_of_PL];

POWER_Pair_AP_CUE_P_S_ARRAY_BAR2
 =[sum(POWER_Pair_AP_CUE_P_S_ARRAY_BAR)/POWER_PAIR_Number_of_PL];

POWER_Pair_CUE_P_S_BAR =
 [POWER_Pair_Fixed_CUE_ARRAY_BAR2,POWER_Pair_CUE_ARRAY_BAR2,POWER_Pair_AP_CUE_P_S_ARRAY_BAR2]

% POWER COLLECTION OF D2D

POWER_Pair_D2DT_ARRAY_BAR =
 [POWER_UE_D2DT_ARRAY{1},POWER_UE_D2DT_ARRAY{2},POWER_UE_D2DT_ARRAY{3},POWER_UE_D2DT_ARRAY{4},POWER_UE_D2DT_ARRAY{5},POWER_UE_D2DT_ARRAY{6},POWER_UE_D2DT_ARRAY{7},POWER_UE_D2DT_ARRAY{8},POWER_UE_D2DT_ARRAY{9},POWER_UE_D2DT_ARRAY{10},POWER_UE_D2DT_ARRAY{11},POWER_UE_D2DT_ARRAY{12},POWER_UE_D2DT_ARRAY{13},POWER_UE_D2DT_ARRAY{14},POWER_UE_D2DT_ARRAY{15},POWER_UE_D2DT_ARRAY{16},POWER_UE_D2DT_ARRAY{17},POWER_UE_D2DT_ARRAY{18},POWER_UE_D2DT_ARRAY{19},POWER_UE_D2DT_ARRAY{20}]

POWER_Pair_Fixed_D2DT_ARRAY_BAR =
 [POWER_UE_Fixed_D2DT_ARRAY{1},POWER_UE_Fixed_D2DT_ARRAY{2},POWER_UE_Fixed_D2DT_ARRAY{3},POWER_UE_Fixed_D2DT_ARRAY{4},POWER_UE_Fixed_D2DT_ARRAY{5},POWER_UE_Fixed_D2DT_ARRAY{6},POWER_UE_Fixed_D2DT_ARRAY{7},POWER_UE_Fixed_D2DT_ARRAY{8},POWER_UE_Fixed_D2DT_ARRAY{9},POWER_UE_Fixed_D2DT_ARRAY{10},POWER_UE_Fixed_D2DT_ARRAY{11},POWER_UE_Fixed_D2DT_ARRAY{12},POWER_UE_Fixed_D2DT_ARRAY{13},POWER_UE_Fixed_D2DT_ARRAY{14},POWER_UE_Fixed_D2DT_ARRAY{15},POWER_UE_Fixed_D2DT_ARRAY{16},POWER_UE_Fixed_D2DT_ARRAY{17},POWER_UE_Fixed_D2DT_ARRAY{18},POWER_UE_Fixed_D2DT_ARRAY{19},POWER_UE_Fixed_D2DT_ARRAY{20}]

```

T_ARRAY{6},POWER_UE_Fixed_D2DT_ARRAY{7},POWER_UE_Fixed_
D2DT_ARRAY{8},POWER_UE_Fixed_D2DT_ARRAY{9},POWER_UE_Fi
xed_D2DT_ARRAY{10},POWER_UE_Fixed_D2DT_ARRAY{11},POWER_
UE_Fixed_D2DT_ARRAY{12},POWER_UE_Fixed_D2DT_ARRAY{13},PO
WER_UE_Fixed_D2DT_ARRAY{14},POWER_UE_Fixed_D2DT_ARRAY{
15},POWER_UE_Fixed_D2DT_ARRAY{16},POWER_UE_Fixed_D2DT_AR
RAY{17},POWER_UE_Fixed_D2DT_ARRAY{18},POWER_UE_Fixed_D2
DT_ARRAY{19},POWER_UE_Fixed_D2DT_ARRAY{20}]
POWER_Pair_AP_D2DT_P_S_ARRAY_BAR =
[POWER_UE_AP_D2DT_P_S_ARRAY{1},POWER_UE_AP_D2DT_P_S_A
RRAY{2},POWER_UE_AP_D2DT_P_S_ARRAY{3},POWER_UE_AP_D2D
T_P_S_ARRAY{4},POWER_UE_AP_D2DT_P_S_ARRAY{5},POWER_UE
_AP_D2DT_P_S_ARRAY{6},POWER_UE_AP_D2DT_P_S_ARRAY{7},PO
WER_UE_AP_D2DT_P_S_ARRAY{8},POWER_UE_AP_D2DT_P_S_ARR
AY{9},POWER_UE_AP_D2DT_P_S_ARRAY{10},POWER_UE_AP_D2DT
_P_S_ARRAY{11},POWER_UE_AP_D2DT_P_S_ARRAY{12},POWER_UE
_AP_D2DT_P_S_ARRAY{13},POWER_UE_AP_D2DT_P_S_ARRAY{14},P
OWER_UE_AP_D2DT_P_S_ARRAY{15},POWER_UE_AP_D2DT_P_S_AR
RAY{16},POWER_UE_AP_D2DT_P_S_ARRAY{17},POWER_UE_AP_D2
DT_P_S_ARRAY{18},POWER_UE_AP_D2DT_P_S_ARRAY{19},POWER_
UE_AP_D2DT_P_S_ARRAY{20}]

POWER_Pair_AVG_D2D_P_S_ARRAY =
[(sum(POWER_Pair_D2DT_ARRAY_BAR)/(POWER_PAIR_Number_of_PL
));0];
POWER_Pair_Fixed_AVG_D2D_P_S_ARRAY =
[(sum(POWER_Pair_Fixed_D2DT_ARRAY_BAR)/(POWER_PAIR_Number_
of_PL));0];
POWER_Pair_AP_AVG_D2D_P_S_ARRAY =
[(sum(POWER_Pair_AP_D2DT_P_S_ARRAY_BAR)/(POWER_PAIR_Numb
er_of_PL));0];

POWER_Pair_D2D_P_S_BAR =
[POWER_Pair_Fixed_AVG_D2D_P_S_ARRAY,POWER_Pair_AVG_D2D_P
_S_ARRAY,POWER_Pair_AP_AVG_D2D_P_S_ARRAY]
% ARRAY OF SINR BAR
% array of eNB SINR
POWER_Pair_PC_SINR_eNB_Array_BAR =
[POWER_Pair_PC_SINR_eNB_Array{1},POWER_Pair_PC_SINR_eNB_Arra
y{2},POWER_Pair_PC_SINR_eNB_Array{3},POWER_Pair_PC_SINR_eNB_
Array{4},POWER_Pair_PC_SINR_eNB_Array{5},POWER_Pair_PC_SINR_e
NB_Array{6},POWER_Pair_PC_SINR_eNB_Array{7},POWER_Pair_PC_SI
NR_eNB_Array{8},POWER_Pair_PC_SINR_eNB_Array{9},POWER_Pair_P
C_SINR_eNB_Array{10},POWER_Pair_PC_SINR_eNB_Array{11},POWER
_Pair_PC_SINR_eNB_Array{12},POWER_Pair_PC_SINR_eNB_Array{13},P
OWER_Pair_PC_SINR_eNB_Array{14},POWER_Pair_PC_SINR_eNB_Array
{15},POWER_Pair_PC_SINR_eNB_Array{16},POWER_Pair_PC_SINR_eNB

```

```

_Array{17},POWER_Pair_PC_SINR_eNB_Array{18},POWER_Pair_PC_SIN
R_eNB_Array{19},POWER_Pair_PC_SINR_eNB_Array{20}]
POWER_Pair_Fixed_SINR_eNB_Array_BAR =
[POWER_Pair_Fixed_SINR_eNB_Array{1},POWER_Pair_Fixed_SINR_eNB
_Array{2},POWER_Pair_Fixed_SINR_eNB_Array{3},POWER_Pair_Fixed_S
INR_eNB_Array{4},POWER_Pair_Fixed_SINR_eNB_Array{5},POWER_Pai
r_Fixed_SINR_eNB_Array{6},POWER_Pair_Fixed_SINR_eNB_Array{7},PO
WER_Pair_Fixed_SINR_eNB_Array{8},POWER_Pair_Fixed_SINR_eNB_Arr
ay{9},POWER_Pair_Fixed_SINR_eNB_Array{10},POWER_Pair_Fixed_SIN
R_eNB_Array{11},POWER_Pair_Fixed_SINR_eNB_Array{12},POWER_Pair
_Fixed_SINR_eNB_Array{13},POWER_Pair_Fixed_SINR_eNB_Array{14},P
OWER_Pair_Fixed_SINR_eNB_Array{15},POWER_Pair_Fixed_SINR_eNB_
Array{16},POWER_Pair_Fixed_SINR_eNB_Array{17},POWER_Pair_Fixed_
SINR_eNB_Array{18},POWER_Pair_Fixed_SINR_eNB_Array{19},POWER_
Pair_Fixed_SINR_eNB_Array{20}]
POWER_Pair_AP_SINR_eNB_Array_BAR =
[POWER_Pair_AP_SINR_eNB_Array{1},POWER_Pair_AP_SINR_eNB_Arra
y{2},POWER_Pair_AP_SINR_eNB_Array{3},POWER_Pair_AP_SINR_eNB
_Array{4},POWER_Pair_AP_SINR_eNB_Array{5},POWER_Pair_AP_SINR
_eNB_Array{6},POWER_Pair_AP_SINR_eNB_Array{7},POWER_Pair_AP_
SINR_eNB_Array{8},POWER_Pair_AP_SINR_eNB_Array{9},POWER_Pair
_AP_SINR_eNB_Array{10},POWER_Pair_AP_SINR_eNB_Array{11},POW
ER_Pair_AP_SINR_eNB_Array{12},POWER_Pair_AP_SINR_eNB_Array{13
},POWER_Pair_AP_SINR_eNB_Array{14},POWER_Pair_AP_SINR_eNB_A
rray{15},POWER_Pair_AP_SINR_eNB_Array{16},POWER_Pair_AP_SINR_
eNB_Array{17},POWER_Pair_AP_SINR_eNB_Array{18},POWER_Pair_AP
_SINR_eNB_Array{19},POWER_Pair_AP_SINR_eNB_Array{20}]

% array of D2D SINR
POWER_Pair_PC_SINR_D2DR_Array_BAR =
[POWER_Pair_PC_SINR_D2DR_Array{1},POWER_Pair_PC_SINR_D2DR_
Array{2},POWER_Pair_PC_SINR_D2DR_Array{3},POWER_Pair_PC_SINR
_D2DR_Array{4},POWER_Pair_PC_SINR_D2DR_Array{5},POWER_Pair_P
C_SINR_D2DR_Array{6},POWER_Pair_PC_SINR_D2DR_Array{7},POWE
R_Pair_PC_SINR_D2DR_Array{8},POWER_Pair_PC_SINR_D2DR_Array{9
},POWER_Pair_PC_SINR_D2DR_Array{10},POWER_Pair_PC_SINR_D2D
R_Array{11},POWER_Pair_PC_SINR_D2DR_Array{12},POWER_Pair_PC_
SINR_D2DR_Array{13},POWER_Pair_PC_SINR_D2DR_Array{14},POWER
_Pair_PC_SINR_D2DR_Array{15},POWER_Pair_PC_SINR_D2DR_Array{1
6},POWER_Pair_PC_SINR_D2DR_Array{17},POWER_Pair_PC_SINR_D2D
R_Array{18},POWER_Pair_PC_SINR_D2DR_Array{19},POWER_Pair_PC_
SINR_D2DR_Array{20}]
POWER_Pair_Fixed_SINR_D2DR_Array_BAR =
[POWER_Pair_Fixed_SINR_D2DR_Array{1},POWER_Pair_Fixed_SINR_D2
DR_Array{2},POWER_Pair_Fixed_SINR_D2DR_Array{3},POWER_Pair_Fi
xed_SINR_D2DR_Array{4},POWER_Pair_Fixed_SINR_D2DR_Array{5},PO
WER_Pair_Fixed_SINR_D2DR_Array{6},POWER_Pair_Fixed_SINR_D2DR
_Array{7},POWER_Pair_Fixed_SINR_D2DR_Array{8},POWER_Pair_Fixed

```

```

_SINR_D2DR_Array{9},POWER_Pair_Fixed_SINR_D2DR_Array{10},POW
ER_Pair_Fixed_SINR_D2DR_Array{11},POWER_Pair_Fixed_SINR_D2DR_
Array{12},POWER_Pair_Fixed_SINR_D2DR_Array{13},POWER_Pair_Fixe
d_SINR_D2DR_Array{14},POWER_Pair_Fixed_SINR_D2DR_Array{15},PO
WER_Pair_Fixed_SINR_D2DR_Array{16},POWER_Pair_Fixed_SINR_D2D
R_Array{17},POWER_Pair_Fixed_SINR_D2DR_Array{18},POWER_Pair_Fi
xed_SINR_D2DR_Array{19},POWER_Pair_Fixed_SINR_D2DR_Array{20}]
POWER_Pair_AP_SINR_D2DR_Array_BAR =
[POWER_Pair_AP_SINR_D2DR_Array{1},POWER_Pair_AP_SINR_D2DR_
Array{2},POWER_Pair_AP_SINR_D2DR_Array{3},POWER_Pair_AP_SINR
_D2DR_Array{4},POWER_Pair_AP_SINR_D2DR_Array{5},POWER_Pair_
AP_SINR_D2DR_Array{6},POWER_Pair_AP_SINR_D2DR_Array{7},POW
ER_Pair_AP_SINR_D2DR_Array{8},POWER_Pair_AP_SINR_D2DR_Array{
9},POWER_Pair_AP_SINR_D2DR_Array{10},POWER_Pair_AP_SINR_D2D
R_Array{11},POWER_Pair_AP_SINR_D2DR_Array{12},POWER_Pair_AP_
SINR_D2DR_Array{13},POWER_Pair_AP_SINR_D2DR_Array{14},POWE
R_Pair_AP_SINR_D2DR_Array{15},POWER_Pair_AP_SINR_D2DR_Array{
16},POWER_Pair_AP_SINR_D2DR_Array{17},POWER_Pair_AP_SINR_D2
DR_Array{18},POWER_Pair_AP_SINR_D2DR_Array{19},POWER_Pair_AP
_SINR_D2DR_Array{20}]

% AVERAGE SINR
% Average eNB SINR
POWER_Pair_PC_SINR_CUE_AVG =
[(sum(POWER_Pair_PC_SINR_eNB_Array_BAR)/(POWER_PAIR_Number_
of_PL));0];
POWER_Pair_Fixed_SINR_CUE_AVG =
[(sum(POWER_Pair_Fixed_SINR_eNB_Array_BAR)/(POWER_PAIR_Numb
er_of_PL));0];
POWER_Pair_AP_SINR_CUE_AVG =
[(sum(POWER_Pair_AP_SINR_eNB_Array_BAR)/(POWER_PAIR_Number_
of_PL));0];
% Average D2DR SINR
POWER_Pair_PC_SINR_D2DR_AVG =
[(sum(POWER_Pair_PC_SINR_D2DR_Array_BAR)/POWER_PAIR_Number_
of_PL);0];
POWER_Pair_Fixed_SINR_D2DR_AVG =
[(sum(POWER_Pair_Fixed_SINR_D2DR_Array_BAR)/POWER_PAIR_Num
ber_of_PL);0];
POWER_Pair_AP_SINR_D2DR_AVG =
[(sum(POWER_Pair_AP_SINR_D2DR_Array_BAR)/POWER_PAIR_Number_
of_PL);0];
% average D2DR SINR analysis
POWER_Pair_PC_SINR_D2DR_bar=
[POWER_Pair_Fixed_SINR_D2DR_AVG,POWER_Pair_PC_SINR_D2DR_A
VG,POWER_Pair_AP_SINR_D2DR_AVG]
% AVERAGE eNB SINR BAR

```

```

POWER_Pair_Average_CUE_SINR =
    [POWER_Pair_Fixed_SINR_CUE_AVG,POWER_Pair_PC_SINR_CUE_AVG
    ,POWER_Pair_AP_SINR_CUE_AVG];

```

```

% ARRAY OF DATA RATE BAR

```

```

% data rate of eNB

```

```

POWER_Pair_PC_Data_rate_CUE_Array_BAR =
    [POWER_Pair_PC_Data_rate_eNB_Array{1},POWER_Pair_PC_Data_rate_e
    NB_Array{2},POWER_Pair_PC_Data_rate_eNB_Array{3},POWER_Pair_PC
    _Data_rate_eNB_Array{4},POWER_Pair_PC_Data_rate_eNB_Array{5},POW
    ER_Pair_PC_Data_rate_eNB_Array{6},POWER_Pair_PC_Data_rate_eNB_Ar
    ray{7},POWER_Pair_PC_Data_rate_eNB_Array{8},POWER_Pair_PC_Data_r
    ate_eNB_Array{9},POWER_Pair_PC_Data_rate_eNB_Array{10},POWER_Pa
    ir_PC_Data_rate_eNB_Array{11},POWER_Pair_PC_Data_rate_eNB_Array{1
    2},POWER_Pair_PC_Data_rate_eNB_Array{13},POWER_Pair_PC_Data_rate
    _eNB_Array{14},POWER_Pair_PC_Data_rate_eNB_Array{15},POWER_Pair
    _PC_Data_rate_eNB_Array{16},POWER_Pair_PC_Data_rate_eNB_Array{17
    },POWER_Pair_PC_Data_rate_eNB_Array{18},POWER_Pair_PC_Data_rate_
    eNB_Array{19},POWER_Pair_PC_Data_rate_eNB_Array{20}]

```

```

POWER_Pair_Fixed_Data_rate_CUE_Array_BAR =
    [POWER_Pair_Fixed_Data_rate_eNB_Array{1},POWER_Pair_Fixed_Data_ra
    te_eNB_Array{2},POWER_Pair_Fixed_Data_rate_eNB_Array{3},POWER_P
    air_Fixed_Data_rate_eNB_Array{4},POWER_Pair_Fixed_Data_rate_eNB_Ar
    ray{5},POWER_Pair_Fixed_Data_rate_eNB_Array{6},POWER_Pair_Fixed_D
    ata_rate_eNB_Array{7},POWER_Pair_Fixed_Data_rate_eNB_Array{8},POW
    ER_Pair_Fixed_Data_rate_eNB_Array{9},POWER_Pair_Fixed_Data_rate_eN
    B_Array{10},POWER_Pair_Fixed_Data_rate_eNB_Array{11},POWER_Pair_
    Fixed_Data_rate_eNB_Array{12},POWER_Pair_Fixed_Data_rate_eNB_Array
    {13},POWER_Pair_Fixed_Data_rate_eNB_Array{14},POWER_Pair_Fixed_D
    ata_rate_eNB_Array{15},POWER_Pair_Fixed_Data_rate_eNB_Array{16},PO
    WER_Pair_Fixed_Data_rate_eNB_Array{17},POWER_Pair_Fixed_Data_rate_
    eNB_Array{18},POWER_Pair_Fixed_Data_rate_eNB_Array{19},POWER_Pa
    ir_Fixed_Data_rate_eNB_Array{20}]

```

```

POWER_Pair_AP_Data_rate_CUE_Array_BAR =
    [POWER_Pair_AP_Data_rate_eNB_Array{1},POWER_Pair_AP_Data_rate_e
    NB_Array{2},POWER_Pair_AP_Data_rate_eNB_Array{3},POWER_Pair_AP
    _Data_rate_eNB_Array{4},POWER_Pair_AP_Data_rate_eNB_Array{5},POW
    ER_Pair_AP_Data_rate_eNB_Array{6},POWER_Pair_AP_Data_rate_eNB_Ar
    ray{7},POWER_Pair_AP_Data_rate_eNB_Array{8},POWER_Pair_AP_Data_
    rate_eNB_Array{9},POWER_Pair_AP_Data_rate_eNB_Array{10},POWER_P
    air_AP_Data_rate_eNB_Array{11},POWER_Pair_AP_Data_rate_eNB_Array{
    12},POWER_Pair_AP_Data_rate_eNB_Array{13},POWER_Pair_AP_Data_rat
    e_eNB_Array{14},POWER_Pair_AP_Data_rate_eNB_Array{15},POWER_Pa
    ir_AP_Data_rate_eNB_Array{16},POWER_Pair_AP_Data_rate_eNB_Array{1
    7},POWER_Pair_AP_Data_rate_eNB_Array{18},POWER_Pair_AP_Data_rate
    _eNB_Array{19},POWER_Pair_AP_Data_rate_eNB_Array{20}]

```

```

POWER_Pair_PC_Data_rate_CUE_AVG_Array_BAR =

```



```

air_AP_Data_rate_D2DR_Array{9},POWER_Pair_AP_Data_rate_D2DR_Array{10},POWER_Pair_AP_Data_rate_D2DR_Array{11},POWER_Pair_AP_Data_rate_D2DR_Array{12},POWER_Pair_AP_Data_rate_D2DR_Array{13},POWER_Pair_AP_Data_rate_D2DR_Array{14},POWER_Pair_AP_Data_rate_D2DR_Array{15},POWER_Pair_AP_Data_rate_D2DR_Array{16},POWER_Pair_AP_Data_rate_D2DR_Array{17},POWER_Pair_AP_Data_rate_D2DR_Array{18},POWER_Pair_AP_Data_rate_D2DR_Array{19},POWER_Pair_AP_Data_rate_D2DR_Array{20}]

```

```

POWER_Pair_PC_Data_rate_D2DR_Array_AVG_BAR = [(sum(POWER_Pair_PC_Data_rate_D2DR_Array_BAR)/(POWER_PAIR_Number_of_PL));0];

```

```

POWER_Pair_Fixed_Data_rate_D2DR_Array_AVG_BAR = [(sum(POWER_Pair_Fixed_Data_rate_D2DR_Array_BAR)/(POWER_PAIR_Number_of_PL));0];

```

```

POWER_Pair_AP_Data_rate_D2DR_Array_AVG_BAR = [(sum(POWER_Pair_AP_Data_rate_D2DR_Array_BAR)/(POWER_PAIR_Number_of_PL));0];

```

```

POWER_Pair_Data_Rate_D2D_AVG = [POWER_Pair_Fixed_Data_rate_D2DR_Array_AVG_BAR,POWER_Pair_PC_Data_rate_D2DR_Array_AVG_BAR,POWER_Pair_AP_Data_rate_D2DR_Array_AVG_BAR]

```

% UE data rate array

```

POWER_Pair_PC_data_rate_UE_Array_BAR = [POWER_Pair_PC_Data_rate_UE_Array{1},POWER_Pair_PC_Data_rate_UE_Array{2},POWER_Pair_PC_Data_rate_UE_Array{3},POWER_Pair_PC_Data_rate_UE_Array{4},POWER_Pair_PC_Data_rate_UE_Array{5},POWER_Pair_PC_Data_rate_UE_Array{6},POWER_Pair_PC_Data_rate_UE_Array{7},POWER_Pair_PC_Data_rate_UE_Array{8},POWER_Pair_PC_Data_rate_UE_Array{9},POWER_Pair_PC_Data_rate_UE_Array{10},POWER_Pair_PC_Data_rate_UE_Array{11},POWER_Pair_PC_Data_rate_UE_Array{12},POWER_Pair_PC_Data_rate_UE_Array{13},POWER_Pair_PC_Data_rate_UE_Array{14},POWER_Pair_PC_Data_rate_UE_Array{15},POWER_Pair_PC_Data_rate_UE_Array{16},POWER_Pair_PC_Data_rate_UE_Array{17},POWER_Pair_PC_Data_rate_UE_Array{18},POWER_Pair_PC_Data_rate_UE_Array{19},POWER_Pair_PC_Data_rate_UE_Array{20}]

```

```

POWER_Pair_Fixed_data_rate_UE_Array_BAR = [POWER_Pair_Fixed_Data_rate_UE_Array{1},POWER_Pair_Fixed_Data_rate_UE_Array{2},POWER_Pair_Fixed_Data_rate_UE_Array{3},POWER_Pair_Fixed_Data_rate_UE_Array{4},POWER_Pair_Fixed_Data_rate_UE_Array{5},POWER_Pair_Fixed_Data_rate_UE_Array{6},POWER_Pair_Fixed_Data_rate_UE_Array{7},POWER_Pair_Fixed_Data_rate_UE_Array{8},POWER_Pair_Fixed_Data_rate_UE_Array{9},POWER_Pair_Fixed_Data_rate_UE_Array{10},POWER_Pair_Fixed_Data_rate_UE_Array{11},POWER_Pair_Fixed_Data_rate_UE_Array{12},POWER_Pair_Fixed_Data_rate_UE_Array{13},POWER_Pair_Fixed_Data_rate_UE_Array{14},POWER_Pair_Fixed_Data_rate_UE_Array{15},POWER_Pair_Fixed_Data_rate_UE_Array{16},POWER_Pair_Fixed_Data_rate_UE_Array{17},POWER_Pair_Fixed_Data_rate_UE_Array{18},POWER_Pair_Fixed_Data_rate_UE_Array{19},POWER_Pair_Fixed_Data_rate_UE_Array{20}]

```

```

ir_Fixed_Data_rate_UE_Array{14},POWER_Pair_Fixed_Data_rate_UE_Array
{15},POWER_Pair_Fixed_Data_rate_UE_Array{16},POWER_Pair_Fixed_Dat
a_rate_UE_Array{17},POWER_Pair_Fixed_Data_rate_UE_Array{18},POWE
R_Pair_Fixed_Data_rate_UE_Array{19},POWER_Pair_Fixed_Data_rate_UE_
Array{20}]
POWER_Pair_AP_data_rate_UE_Array_BAR =
[POWER_Pair_AP_Data_rate_UE_Array{1},POWER_Pair_AP_Data_rate_UE
_Array{2},POWER_Pair_AP_Data_rate_UE_Array{3},POWER_Pair_AP_Dat
a_rate_UE_Array{4},POWER_Pair_AP_Data_rate_UE_Array{5},POWER_Pa
ir_AP_Data_rate_UE_Array{6},POWER_Pair_AP_Data_rate_UE_Array{7},P
OWER_Pair_AP_Data_rate_UE_Array{8},POWER_Pair_AP_Data_rate_UE_
Array{9},POWER_Pair_AP_Data_rate_UE_Array{10},POWER_Pair_AP_Dat
a_rate_UE_Array{11},POWER_Pair_AP_Data_rate_UE_Array{12},POWER_
Pair_AP_Data_rate_UE_Array{13},POWER_Pair_AP_Data_rate_UE_Array{1
4},POWER_Pair_AP_Data_rate_UE_Array{15},POWER_Pair_AP_Data_rate_
UE_Array{16},POWER_Pair_AP_Data_rate_UE_Array{17},POWER_Pair_A
P_Data_rate_UE_Array{18},POWER_Pair_AP_Data_rate_UE_Array{19},PO
WER_Pair_AP_Data_rate_UE_Array{20}]

% average data rate of UE
POWER_Pair_PC_Data_rate_UE_Array_AVG_BAR =
[(sum(POWER_Pair_PC_Data_rate_D2DR_Array_BAR)+sum(POWER_Pair_
PC_Data_rate_CUE_Array_BAR))/POWER_PAIR_Number_of_PL;0];
POWER_Pair_Fixed_Data_rate_UE_Array_AVG_BAR =
[(sum(POWER_Pair_Fixed_Data_rate_D2DR_Array_BAR)+sum(POWER_Pai
r_Fixed_Data_rate_CUE_Array_BAR))/POWER_PAIR_Number_of_PL;0];
POWER_Pair_AP_Data_rate_UE_Array_AVG_BAR =
[(sum(POWER_Pair_AP_Data_rate_D2DR_Array_BAR)+sum(POWER_Pair_
AP_Data_rate_CUE_Array_BAR))/POWER_PAIR_Number_of_PL;0];
POWER_Pair_Data_rate_UE_Array_AVG_BAR
=[abs(POWER_Pair_Fixed_Data_rate_UE_Array_AVG_BAR),abs(POWER_P
air_PC_Data_rate_UE_Array_AVG_BAR),abs(POWER_Pair_AP_Data_rate_
UE_Array_AVG_BAR)]

POWER_PAIR_X_axis= 1:1:20; % DISTANCE OF D2D PAIR

```

figure (26)

```

J5= plot(POWER_PAIR_X_axis,POWER_Pair_Fixed_SINR_D2DR_Array_BAR,'-
*g') ;
hold on;
J6= plot(POWER_PAIR_X_axis,POWER_Pair_PC_SINR_D2DR_Array_BAR,'-*b')
;
J7= plot(POWER_PAIR_X_axis,POWER_Pair_AP_SINR_D2DR_Array_BAR,'-or')
;

```

```

    title('SINR OF DUE against number of D2D pairs
','FontSize',12) xlabel('Number of D2D pairs','FontSize',12)
ylabel('SINR OF D2D','FontSize',12) legend([J5 J6
J7],'FPC','PCS1','D2D-PCS') hold off;

```

figure (27)

```

bar(POWER_Pair_PC_SINR_D2DR_bar)
    title('Average DUE SINR when varying D2D
pairs','FontSize',12) xlabel ('Scheme','FontSize',12) ylabel
('DUE SINR','FontSize',12) legend ('FPC','PCS1','D2D-PCS')

```

figure(28)

```

J8=
    plot(POWER_PAIR_X_axis,POWER_Pair_Fixed_Data_rate_D2DR_Array_B
AR,'-*g')
hold on;
J9= plot(POWER_PAIR_X_axis,POWER_Pair_PC_Data_rate_D2DR_Array_BAR,'-
*b')
J10=
    plot(POWER_PAIR_X_axis,POWER_Pair_AP_Data_rate_D2DR_Array_BAR
,'-or')
    title('Data rate of DUE against number of D2D pairs
','FontSize',12) xlabel('Number of D2D pairs ','FontSize',12)
ylabel('data rate of D2D(Mbps)','FontSize',12) legend([J8 J9
J10],'FPC','PCS1','D2D-PCS') hold off;

```

figure(29)

```

bar(POWER_Pair_Data_Rate_D2D_AVG)
    title('Average DUE data rate when varying D2D
pairs','FontSize',12) xlabel ('Scheme','FontSize',12) ylabel ('DUE
data rate (Mbps)','FontSize',12) legend ('FPC','PCS1','D2D-PCS')

```

figure(30)

```

bar(POWER_Pair_D2D_P_S_BAR)
    title('Average DUE power consumption when varying D2D
pairs','FontSize',12) xlabel ('Scheme','FontSize',12) ylabel ('Power
(dBm)','FontSize',12)
    legend ('FPC','PCS1','D2D-PCS')

```

figure (31)

```

J11= plot(POWER_PAIR_X_axis,POWER_Pair_Fixed_Data_rate_CUE_Array_BA
R,'-*g');
hold on;
J12= plot(POWER_PAIR_X_axis,POWER_Pair_PC_Data_rate_CUE_Array_BAR,'-
*b');
J13= plot(POWER_PAIR_X_axis,POWER_Pair_AP_Data_rate_CUE_Array_BAR,'-
or');
    title('Data rate of CUE against number of D2D pairs
','FontSize',12) xlabel('Number of D2D pairs ','FontSize',12)

```

```
ylabel('data rate of CUE(Mbps)','FontSize',12) legend([J11 J12
J13],'FPC','PCS1','D2D-PCS') hold off;
```

```
figure(32)
% barchart of average CUE data rate
bar(POWER_Pair_Data_Rate_CUE_AVG)
title('Average CUE data rate when varying D2D
pairs','FontSize',12) xlabel ('Scheme','FontSize',12) ylabel ('Power
(dBm)','FontSize',12)
legend ('FPC','PCS1','D2D-PCS')
```

```
figure(33) % data
rate of UE
J14 = plot(POWER_PAIR_X_axis,POWER_Pair_Fixed_data_rate_UE_Array_BAR,'-
*g');
hold on;
J15 = plot(POWER_PAIR_X_axis,POWER_Pair_PC_data_rate_UE_Array_BAR,'-
*b') ;
J16 = plot(POWER_PAIR_X_axis,POWER_Pair_AP_data_rate_UE_Array_BAR,'-
or');
title('Data rate of UE against number of D2D pairs
','FontSize',12) xlabel('Number of D2D pairs ','FontSize',12)
ylabel('data rate of UE(Mbps)','FontSize',12) legend([J14 J15
J16],'FPC','PCS1','D2D-PCS') hold off;
```

```
figure(34)
bar(POWER_Pair_Data_rate_UE_Array_AVG_BAR)
title('Average UE data rate when varying D2D
pairs','FontSize',12) xlabel ('Scheme','FontSize',12) ylabel
('Power (dBm)','FontSize',12) legend ('FPC','PCS1','D2D-PCS')
```